EQUS
Australian Research Council
Centre of Excellence for
Engineered Quantum Systems

THE UNIVERSITY OF WESTERN AUSTRALIA

SEEK WISDOM

Frequency and Quantum Metrology Research Group at UWA

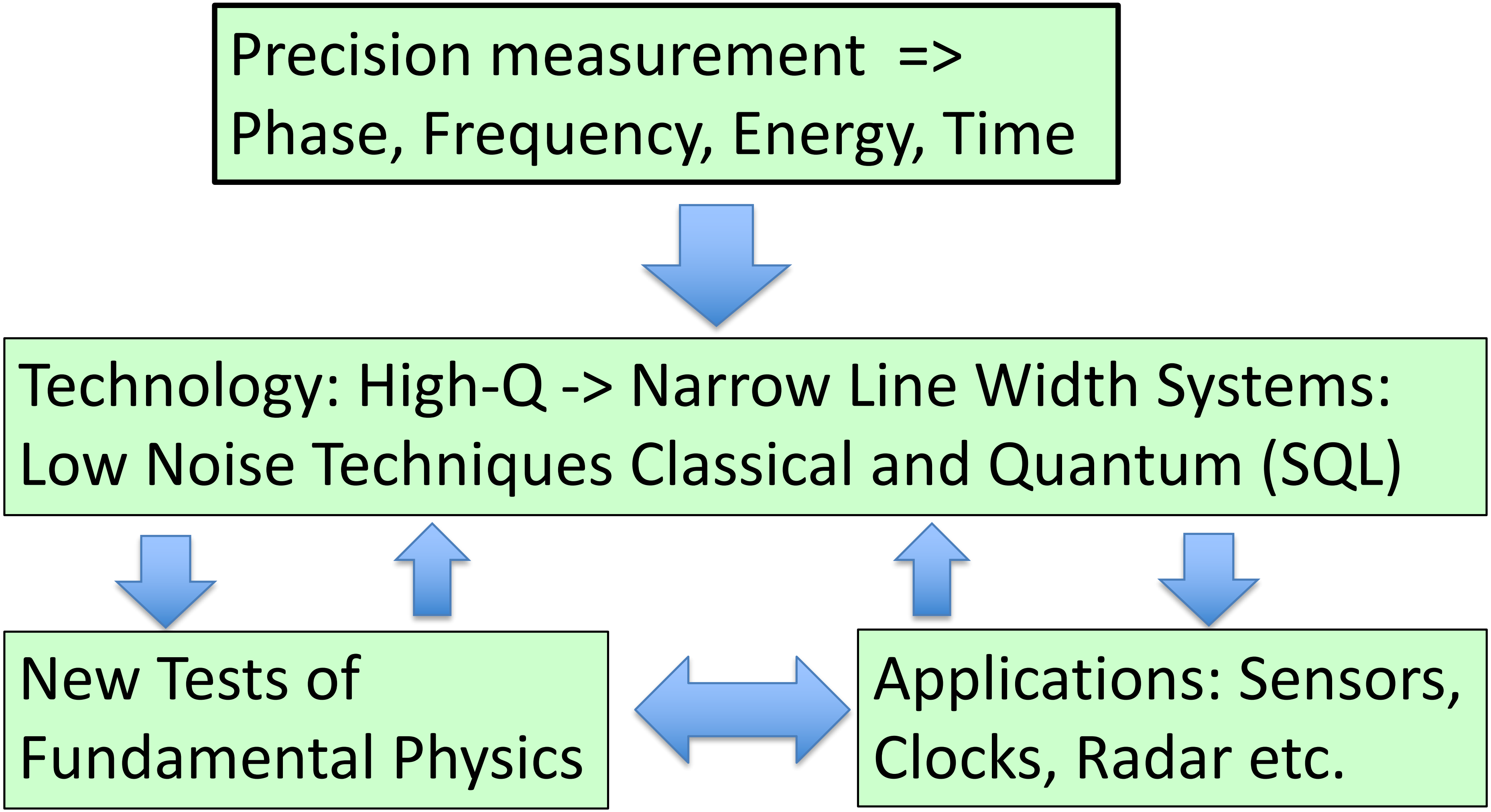
Precision measurement =>
Phase, Frequency, Energy, Time
Technology: High-Q -> Narrow Line Width Systems:
Low Noise Techniques Classical and Quantum (SQL)
New Tests of
Fundamental Physics
Applications: Sensors,
Clocks, Radar etc.

A Short History of My Attempt to Measure Nothing with Precision Measurement

Re-entrant Parametric Transducers

Microwave Readout with Automatic Carrier Suppression

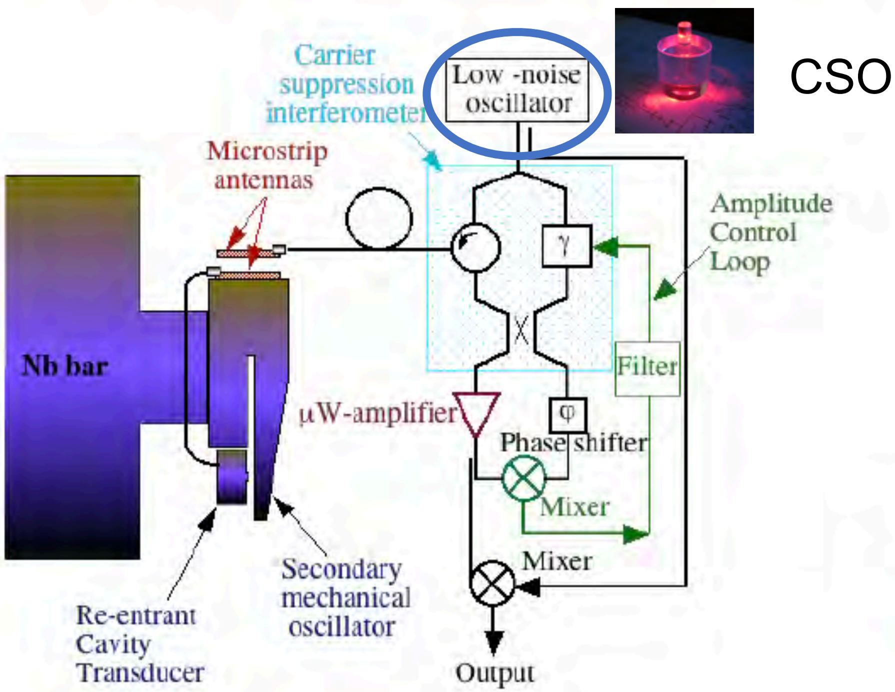

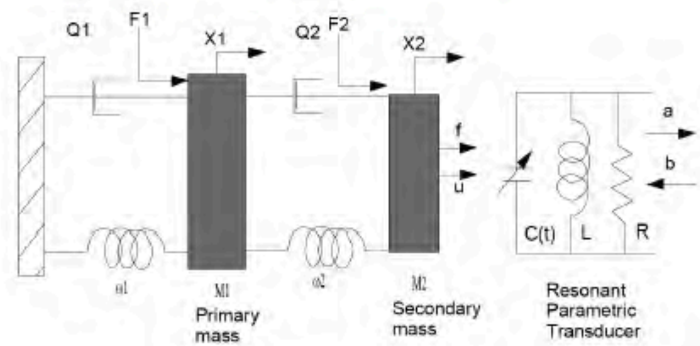

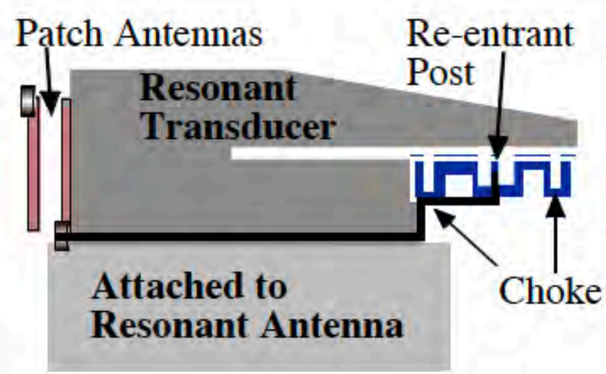

CARRIER SUPPRESSION INTERFEROMETER

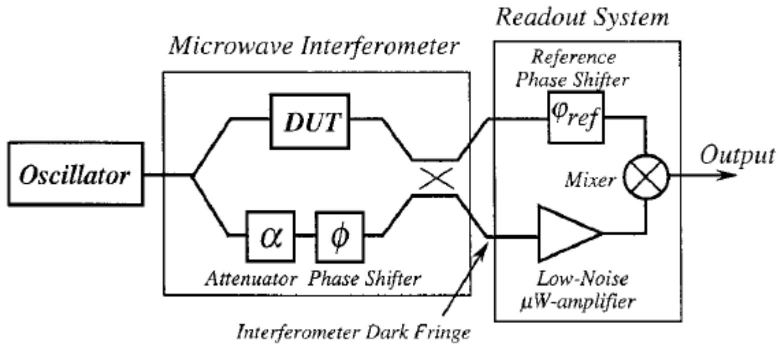

Fig. 1. Interferometric noise measurement system.

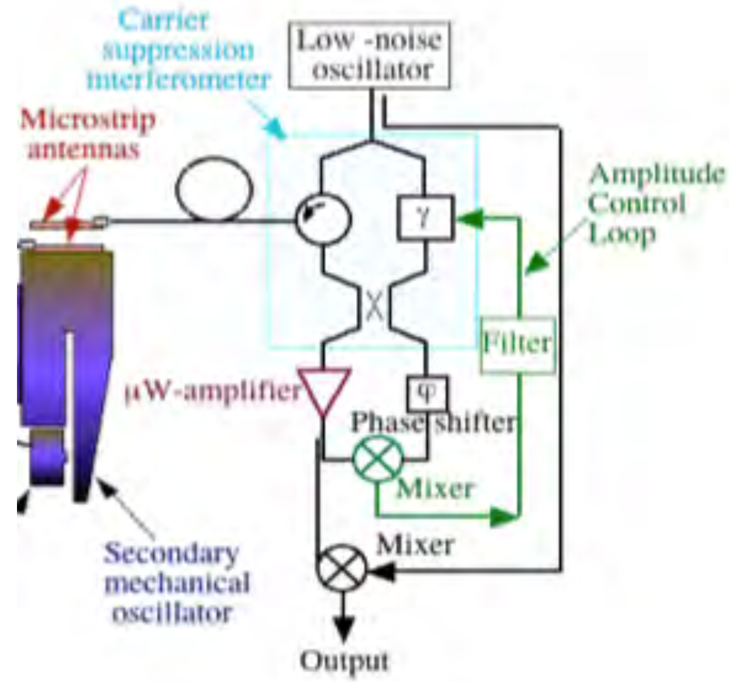

1526 IEEE TRANSACTIONS ON ULTRASONICS, FERROELECTRICS, AND FREQUENCY CONTROL, VOL. 45, NO. 6, NOVEMBER 1998

Microwave Interferometry: Application to Precision Measurements and Noise Reduction Techniques

Eugene N. Ivanov, M. E. Tobar, *Member, IEEE*, and R. A. Woode

$$\mathcal{L}_{\varphi}^{n/f(1)}(f) = \mathcal{L}_{\mathrm{AM}}^{n/f(1)}(f) = \frac{k_B T_{\mathrm{RS}}}{P_{\mathrm{inp}} L_{\mathrm{DUT}}}, \qquad (1)$$

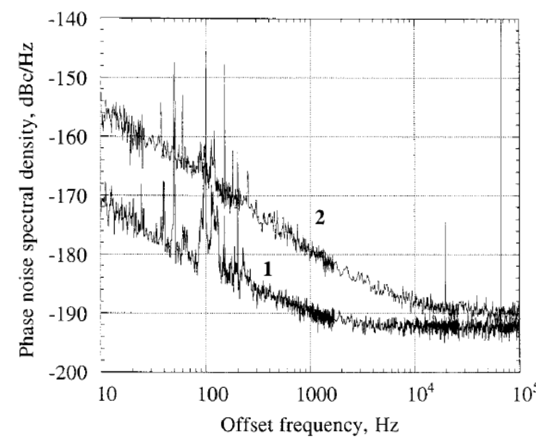

Fig. 2. The phase noise floor of interferometric noise measurement system (curve 1), phase noise of 6 microwave isolators connected in series (curve 2). Input power is 20 dBm, carrier frequency 9 GHz.

REVIEW OF SCIENTIFIC INSTRUMENTS **80**, 044701 (2009)

Microwave phase detection at the level of 10^{-11} rad

Eugene N. Ivanov[a] and Michael E. Tobar[b]
School of Physics M013, University of Western Australia, 35 Stirling Hwy., Crawley, 6009 Western Australia, Australia

(Received 7 December 2008; accepted 15 March 2009; published online 10 April 2009)

We report on a noise measurement system with the highest spectral resolution ever achieved in the microwave domain. It is capable of detecting the phase fluctuations in rms amplitude of 2×10^{-11} rad/$\sqrt{\text{Hz}}$ at Fourier frequencies above a few kilohertz. Such precision allows the study of intrinsic fluctuations in various microwave components and materials, as well as precise tests of fundamental physics. Employing this system we discovered a previously unknown phenomenon of down-conversion of pump oscillator phase noise into the low-frequency voltage fluctuations.
 [DOI: 10.1063/1.3115206]

Sapphire Loaded Cavity (SLC) Resonators

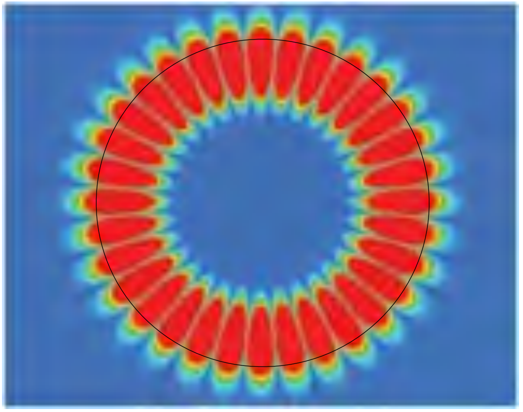

Electric field density plot
($H_{16,1,1}$ – mode)

Key features

Very high Q-factors at WG- modes

Temperature	Q-factor (10 GHz)
300 K	$2\ 10^{5}$
77 K	$3\ 10^{7}$
4. 2 K	$4\ 10^{9}$

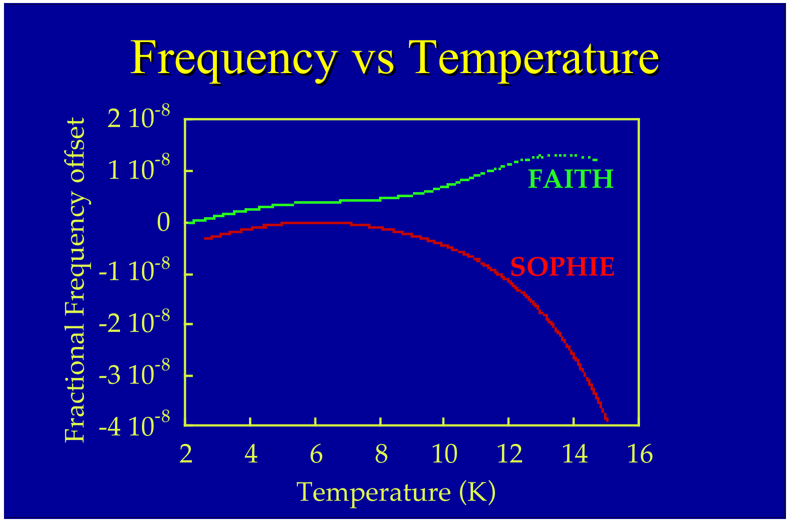

Frequency-temperature turning points

Microwave Oscillators

Room temperature oscillator with interferometric signal processing

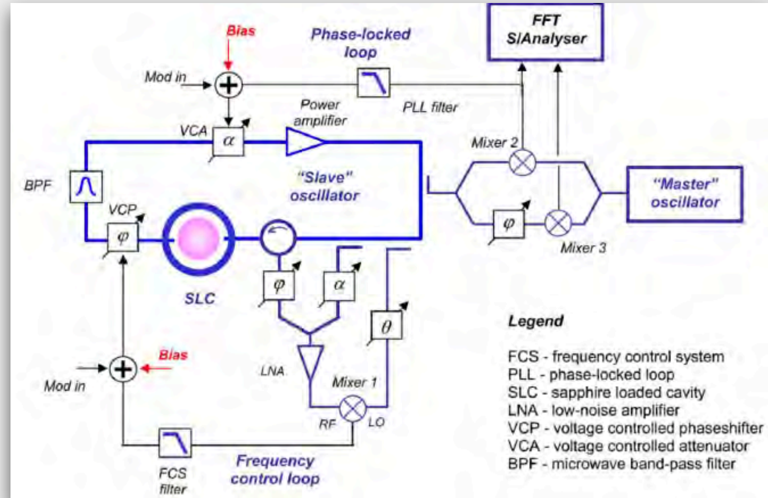

developed @ UWA

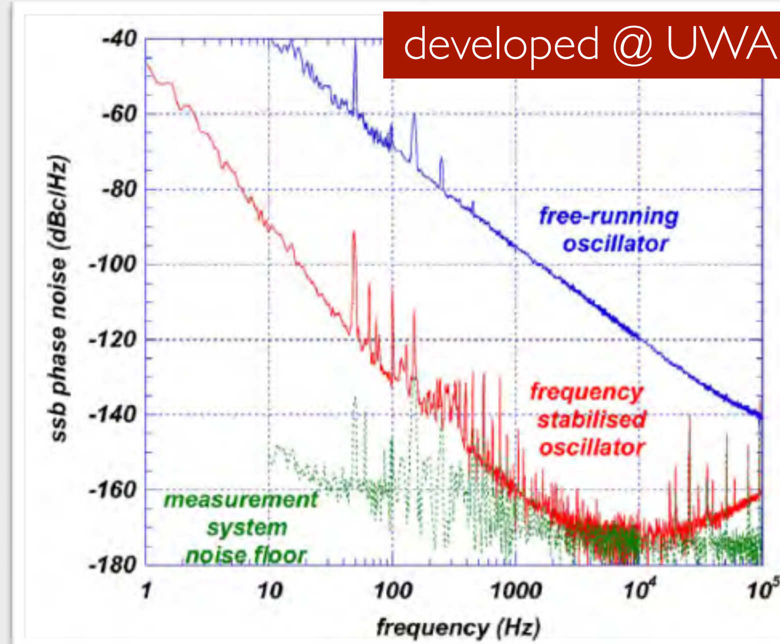

Cryogenic Sapphire Oscillators

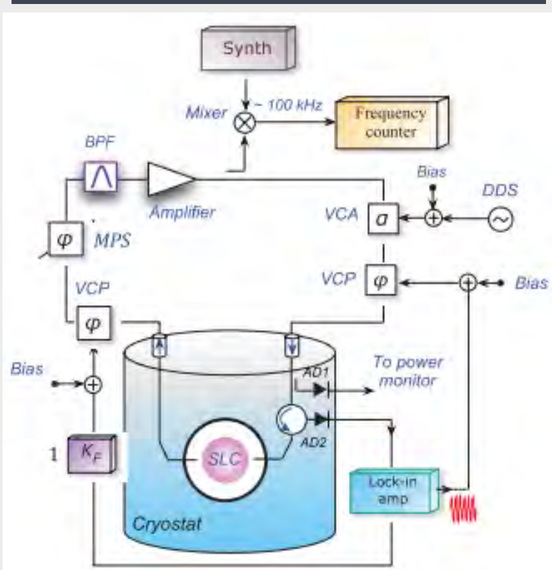

developed @ UWA

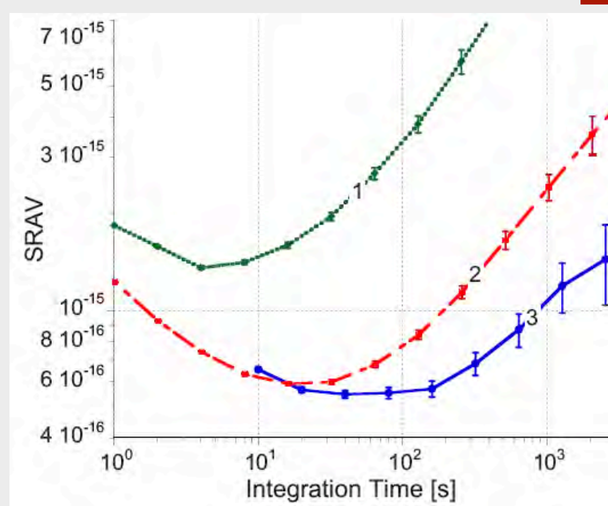

approaching 10^{-16}

EQUS
Australian Research Council
Centre of Excellence for
Engineered Quantum Systems

Microwave Oscillators

National Metrology Laboratories

- Lowest phase and amplitude noise
- Exceptional spectral purity
- Low spurious content
- Low vibrational sensitivity
- Unequalled short-term stability.

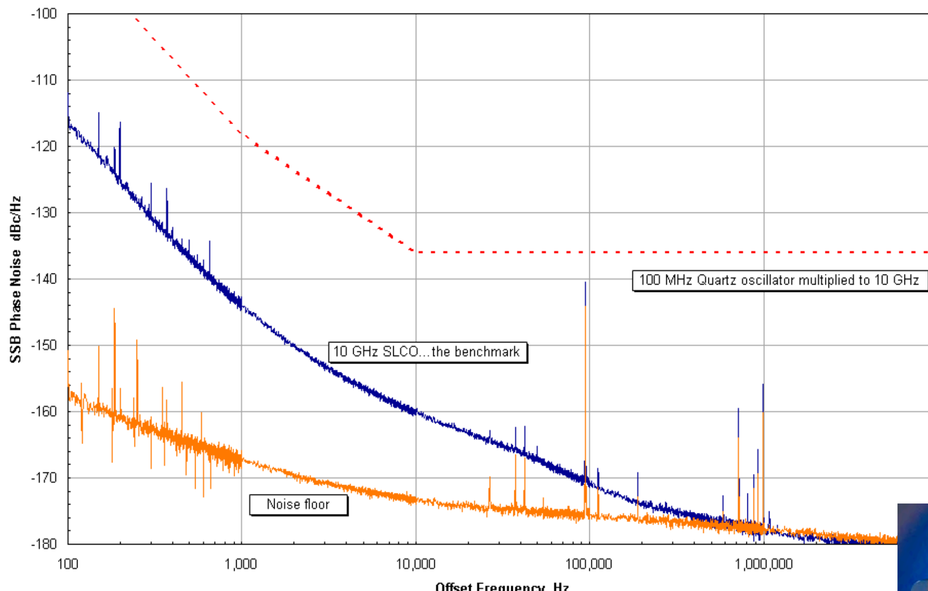

SAPPHIRE LOADED CAVITYOSCILLATORS

Compact low noise oscillator: Defence Radar Applications

Oscillator/Clock Zoo

Photons

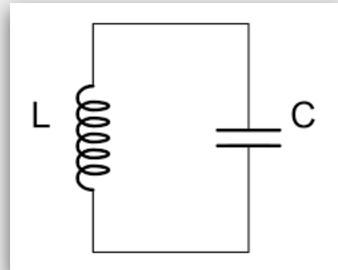

LC-circuits

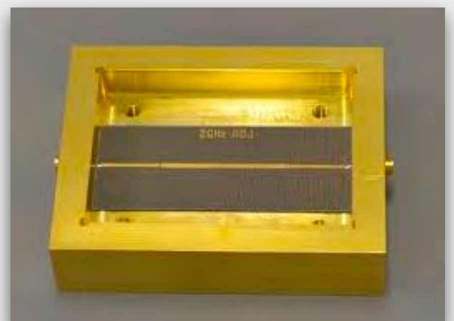

Metallic Cavities

Dielectric Cavities

Phonons

SAW

BAW

Structures

Magnons

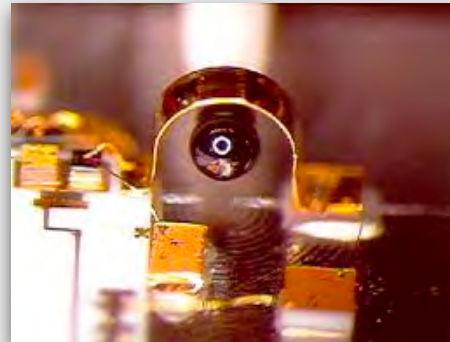

Bulk

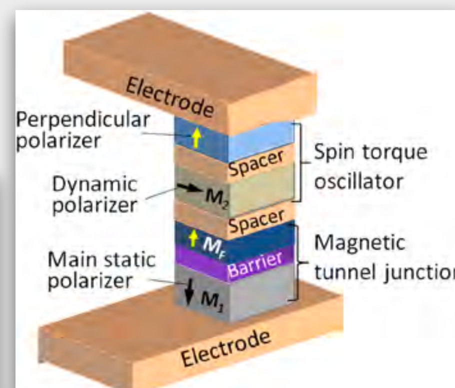

Spin-Torque

Atoms

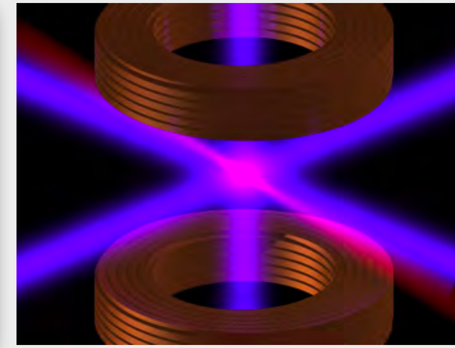

Electron transitions

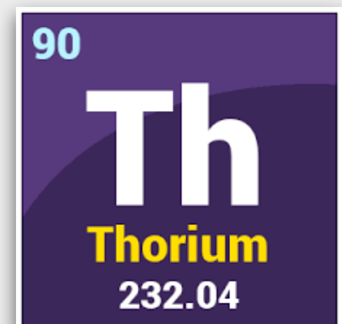

Nuclear transitions

EQUS
Australian Research Council
Centre of Excellence for
Engineered Quantum Systems

Collaboration with SYRTE at Paris Observatory

Long term operation of CSO -> 5.5 yrs
76% Duty cycle since August 2003

Before 2003 with less duty cycle

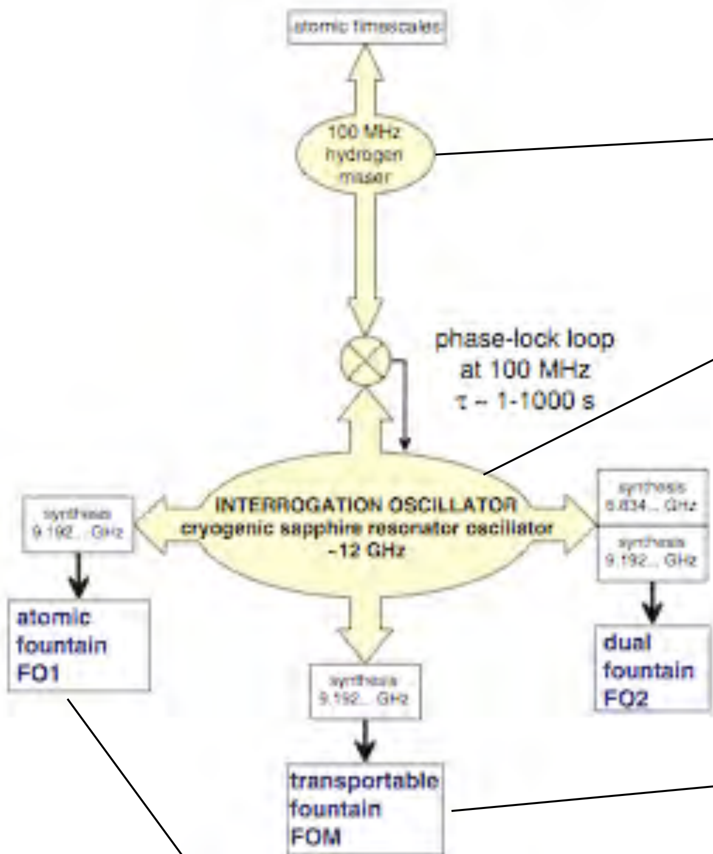

Test Relativity

Varying Fundamental Constants

Experiment:
Resonators

Cylindrical Sapphire crystal

Superconducting Niobium Cavity

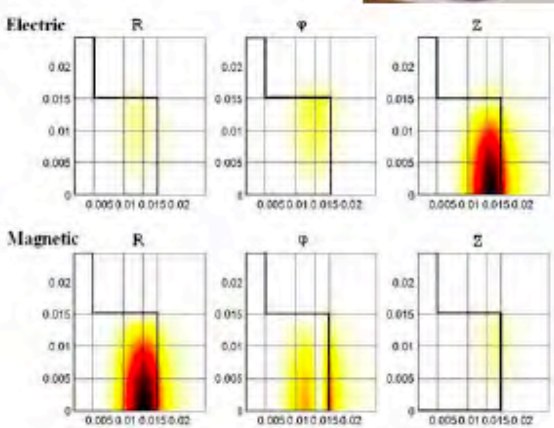

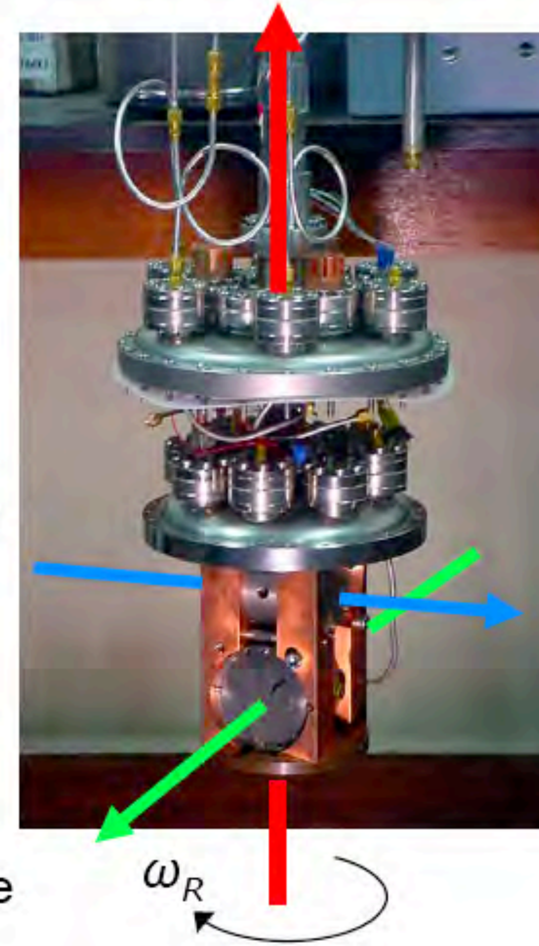

Operate the E8,1,1 mode
Frequency ~ 10GHz
Q ~ 1 x 10^8

Experiment:
Rotation system

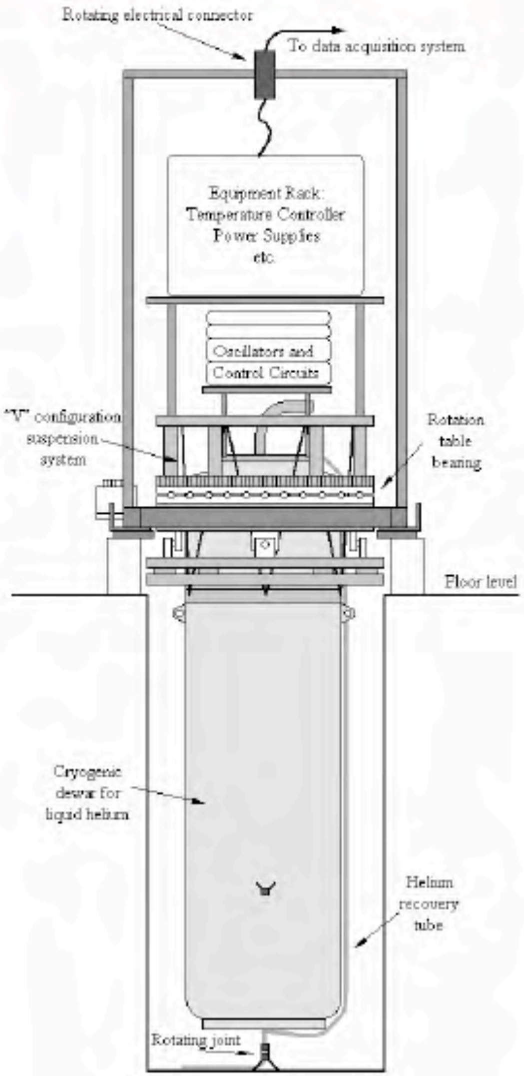

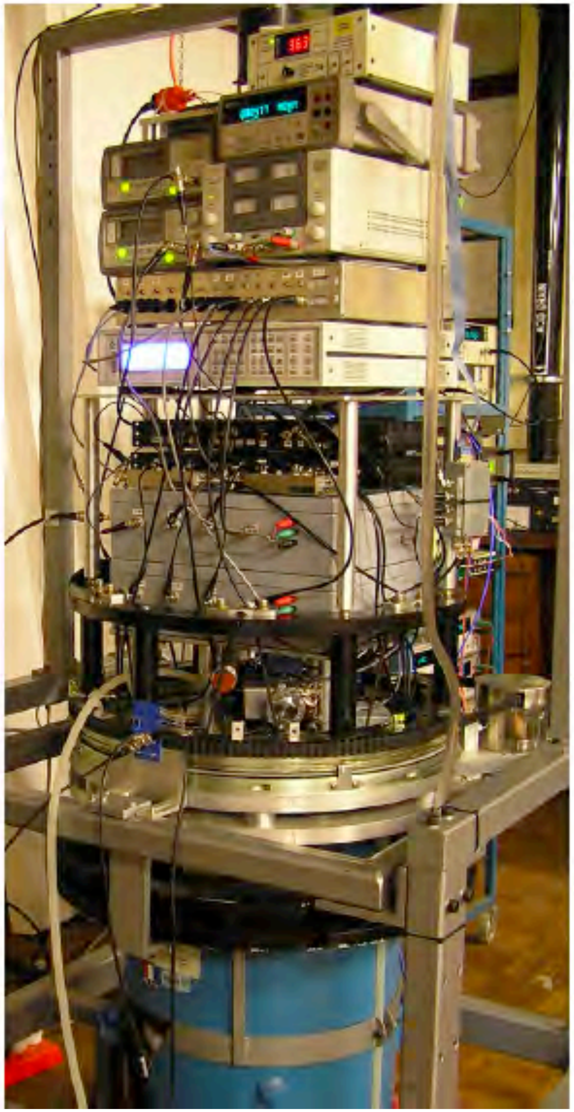

natu
COMM

ARTIC

Received 1

Dire
in e

Moritz N
Eugene I

Lorentz sy
model of
low-energ
scale. Mai
appearing
to assess
to perforr
terrestrial
orientatio
confidenc
experiments allows us to set comprehensive simultaneous bounds on nine boost and rotation

INTERNATIONAL BUSINESS TIMES
AU EDITION | MONDAY, SEPTEMBER 21, 2015 AS OF 8:04 PM AEST

SCIENCE

Australian researchers test speed of light with never-before made precision

By Darwin Malicdem on September 15 2015 4:17 PM

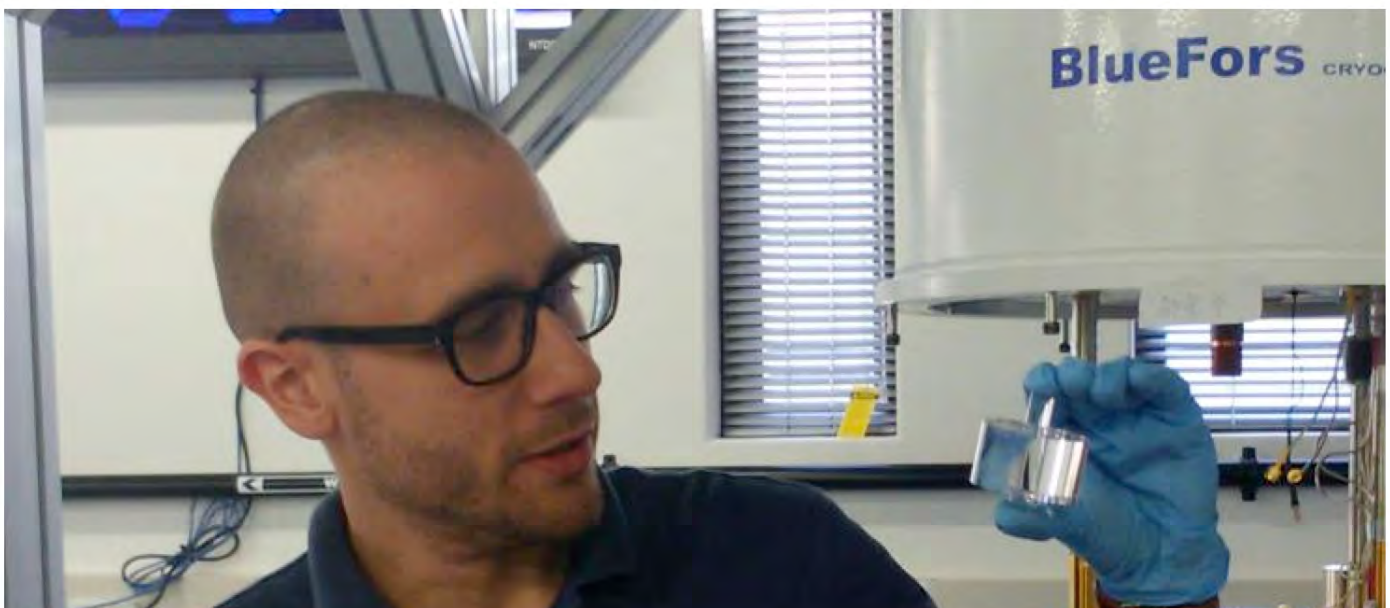

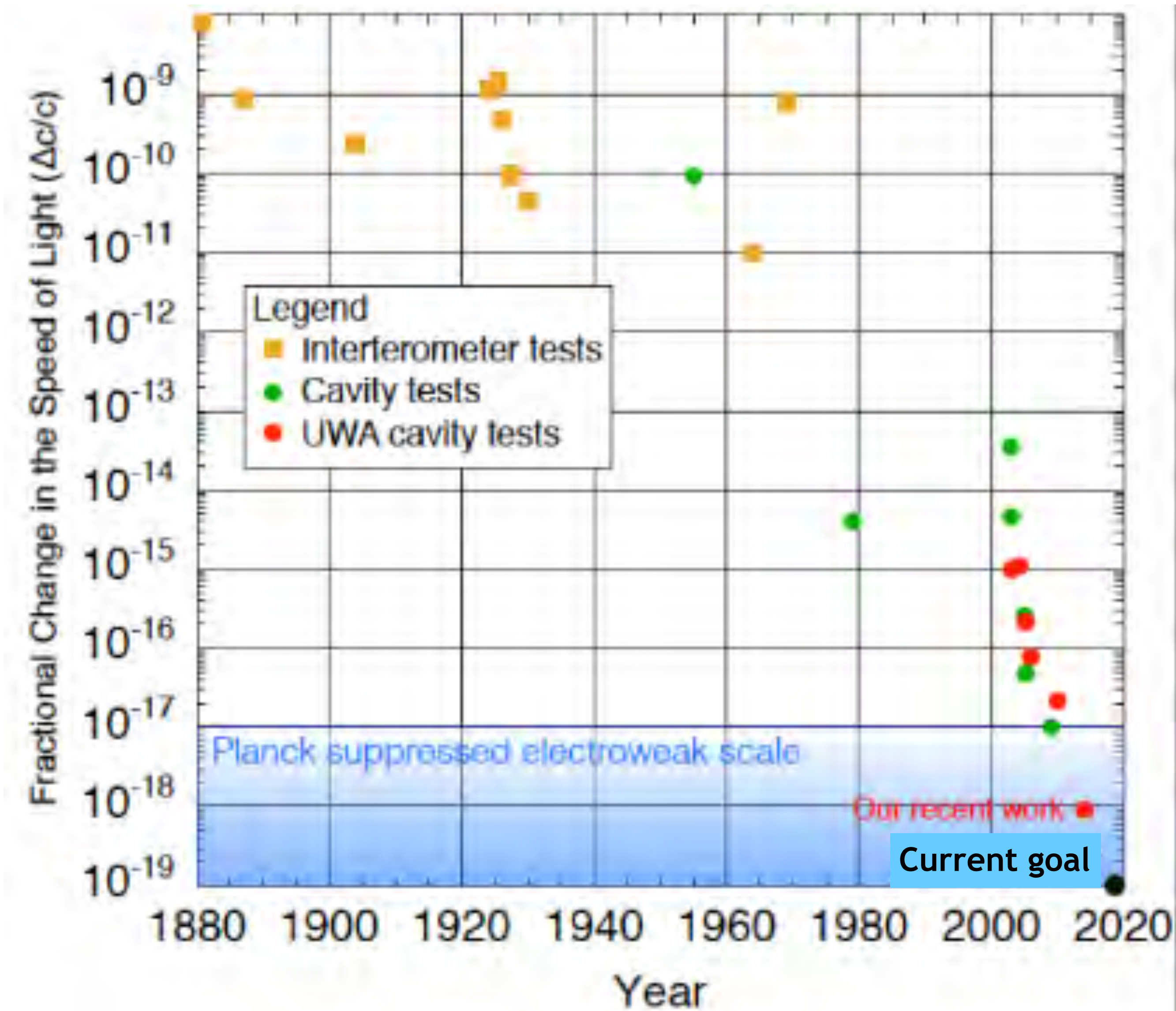

Planck energy suppressed by the energy scale of electroweak unification (100 GeV) dimensionless ratio of ~ 8×10^{18}

PHYSICAL REVIEW X 6, 011018 (2016)

Next Generation of Phonon Tests of Lorentz Invariance Using Quartz BAW Resonators

Maxim Goryachev, Zeyu Kuang, Eugene N. Ivanov, Philipp Haslinger,
Holger Müller, and Michael E. Tobar, *Fellow, IEEE*

***Abstract*— We demonstrate technological improvements in phonon sector tests of the Lorentz invariance that implement quartz bulk acoustic wave oscillators. In this experiment, room temperature oscillators with state-of-the-art phase noise are continuously compared on a platform that rotates at a rate of order of a cycle per second. The discussion is focused on improvements in noise measurement techniques, data acquisition, and data processing. Preliminary results of the second generation of such tests are given, and indicate that standard model extension coefficients in the matter sector can be measured at a precision of order 10^{-16} GeV after taking a year's worth of data. This is equivalent to an improvement of two orders of magnitude over the prior acoustic phonon sector experiment.**

***Index Terms*— Acoustic waves, data analysis, frequency measurement, low-frequency noise, physics computing.**

Universi ... *lia*
(Received ... 16)
We prop ... uartz
oscillator t ... idard
model ext ... lids,
giving rise ... first
realization ... ress-
compensat ... it of
$\tilde{c}_Q^n = (-1.$ ... f the
standard m ... ents
in accurac ... ton,
electron, a
DOI: 10.11

Rotating Quartz Oscillators

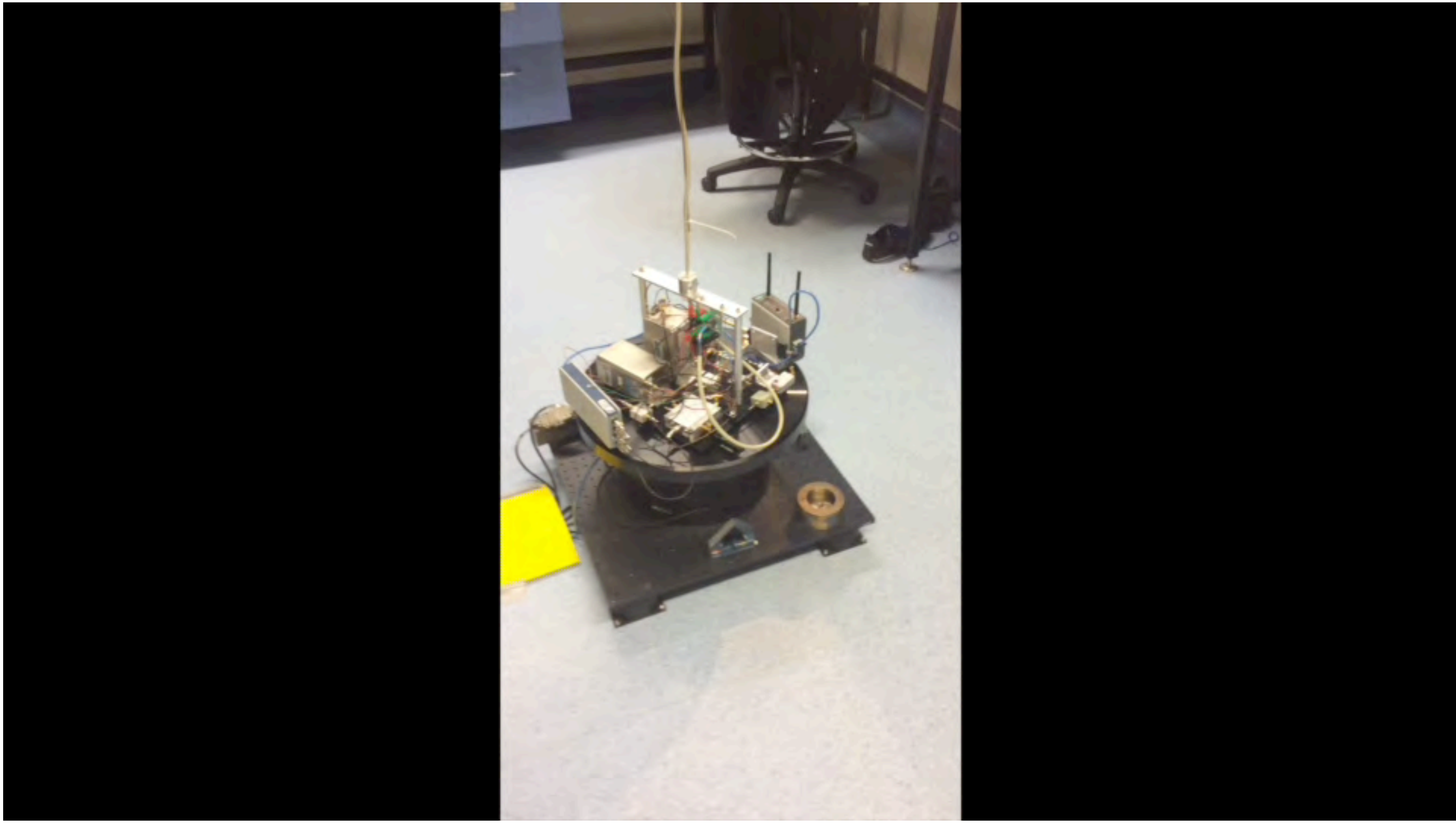

Rotating Bulk Acoustic Wave Oscillators

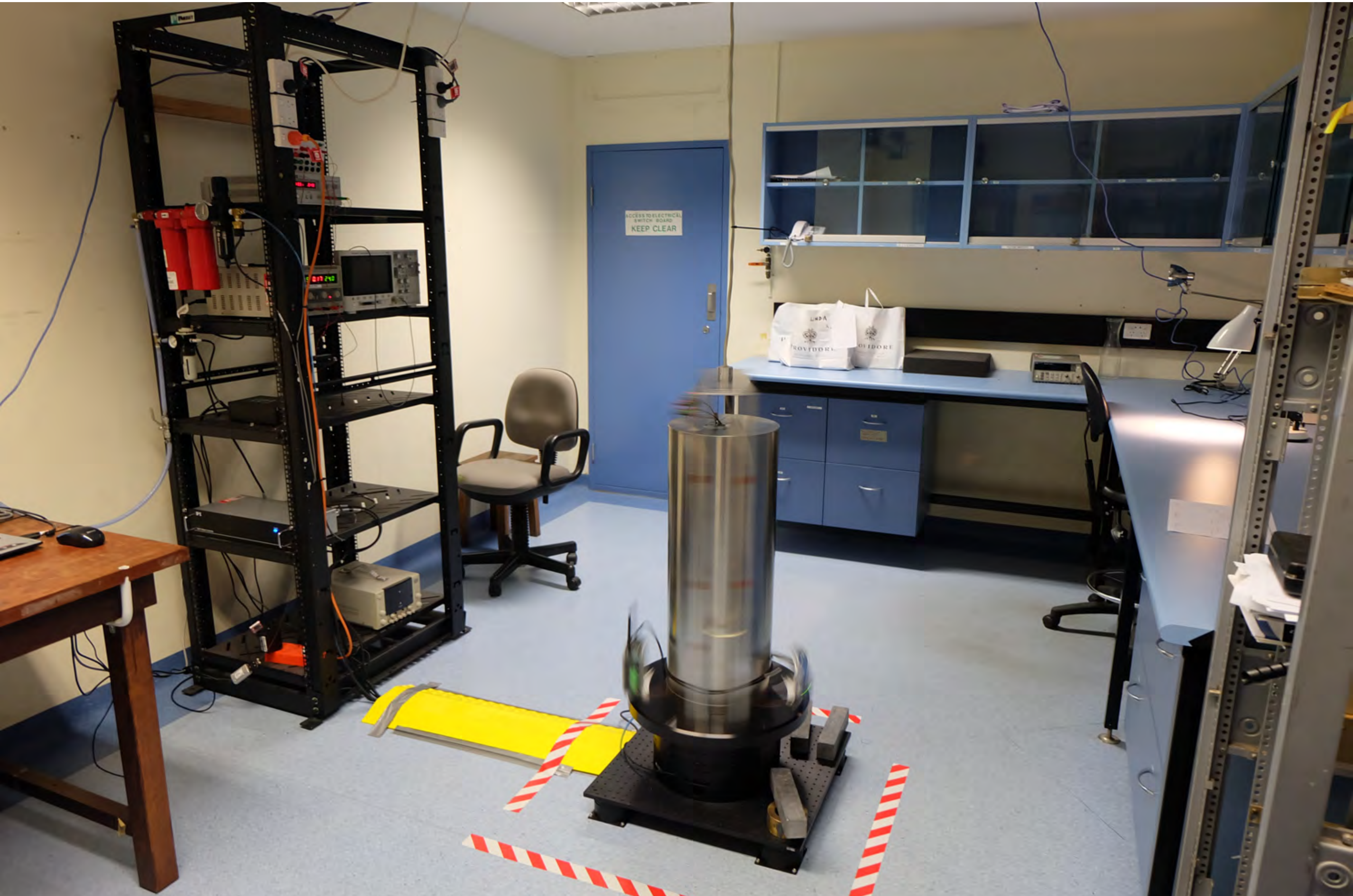

Trying to Enter the Game to Search for the Axion

Physics Letters B 698 (2011) 346–352

Contents lists available at ScienceDirect

PHYSICAL REVIEW D 84, 055023 (2011)

Microwave cavity hidden sector photon threshold crossing

Rhys G. Povey,* John G. Hartnett, and Michael E. Tobar

School of Physics, University of Western Australia, Western Australia 6009, Australia

(Received 31 May 2011; published 27 September 2011)

Hidden sector photons are a weakly interacting slim particle arising from an additional U(1) gauge symmetry predicted by many standard model extensions. We present and demonstrate a new experimental method using a single microwave cavity to search for hidden sector photons. Only photons with a great enough energy are able to oscillate into hidden sector photons of a particular mass. If our cavity is driven on resonance and tuned over the corresponding threshold frequency, an observed drop in the circulating power signifies the creation of hidden sector photons. This approach avoids the problems of microwave leakage and frequency matching inherent in photon regeneration techniques.

Editor: A. Ringwald

Keywords:
Low energy particle physics
Light shining through walls experiments
Tests of quantum interference
Microwave cavities

regeneration rates where on average the cavity contains less than one photon. In this Letter we report on a demonstration experiment using a microwave cavity driven with extremely low power, to show that resonant amplification works also in this regime. In accordance with standard quantum mechanics this is a demonstration that interference also works at the level of less than one quantum. As an additional benefit this experiment shows that thermal photons inside the cavity cause no adverse effects.

Frequency Metrology in Paraphoton Detection

New alternative to Light Shining through a Wall

PHYSICAL REVIEW D **87**, 115008 (2013)

Hidden sector photon coupling of resonant cavities

Stephen R. Parker,[1,*] Gray Rybka,[2] and Michael E. Tobar[1]
[1]*School of Physics, The University of Western Australia, Crawley 6009, Australia*
[2]*University of Washington, Seattle, Washington 98195, USA*
(Received 25 April 2013; published 7 June 2013)

Many beyond the standard model theories introduce light paraphotons, a hypothetical spin-1 field that kinetically mixes with photons. Microwave cavity experiments have traditionally searched for paraphotons via transmission of power from an actively driven cavity to a passive receiver cavity, with the two cavities separated by a barrier that is impenetrable to photons. We extend this measurement technique to account for two-way coupling between the cavities and show that the presence of a paraphoton field can alter the resonant frequencies of the coupled cavity pair. We propose an experiment that exploits this effect and uses measurements of a cavity's resonant frequency to constrain the paraphoton-photon mixing parameter χ. We show that such an experiment can improve the sensitivity to χ over existing experiments for paraphoton masses less than the resonant frequency of the cavity, and that it can eliminate some of the most common systematics for resonant cavity experiments.

coupled mode system

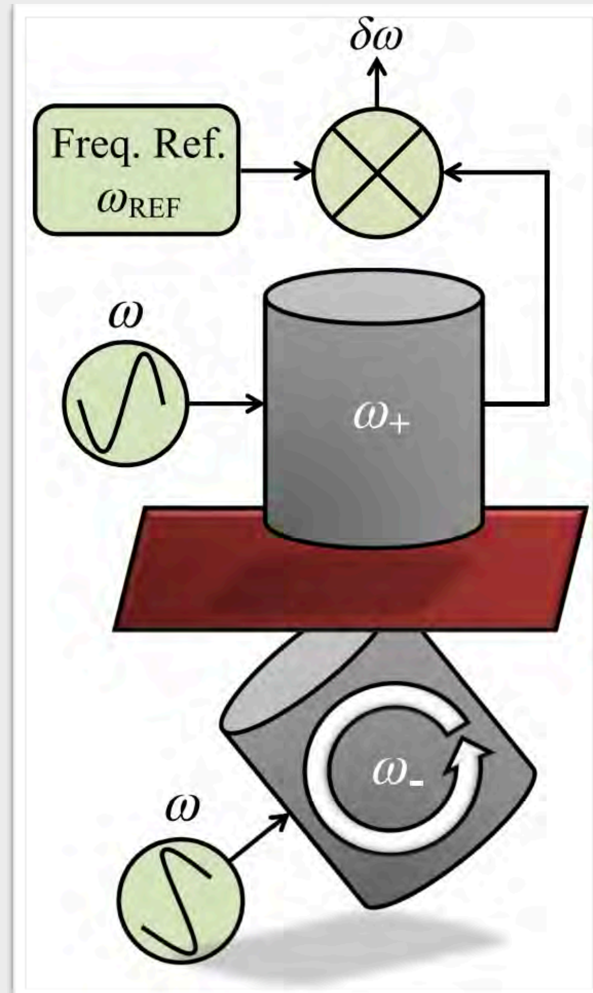

$$\omega_{\pm} \approx \omega_0\left(\frac{1}{1-\frac{x^2}{2}}\left(1+\frac{1}{2Q_1Q_2}+\frac{x^2}{4}+\boxed{\frac{m_{\gamma'}^2\chi^2}{\omega_0^2}-\frac{m_{\gamma'}^4\chi^2G_S}{\omega_0^4}}\pm\left(\frac{1}{Q_1Q_2}+x^2+\boxed{\frac{2m_{\gamma'}^2x^2\chi^2}{\omega_0^2}-\frac{2m_{\gamma'}^4x^2\chi^2G_S}{\omega_0^4}+\frac{m_{\gamma'}^8\chi^4G}{\omega_0^8}}\right)^{\frac{1}{2}}\right)\right)^{\frac{1}{2}},$$

Paraphoton coupling to the 2nd cavity modulate resonance frequency

EQUS
Australian Research Council
Centre of Excellence for
Engineered Quantum Systems

Trying to Enter the Game to Search for the Axion

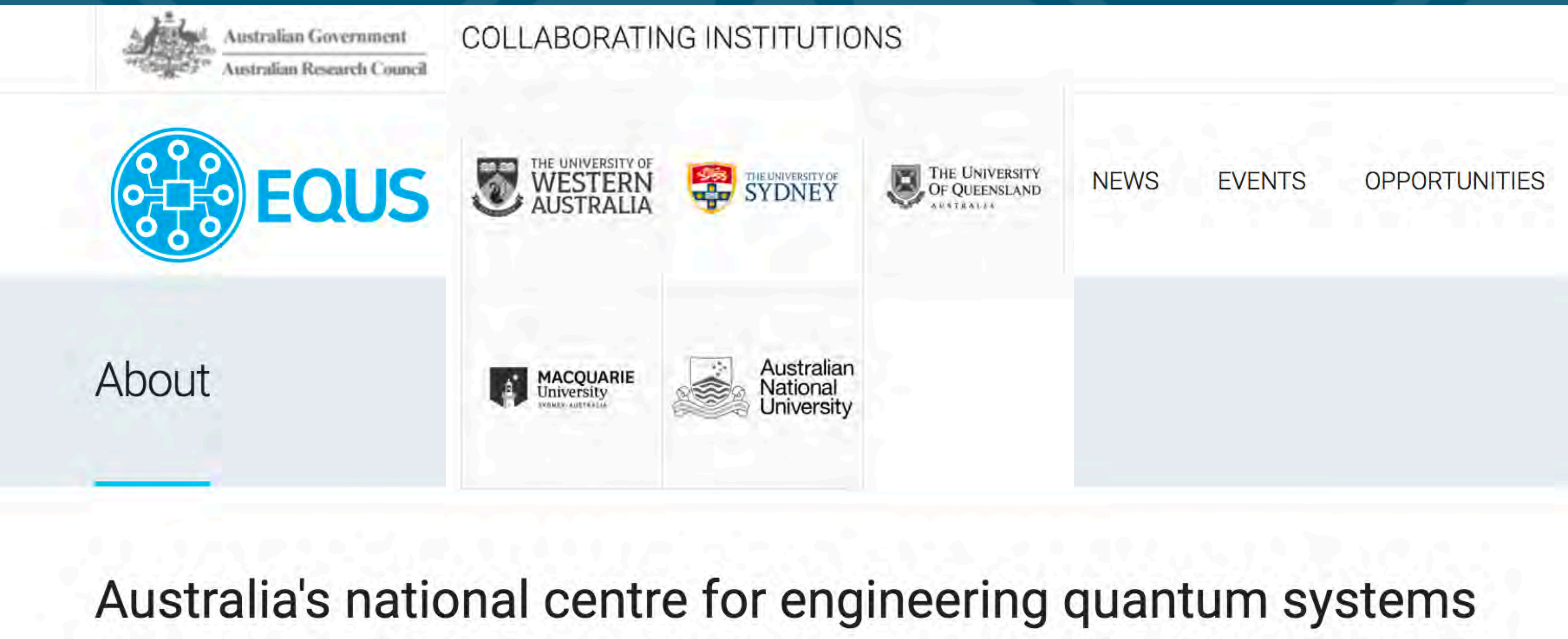

2011-2017 renewed 2018-2024

My lab $350,000 / year 14 years!

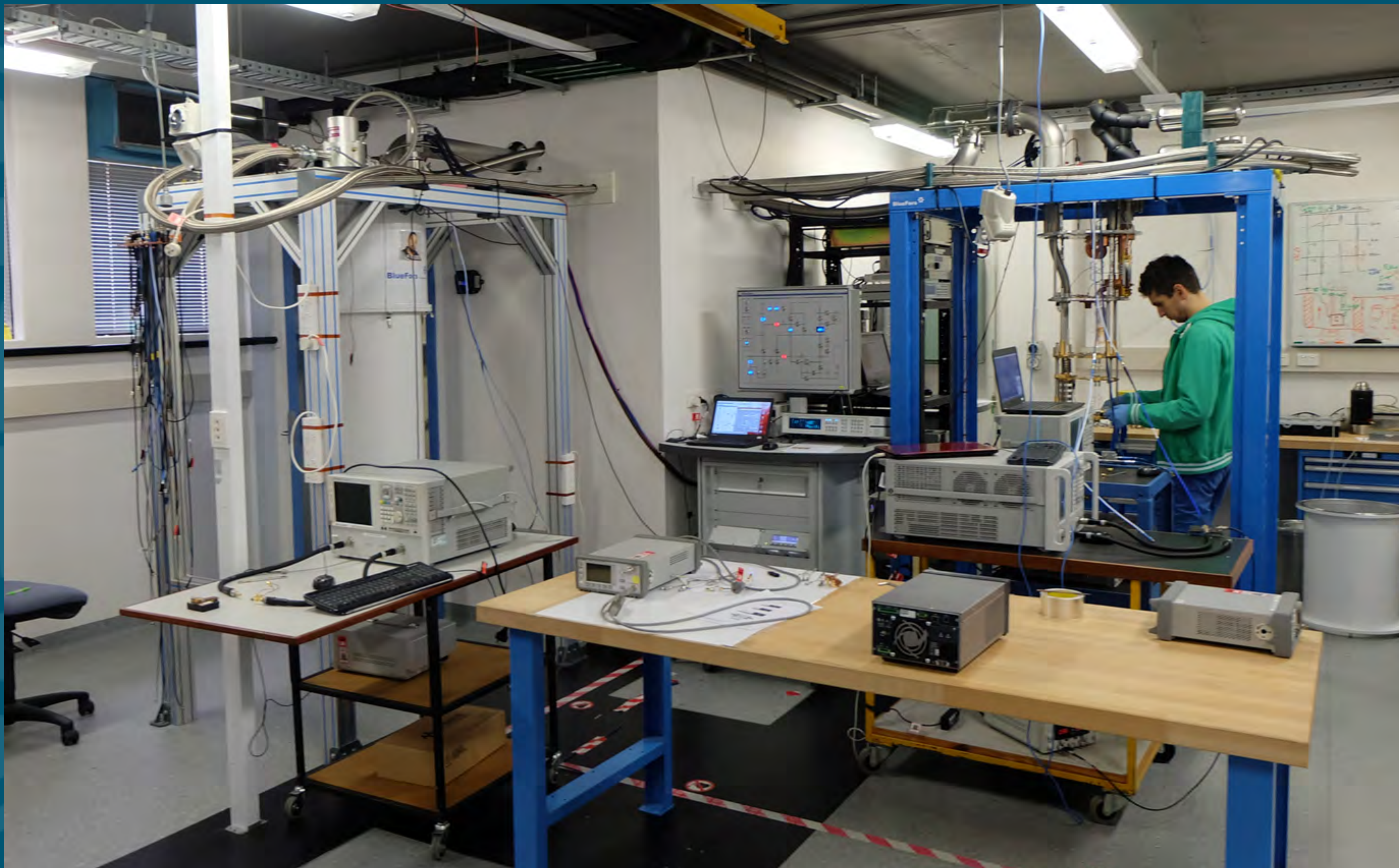

7 T Magnet (10 cm bore)

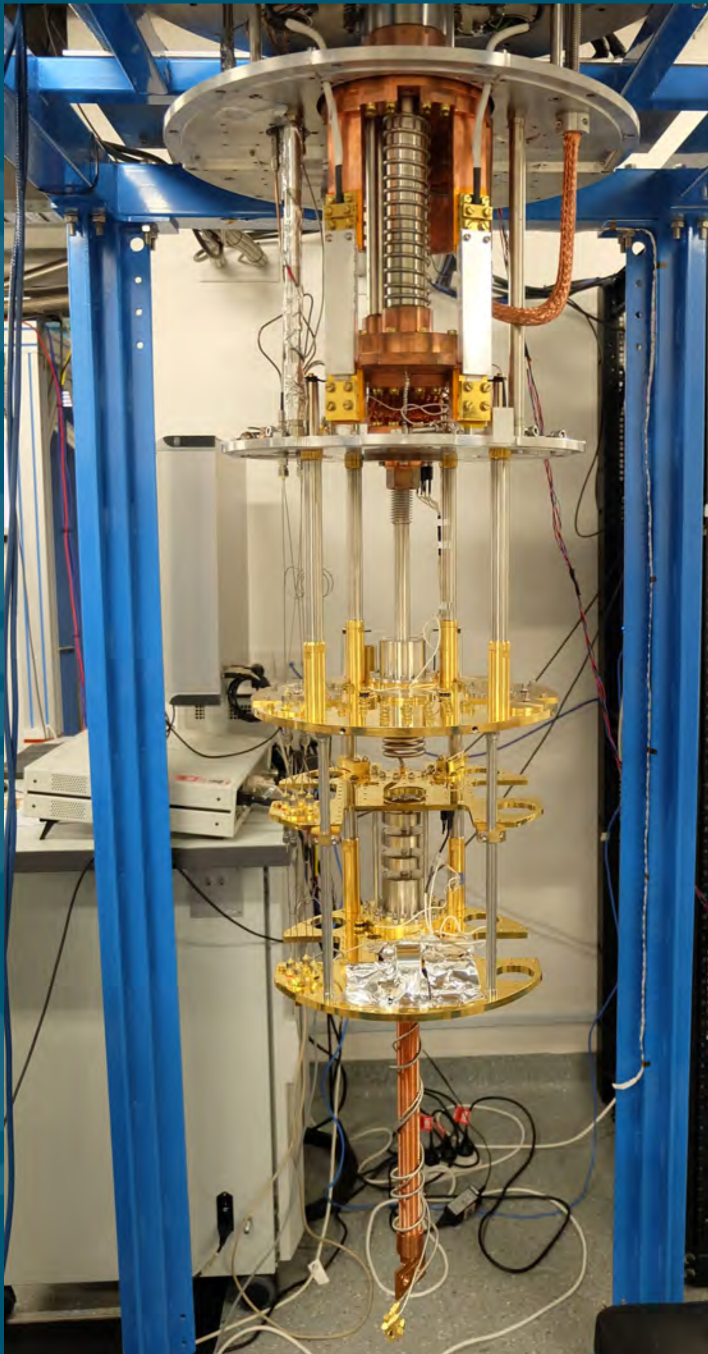

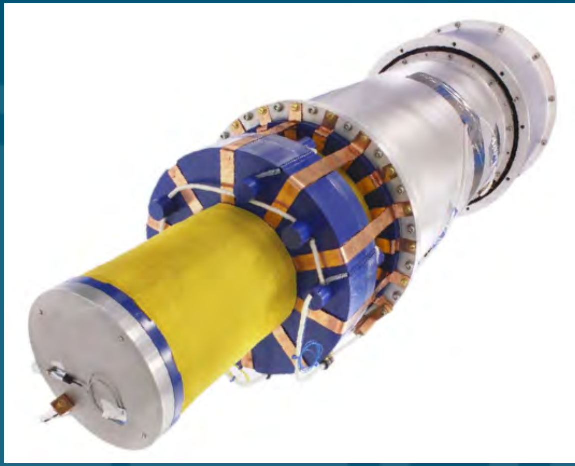

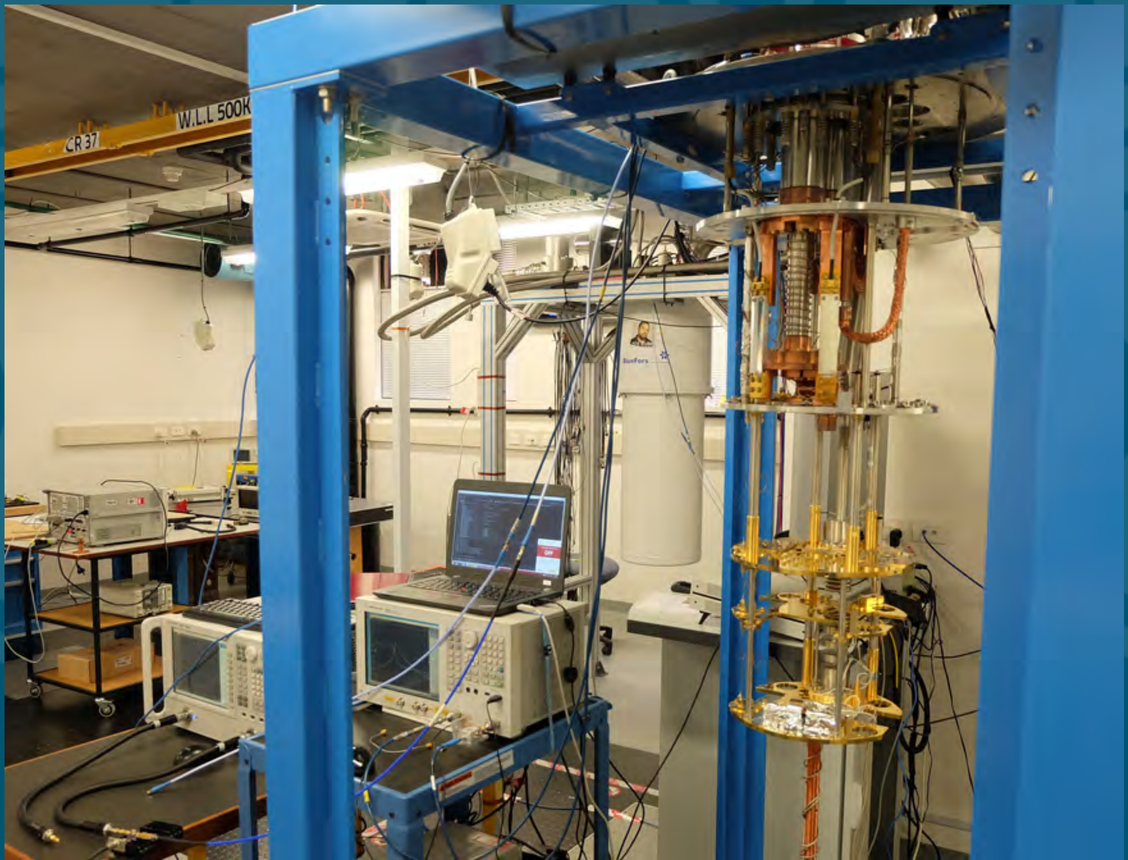


CRYOMECH

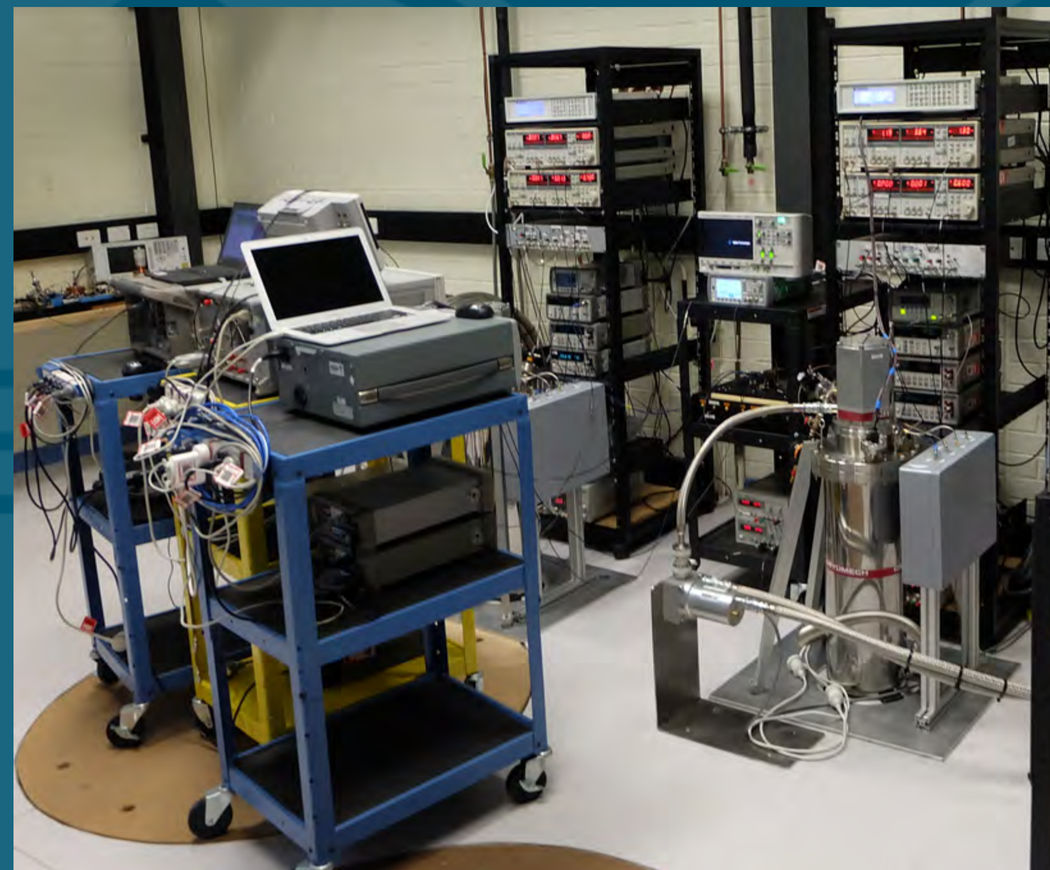

Funding History For Axion Dark Matter at UWA

~~DP160103999~~	~~Finding the dark matter axion~~	~~Prof Michael Tobar~~	~~The University of Western Australia~~
~~DP170102672~~	~~High Mass Dark Matter Axion Halosc~~	~~Prof Michael Tobar~~	~~The University of Western Australia~~
CE170100009	ARC Centre of Excellence for Engineered Quantum Systems	Prof Andrew White	The University of Queensland

Indicative funding by calendar year

2017	2018	2019	2020	2021	2022	2023
$4,650,000.00	$4,500,000.00	$4,500,000.00	$4,550,000.00	$4,550,000.00	$4,550,000.00	$4,600,000.00

PARTICLE PHYSICS DID NOT GET THIER CENTRE RENEWED: New Plan for Centre of Excellence on Dark matter Particle Physics

LE180100042	Australian Dark Matter Detector for High Mass Axions	Prof Michael Tobar	The University of Western Australia

Funded Biggest BlueFors DilFridge 14 T Magnet: Arrive June 2019

DP190100071	Precision Low Energy Experiments to Search for New Physics	Prof Michael Tobar	The University of Western Australia

FUNDED: $530,000 Gray Rybka ADMX, Frank Wilczek

AUSTRALIAN RESEARCH COUNCIL
ARC Centres of Excellence
Proposal for Funding Commencing in 2020

CE

PROJECT ID: CE200100008

First Investigator: Prof Elisabetta Barberio

Admin Org: The University of Melbourne

Total number of sheets contained in this Proposal: 435

Number	Name	Participant Type	Current Organisation(s)	Relevant Organisation
1	Prof Elisabetta Barberio	Centre Director	The University of Melbourne	The University of Melbourne
2	Prof Anthony Williams	Chief Investigator	The University of Adelaide	The University of Adelaide
3	Prof Andrew Stuchbery	Chief Investigator	The Australian National University	The Australian National University
4	A/Prof Nicole Bell	Chief Investigator	The University of Melbourne	The University of Melbourne
5	Prof Michael Tobar	Chief Investigator	The University of Western Australia	The University of Western Australia
6	A/Prof Alan Duffy	Chief Investigator	Swinburne University of Technology	Swinburne University of Technology
29	Asst Prof Gray Rybka	Partner Investigator	University of Washington, Seattle	University of Washington, Seattle
30	Prof Yannis Semertzidis	Partner Investigator	Institute for Basic Science, Center for Axions and Precision Physics Research, South Korea and KAIST (Korea Advanced Institute of Science and Technology)	korea Institute of Science and Technology, Europe
31	Prof Frank Wilczek	Partner Investigator	Stockholm University, Sweden, Massachusetts Institute of Technology	Stockholm University, Sweden

Applying $43 M AUD 7 Years

$2.8 M for Axion Wisp
$1.2 M Quantum Tech WIMPs

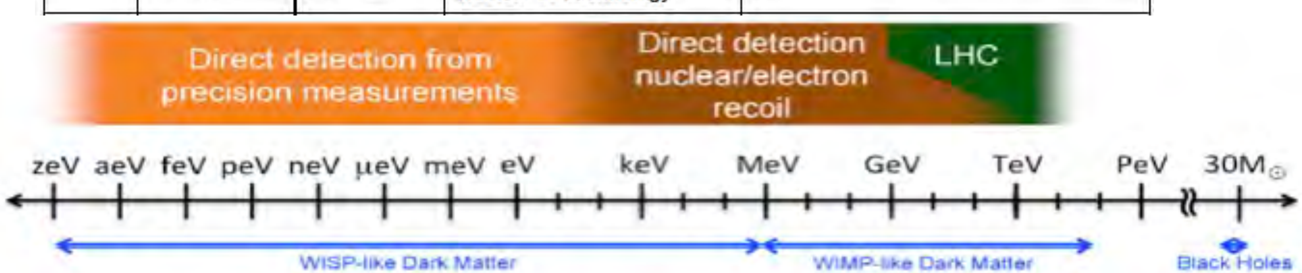

The ORGAN Experiment:

McGillivary Organ at UWA

THE UNIVERSITY OF WESTERN AUSTRALIA

EQUS Australian Research Council Centre of Excellence for Engineered Quantum Systems

What is ORGAN?

- High frequency/high mass axion haloscope
- **O**scillating **R**esonant **G**roup **A**xio**N** Experiment
- Designed to probe promising high mass

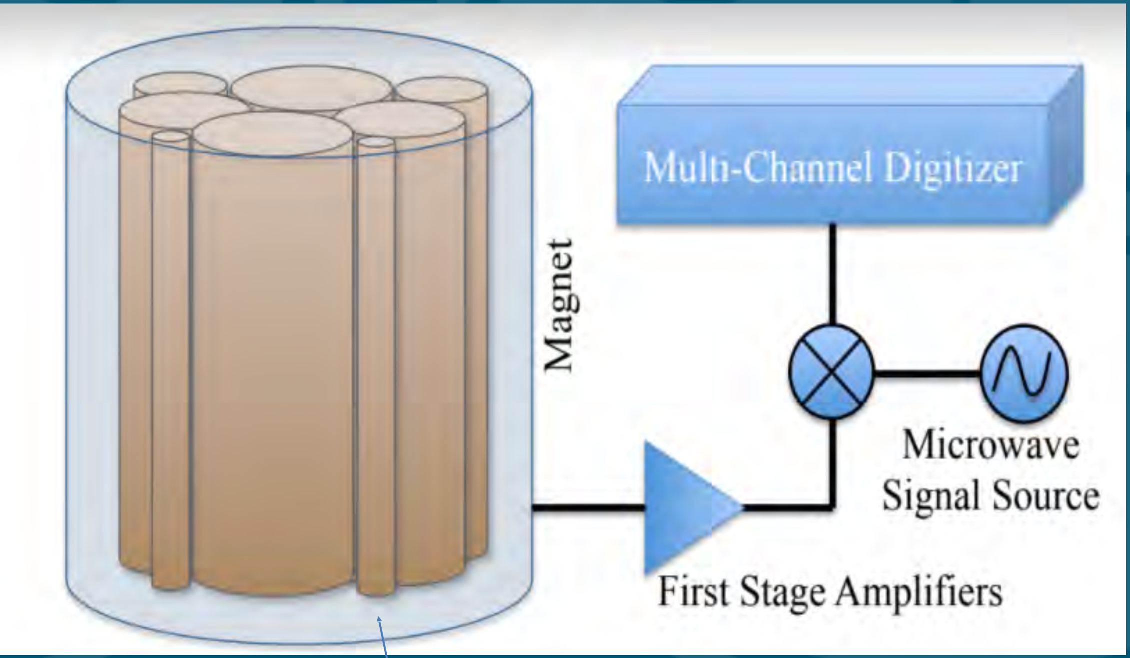

Multiple cylindrical resonators to scan over multiple frequencies

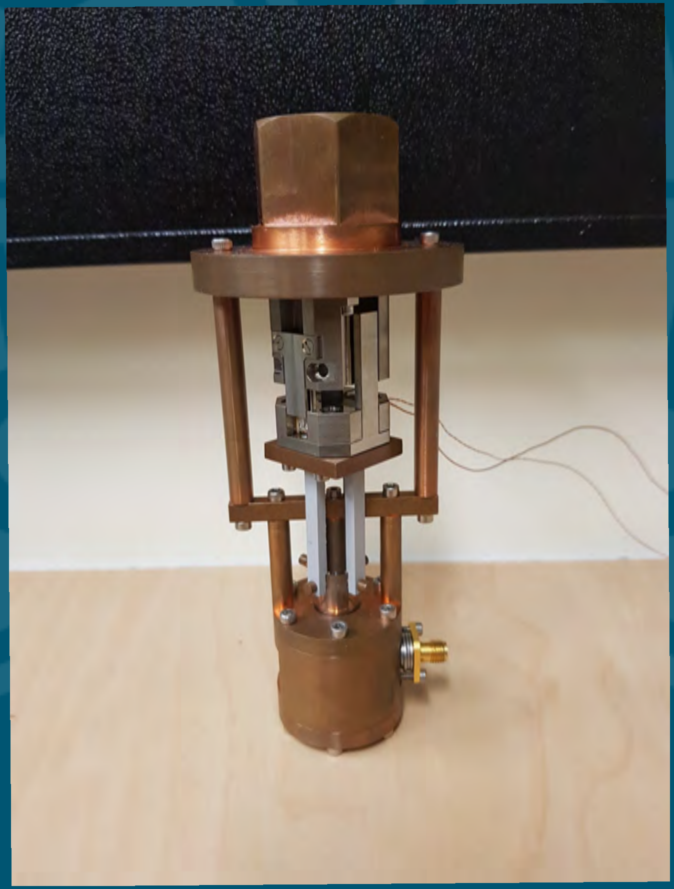

What is ORGAN?

- ORGAN compared to ADMX:
- 15 – 50 GHz rather than ~1 GHz
- 14 T smaller bore magnet rather than
- ~8 T custom magnet
- Been in construction/design phase
- Hosted at UWA
- Part of EQUS CoE program!

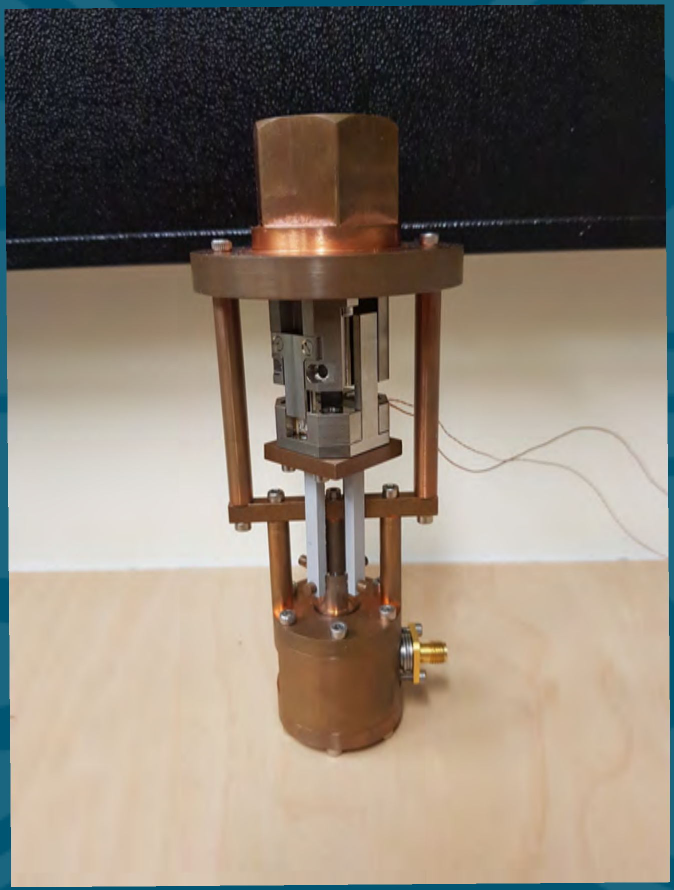

Who is ORGAN?

- Key UWA Personnel:
  - Michael Tobar
  - Ben McAllister
  - Maxim Goryachev
  - Jeremy Bourhill
  - Eugene Ivanov
  - Graeme Flower
  - Catriona Thomson

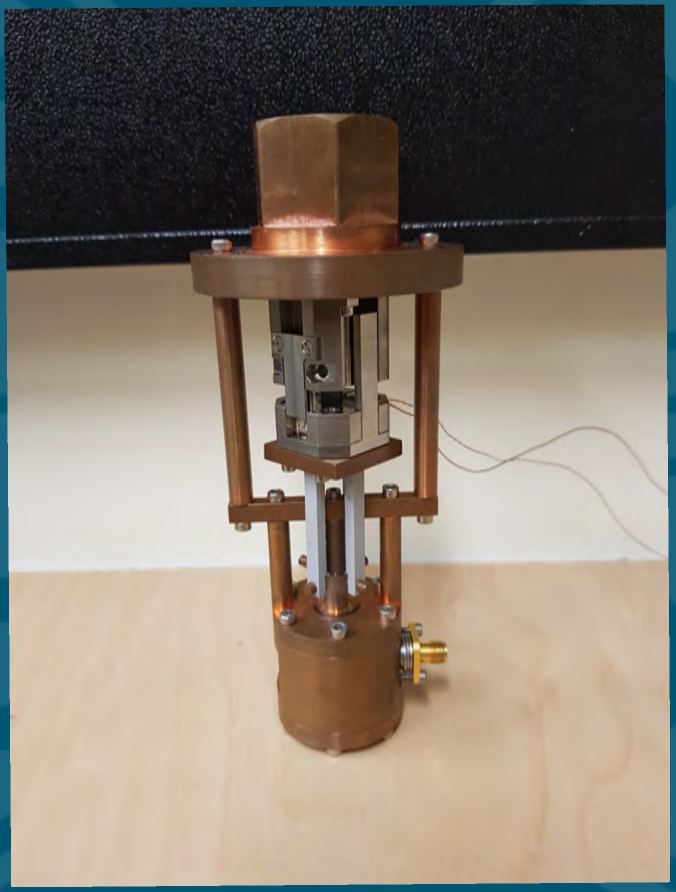

EQuS Collaborators

Number	Name	Participant Type	Current Organisation(s)	Relevant Organisation
1	Prof Michael Tobar	Chief Investigator	The University of Western Australia	The University of Western Australia
2	Dr Maxim Goryachev	Chief Investigator	The University of Western Australia	The University of Western Australia
3	Prof Eugene Ivanov	Chief Investigator	The University of Western Australia	The University of Western Australia
4	Dr Arkady Fedorov	Chief Investigator	The University of Queensland	The University of Queensland
5	Prof Warwick Bowen	Chief Investigator	The University of Queensland, The University of Queensland	The University of Queensland
6	Prof Michael Drinkwater	Chief Investigator	The University of Queensland	The University of Queensland
7	Dr Thomas Volz	Chief Investigator	Macquarie University	Macquarie University
8	A/Prof Gavin Brennen	Chief Investigator	Macquarie University	Macquarie University
9	Prof Jason Twamley	Chief Investigator	Macquarie University	Macquarie University
10	Dr Paul Altin	Chief Investigator	LIQUID INSTRUMENTS PTY. LTD., The Australian National University	The Australian National University
11	Prof Andrew Doherty	Chief Investigator	The University of Sydney	The University of Sydney

Buying Expensive item Can be a Problem 625,000 Euro

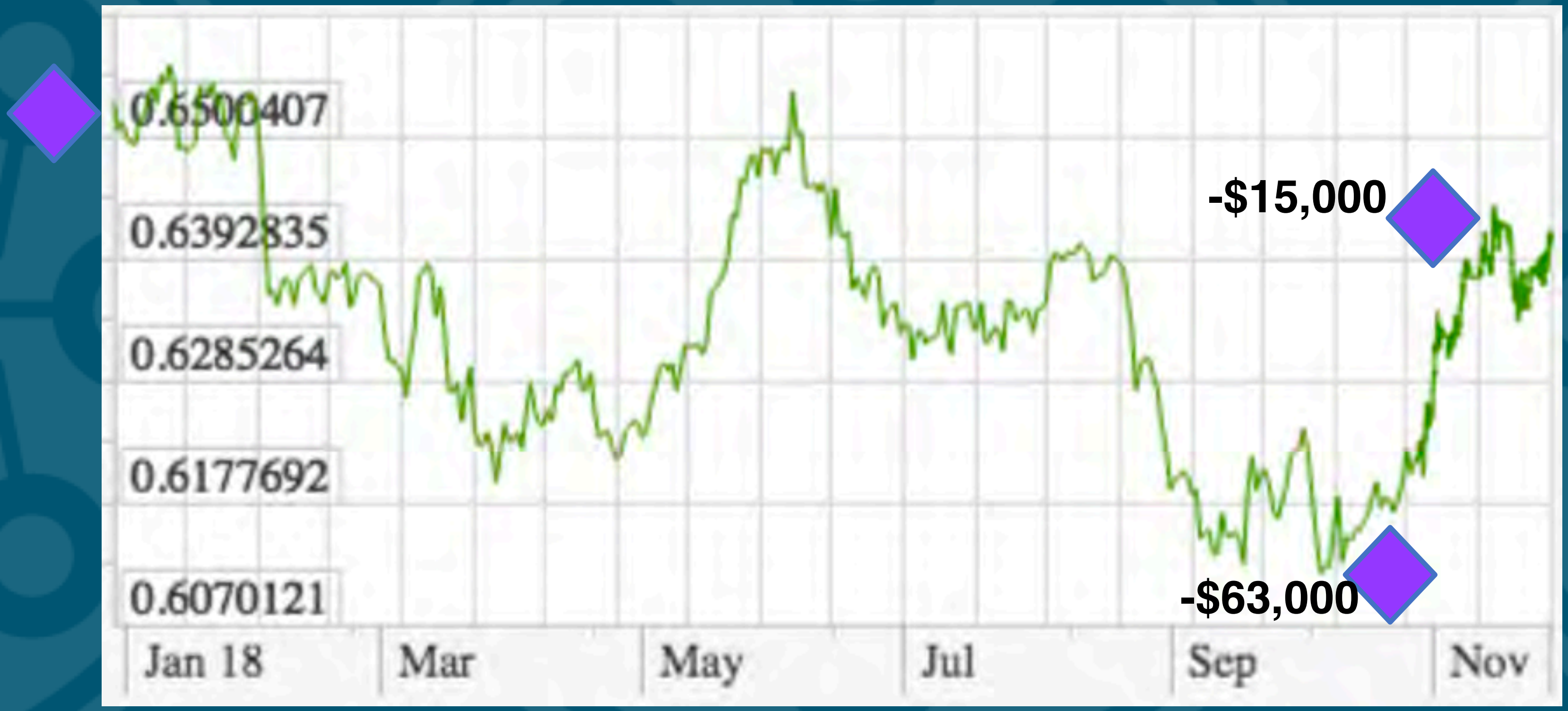

When is ORGAN?

- Now!
- Has been in development
- Path-finding run complete
- Time-line of long term operation:
  - Narrow search (26 – 27 GHz)
  - Wider search in 5 GHz chunks

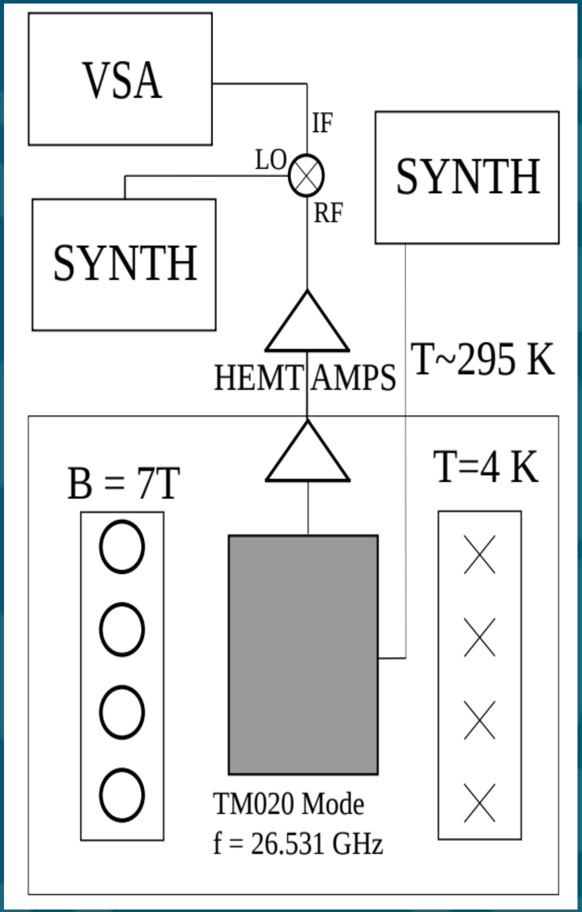

First Experiment

First run complete

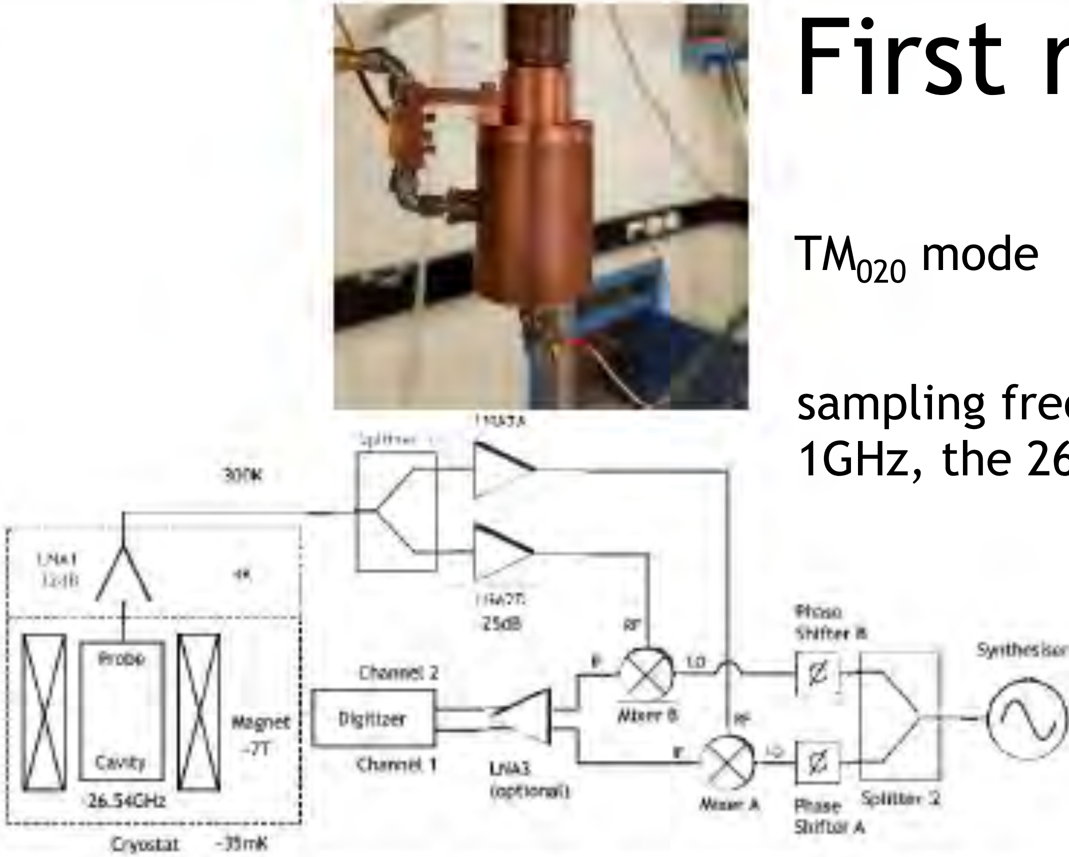

Figure 3.1: **ORGAN configuration.** The copper microwave cavity being used in the initial experiment (top) and a current ORGAN hardware diagram (bottom).

TM_{020} mode

sampling frequency of the digitizer is 1GHz, the 26.54GHz

Where is ORGAN?

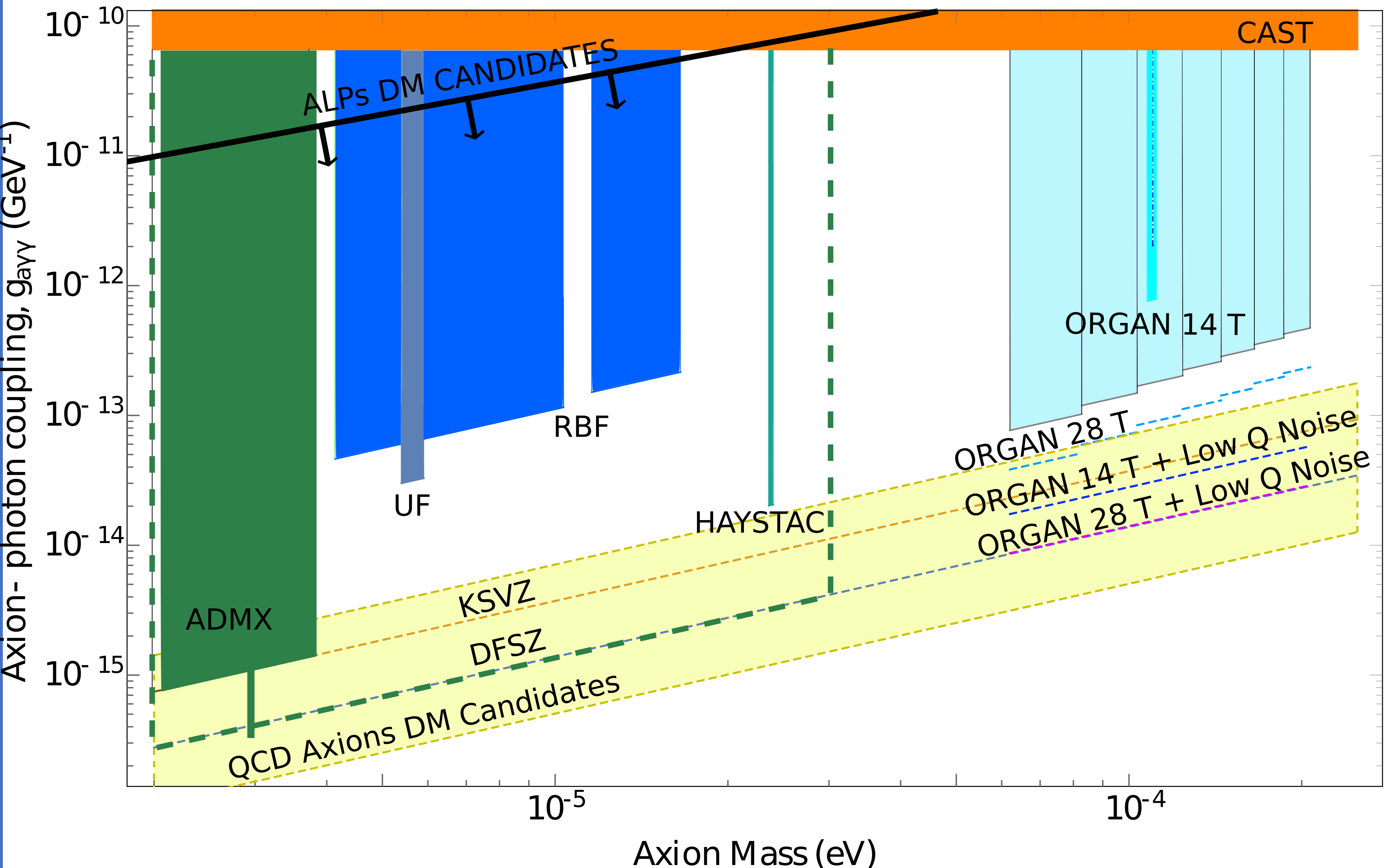

High Mass Haloscopes: Problems

- Signal power in axion haloscope

$$P_a \propto g_{a\gamma\gamma}^2 B^2 C V Q \frac{\wp_a}{m_a}$$

- Shows half of the problem
- High frequency:
  - Low volume for cavities
  - Lossier materials → Lower quality factor
  - Inverse dependence on axion mass
- SQL increases with frequency for amplifiers
- This is a big issue in the community

Form Factor

- Signal power in axion haloscope

$$P_a \propto g_{a\gamma\gamma}^2 B^2 C V Q \frac{\wp_a}{m_a}$$

$$C = \frac{\left| \int dV_c \vec{E}_c \cdot \vec{\hat{z}} \right|^2}{V \int dV_c \epsilon_r \mid E_c \mid^2}.$$

- Geometric integral
- Means we can only use specific modes

ORGAN Phase I and II: Resonator Design

- Think about ways to boost C, for example

$$C = \frac{\left|\int dV_c \vec{E}_c \cdot \vec{\hat{z}}\right|^2}{V \int dV_c \epsilon_r \mid E_c \mid^2}.$$

- Dielectric materials suppress electric field
- Reduce the electric field where there are out of phase field lobes
- We can Apply this to TM modes → Dielectric Rings
- Tuning mechanisms naturally included

ORGAN Phase I and II: Resonator Design

- TM_{030} mode E_z field looks like this:

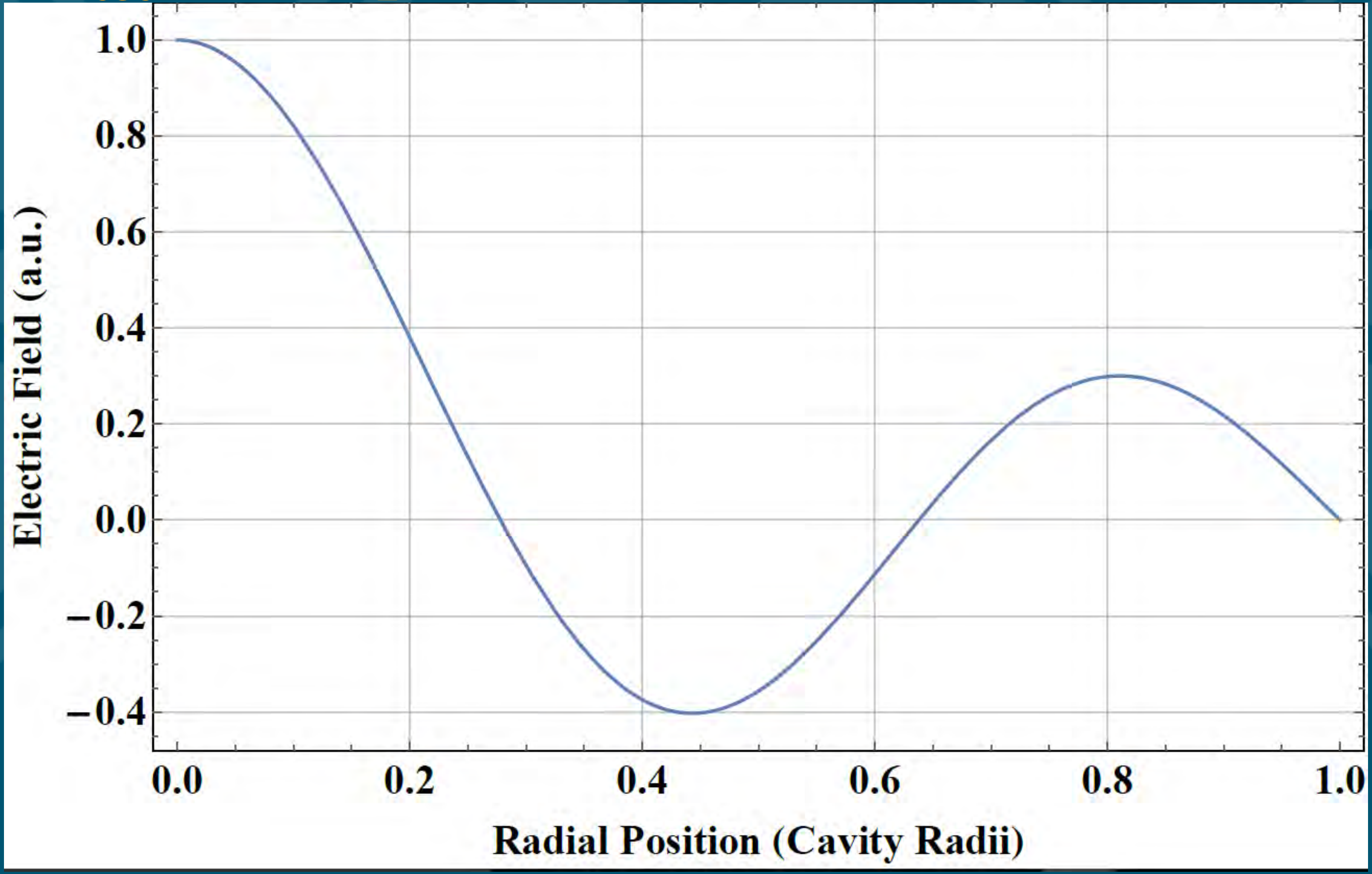

ORGAN Phase I and II: Resonator Design

- TM_{030} mode E_z field looks like this:

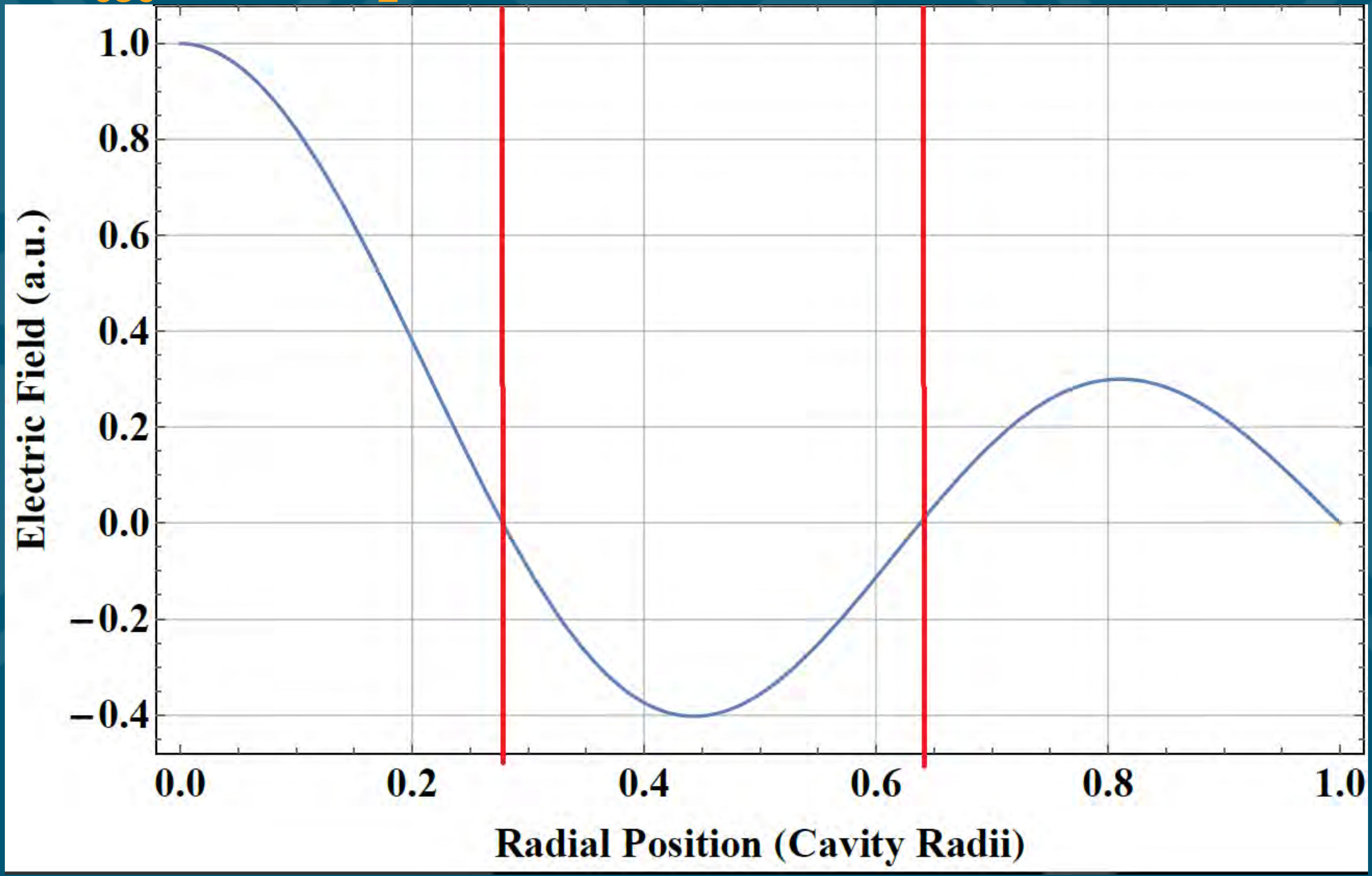

ORGAN Phase I and II: Resonator Design

- We can calculate where these things need to go
- E-field looks like:

$$\vec{E}_c(r) = E_0 \; e^{i\omega t} \; J_0(\frac{\zeta_{0,n}}{R} r) \; \hat{z}$$

- So, required thickness and location:

$$\frac{\zeta_{0,2} - \zeta_{0,1}}{\zeta_{0,3}\sqrt{\epsilon_r}} R$$

$$r = \frac{\zeta_{0,1}}{\zeta_{0,3}} R$$

ORGAN Phase I and II: Resonator Design

- If we do it right, we get this

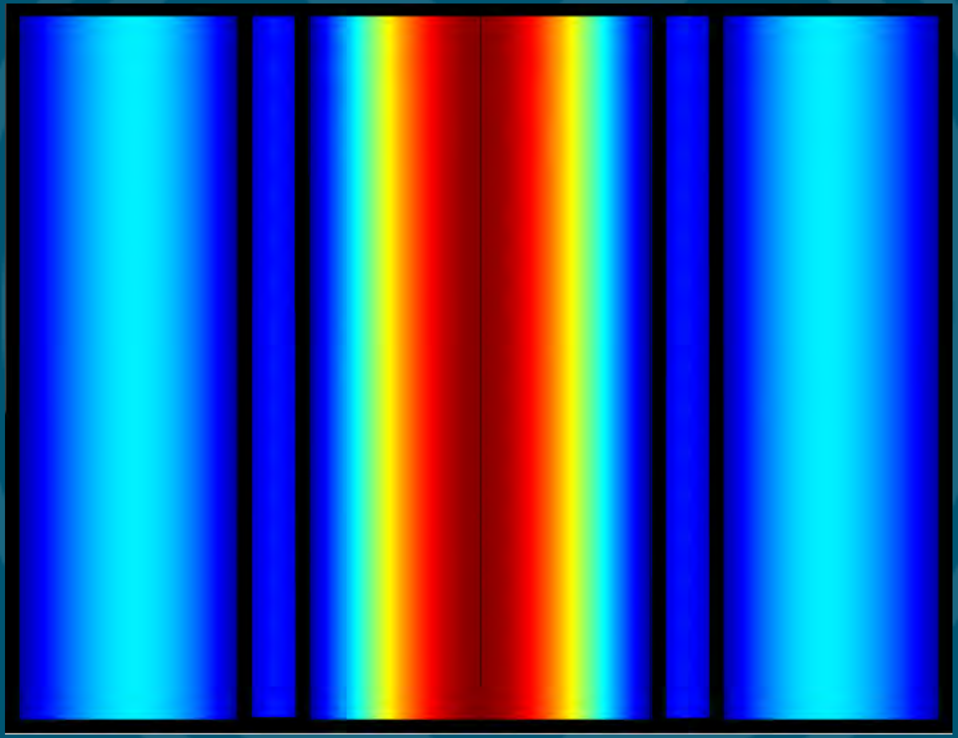

- Finite element simulations → Form factor ~0.45, improved from 0.053
- Can use higher order modes and maintain C while boosting V

ORGAN Phase I and II: Resonator Design

- Even better, we can tune this structure

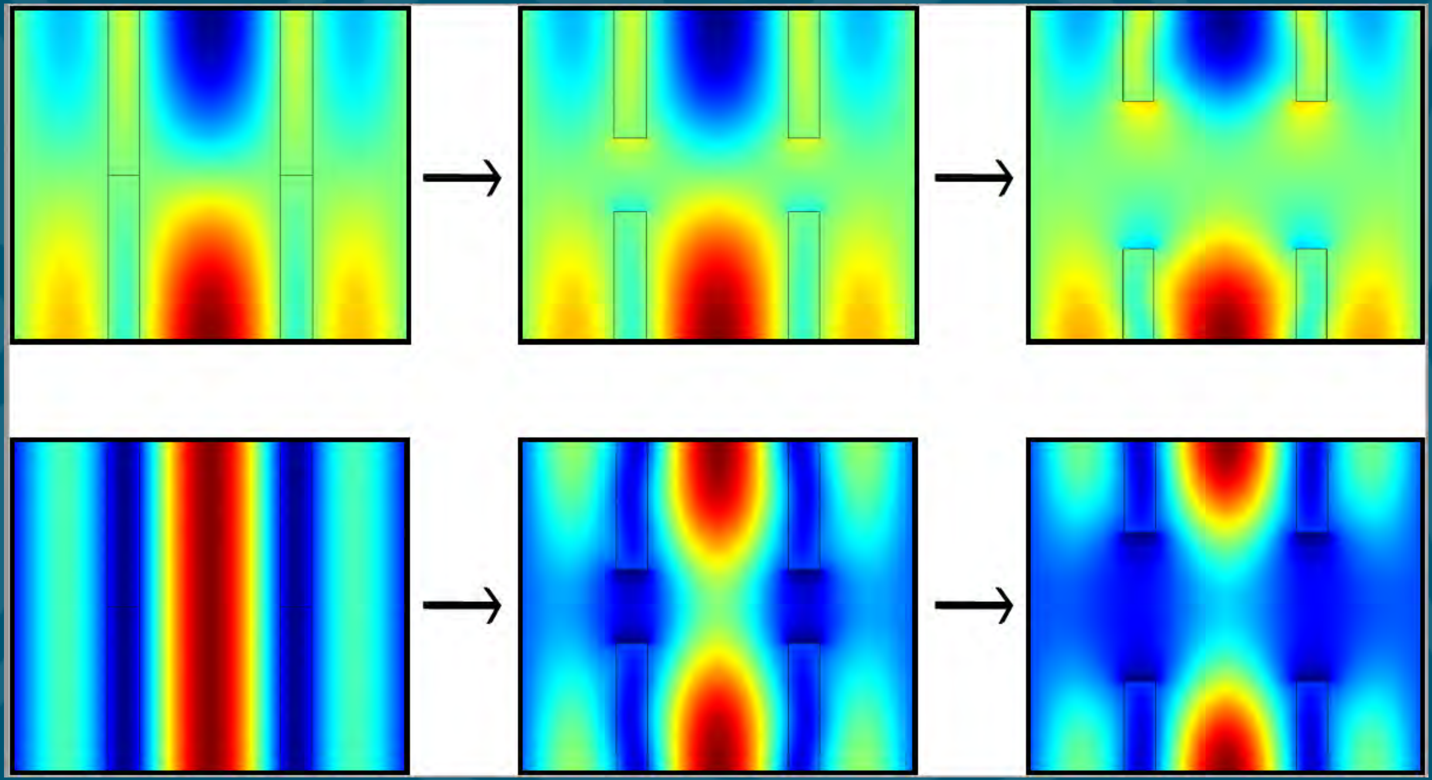

- TM_{030} and TM_{031} modes
- Axial "super-modes"

ORGAN Phase I and II: Resonator Design

- Most sensitive “symmetric super-mode” retains sensitivity as the gap increases
- Frequency tuning grater than 20% of central frequency

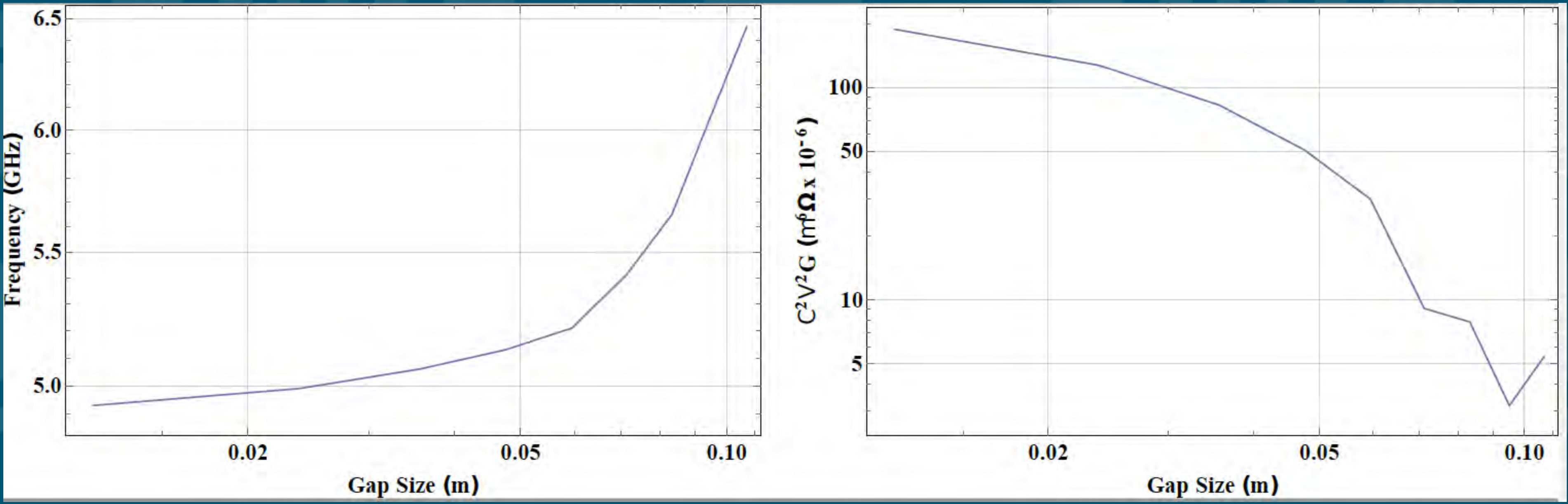

ORGAN Phase I and II: Resonator Design

- We can compare this with an “ADMX-style” tuning rod structure at the same frequency

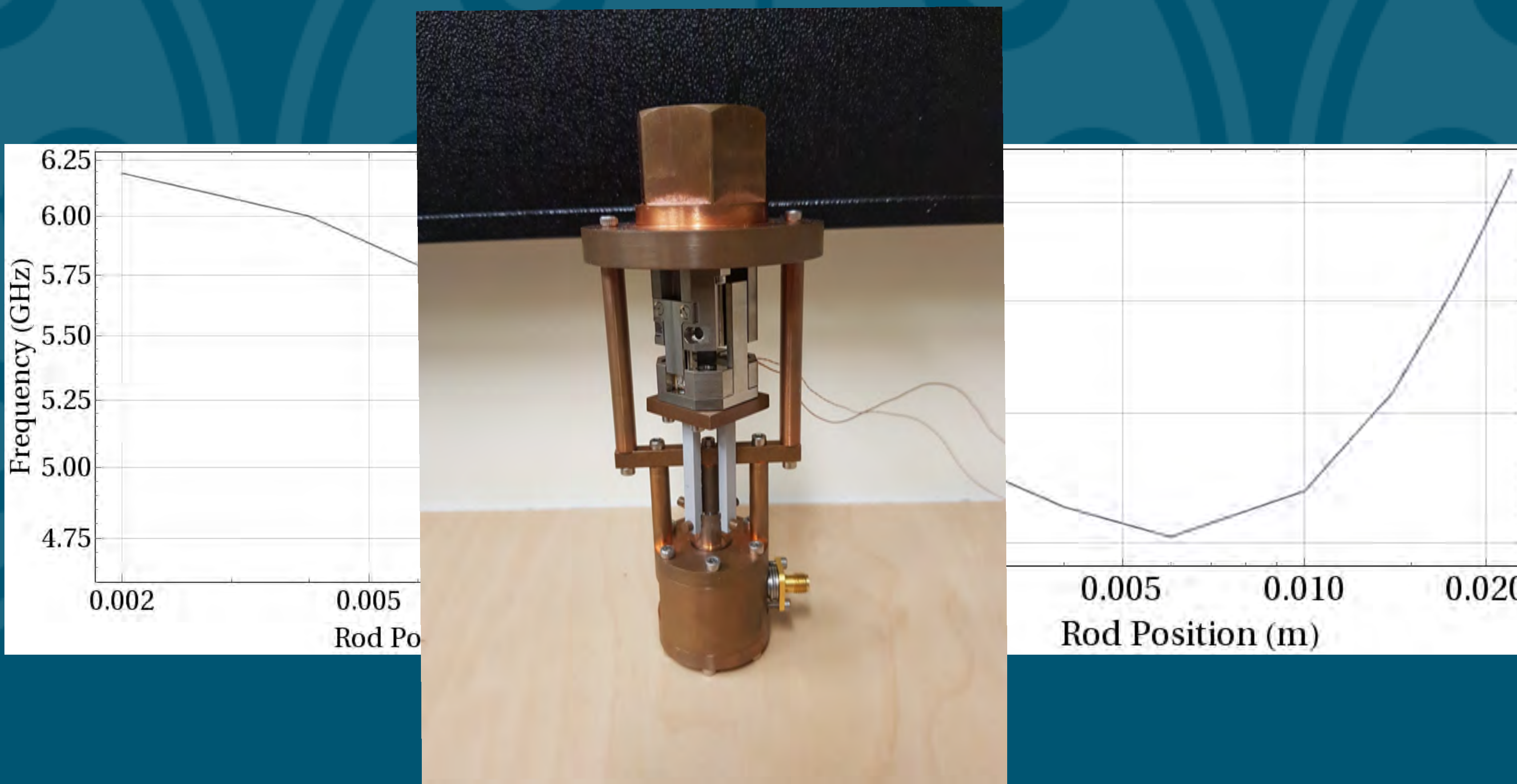

HYBRID QUANTUM SYSTEMS RESEARH WITH SPINS AND PHOTONS

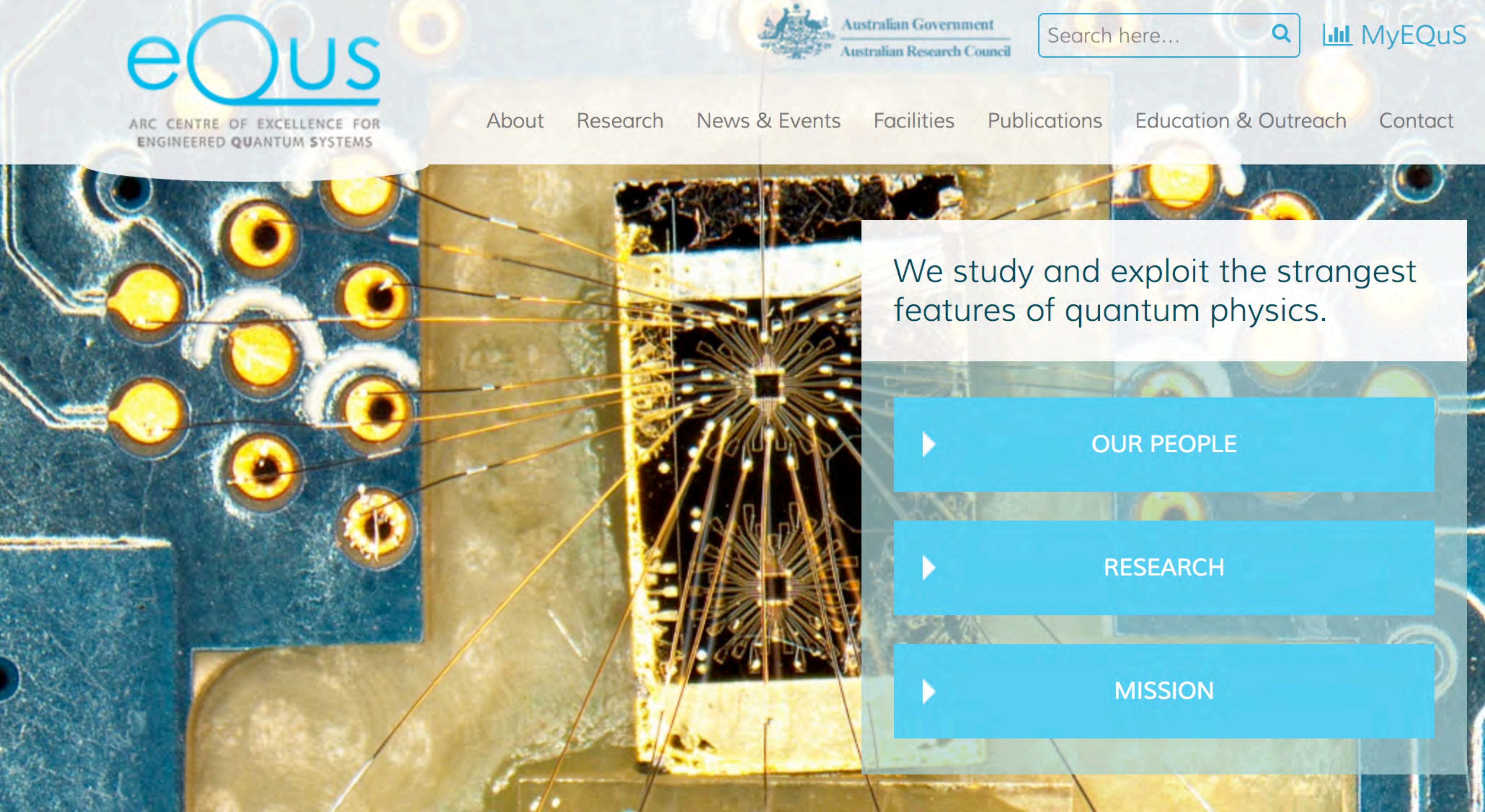

Types of Cavities:

WG Modes

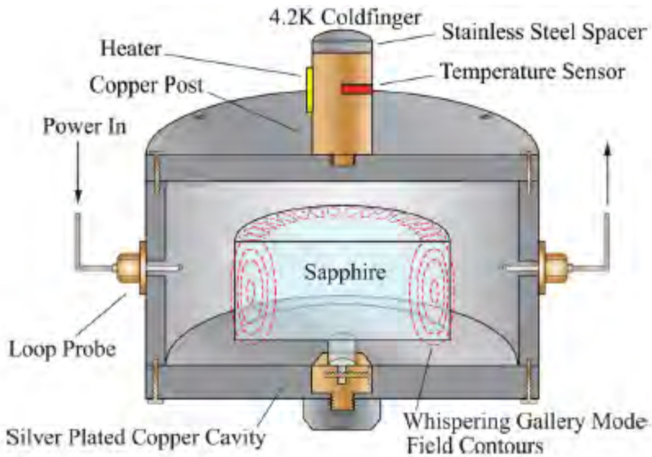

Reentrant Lattice

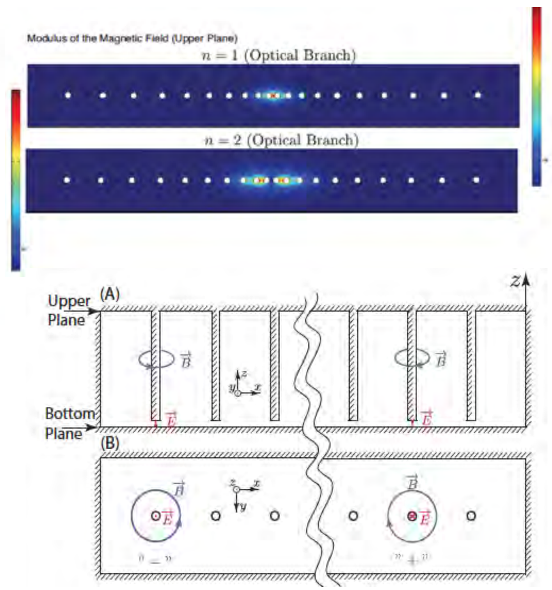

Reentrant

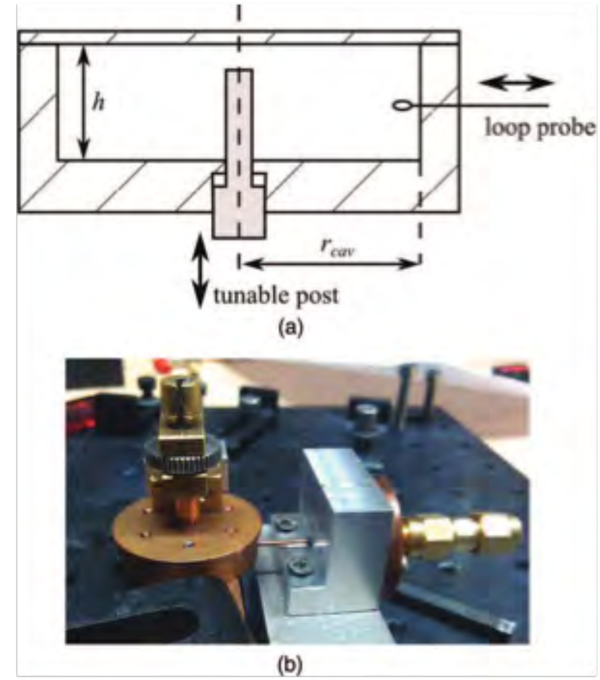

TE + TM Cylindrical modes

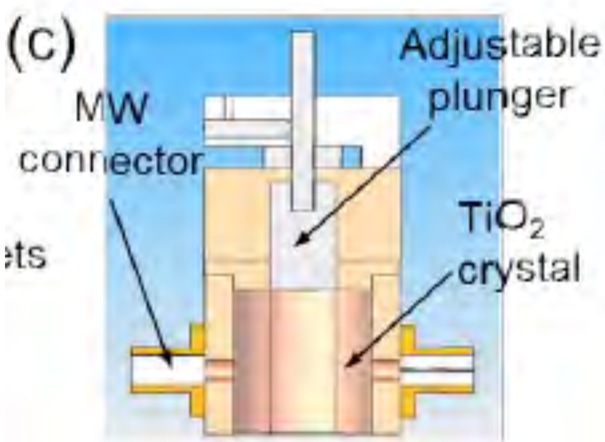

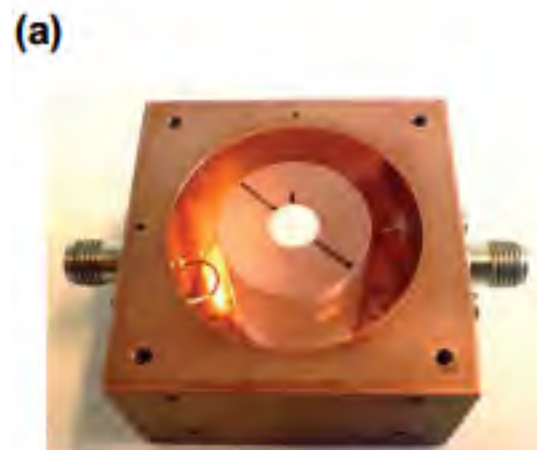

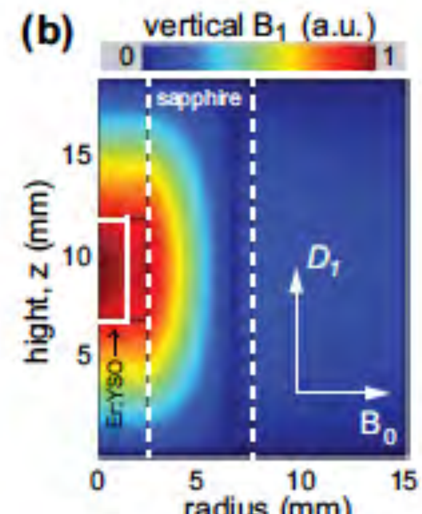

arXiv:1408.2905 [quant-ph] PHYSICAL REVIEW APPLIED **2,** 054002 (2014)

High-Cooperativity Cavity QED with Magnons at Microwave Frequencies

Maxim Goryachev,[1] Warrick G. Farr,[1] Daniel L. Creedon,[1] Yaohui Fan,[1] Mikhail Kostylev,[2] and Michael E. Tobar[1,*]
[1]*ARC Centre of Excellence for Engineered Quantum Systems, School of Physics, University of Western Australia, 35 Stirling Highway, Crawley, Western Australia, 6009, Australia*
[2]*Magnetisation Dynamics and Spintronics Group, School of Physics, University of Western Australia, 35 Stirling Highway, Crawley, Western Australia, 6009, Australia*
(Received 25 July 2014; revised manuscript received 10 October 2014; published 5 November 2014)

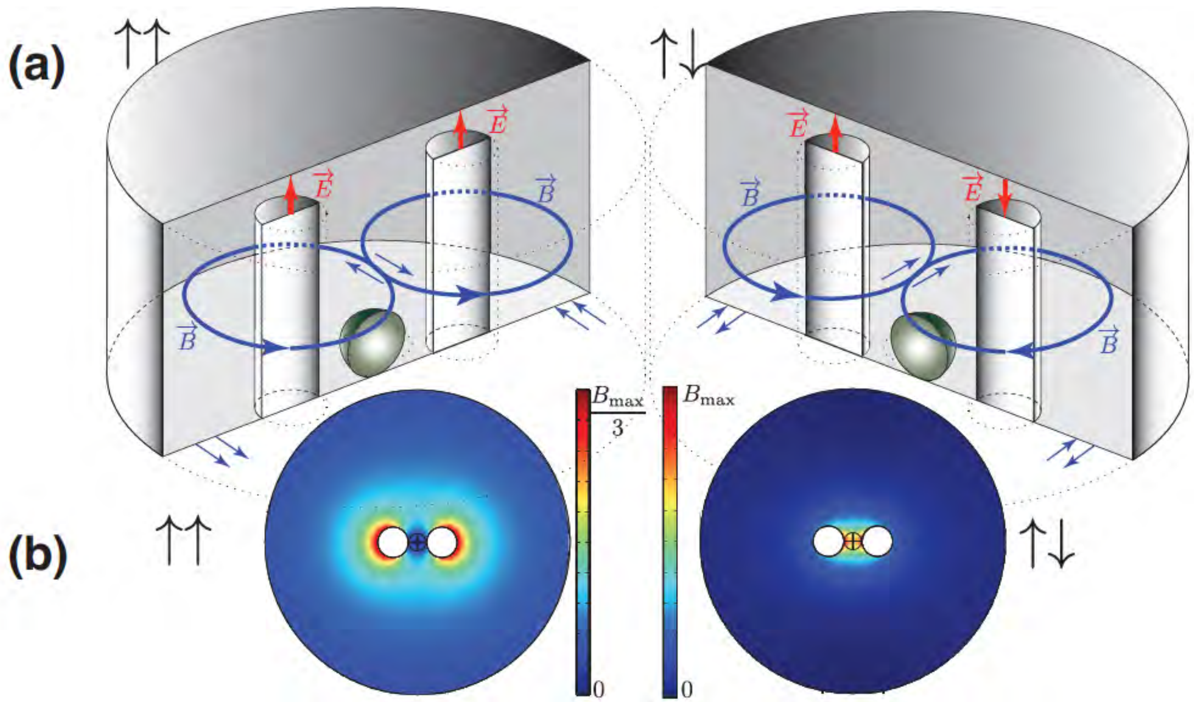

Goryachev and Tobar, 2014, Patent, PNo. AU2014,903,143

Magnons

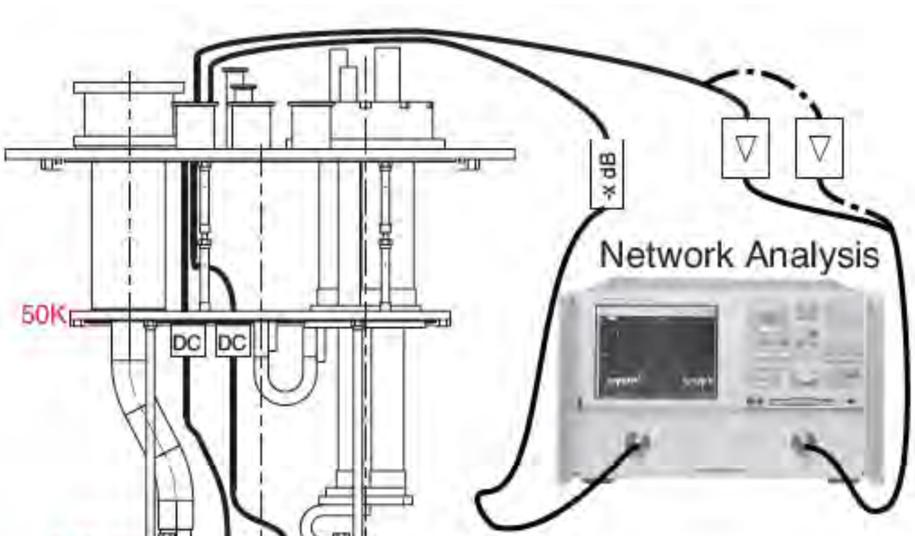

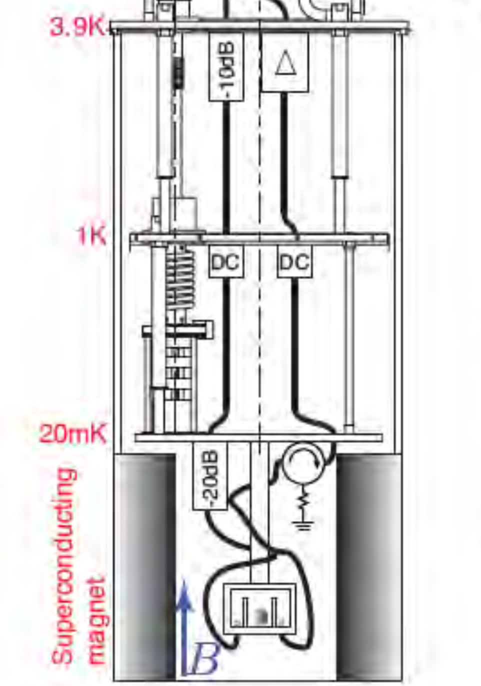

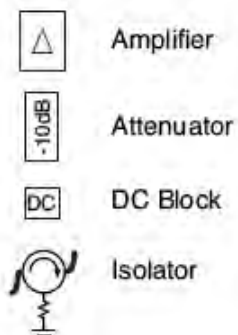

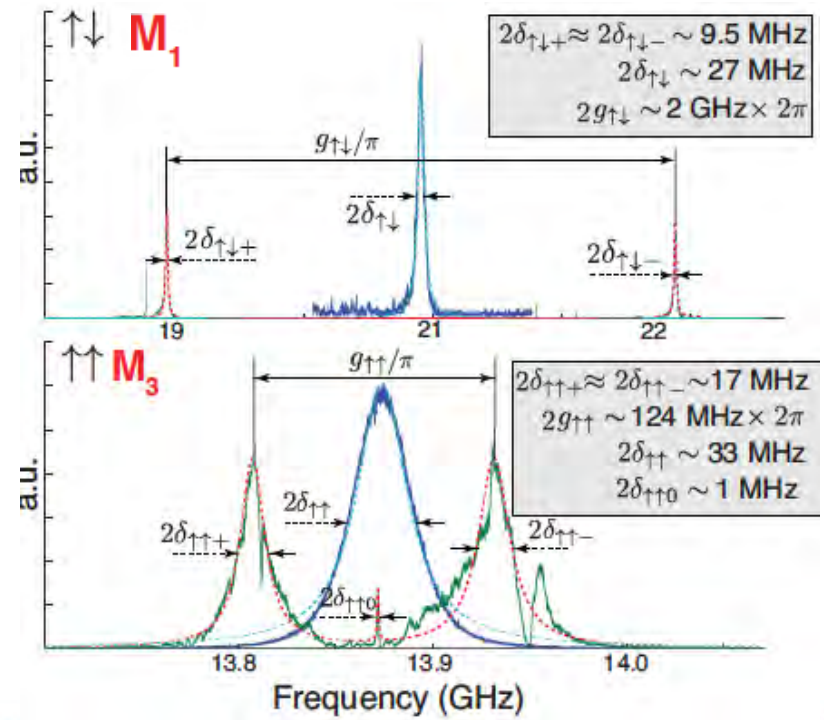

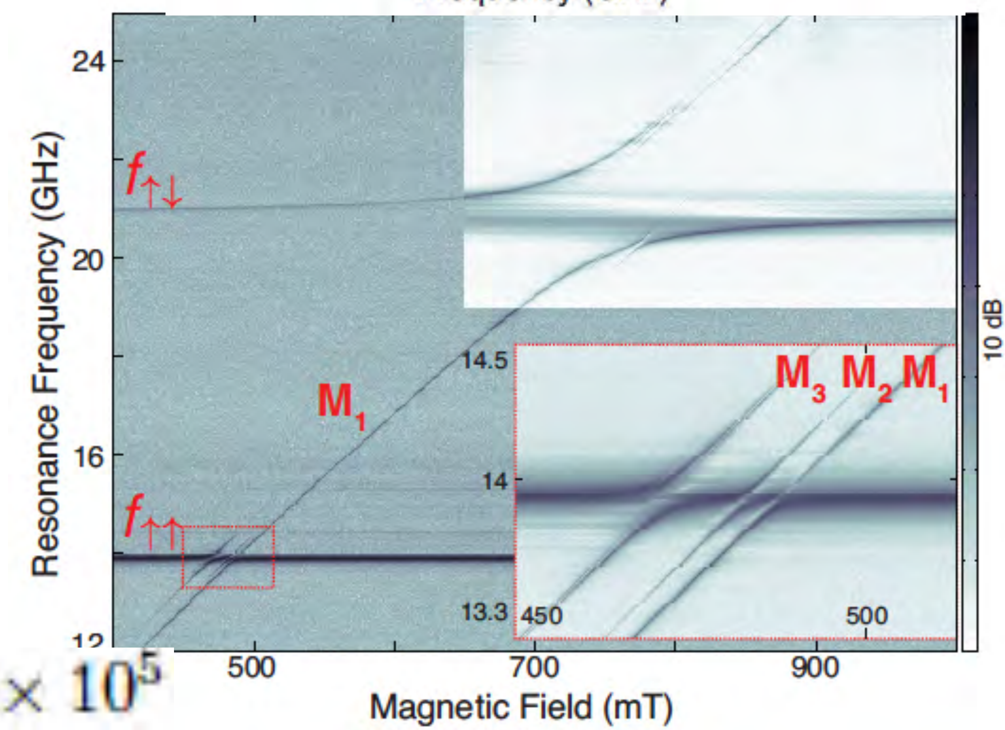

spin cooperativities $\frac{g^2_{\uparrow x}}{(\pi)^2 \gamma_M \gamma_{\uparrow x}}$

dark and bright 1.6×10^3 and 1.3×10^5

Axion Wind Detection with an Improved Ferromagnetic Haloscope

Graeme Flower, Jeremy Bourhill, Maxim Goryachev, Michael E. Tobar

(Submitted on 23 Nov 2018)

With the axion being a prime candidate for dark matter, there has been some recent interest in direct detection through a so called `Ferromagnetic haloscope.' Such devices exploit the coupling between axions and electrons in the form of collective spin excitations of magnetic materials with readout through a microwave cavity. Here, we present a new, more general, theoretical treatment of such experiments in a Hamiltonian framework with coupled magnons and photons. In particular, this opens up the possibility of operating this experiment in the dispersive regime which allows easy searching of the axion mass parameter space. This experiment is implemented in a cryogenic setup, and initial results are presented setting first laboratory limits on the axion-electron coupling strength of $g_{a\gamma\gamma} > 3.7 \times 10^{-9}$ in the range $33.79\mu\text{eV} < m_a < 33.94\mu\text{eV}$ with 95% confidence. Future improvements and requirements to reach the DFSZ axion model are further discussed.

Comments: 10 pages, 5 figures
Subjects: **Instrumentation and Detectors (physics.ins-det)**
Cite as: arXiv:1811.09348 **[physics.ins-det]**
(or **arXiv:1811.09348v1 [physics.ins-det]** for this version)

Submission history

From: Graeme Flower [view email]
[v1] Fri, 23 Nov 2018 03:02:42 UTC (1,459 KB)

Cavity-Magnon polaritons

$$\frac{H}{\hbar} = \omega_c a^\dagger a + \omega_m b^\dagger b + g_{cm}(a^\dagger + a)(b^\dagger + b)$$

Photons — Magnons — Interaction

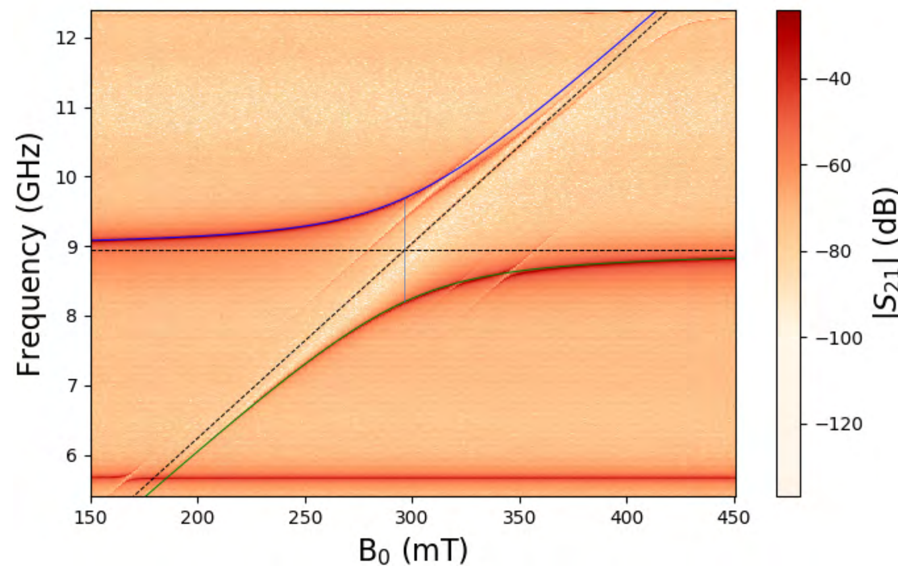

$$\omega_\pm = \frac{\omega_c + \omega_m}{2} \pm \sqrt{(\frac{\omega_m - \omega_c}{2})^2 + g_{cm}^2}$$

First results

36MHz in 6 MHz blocks from 8hrs of averages

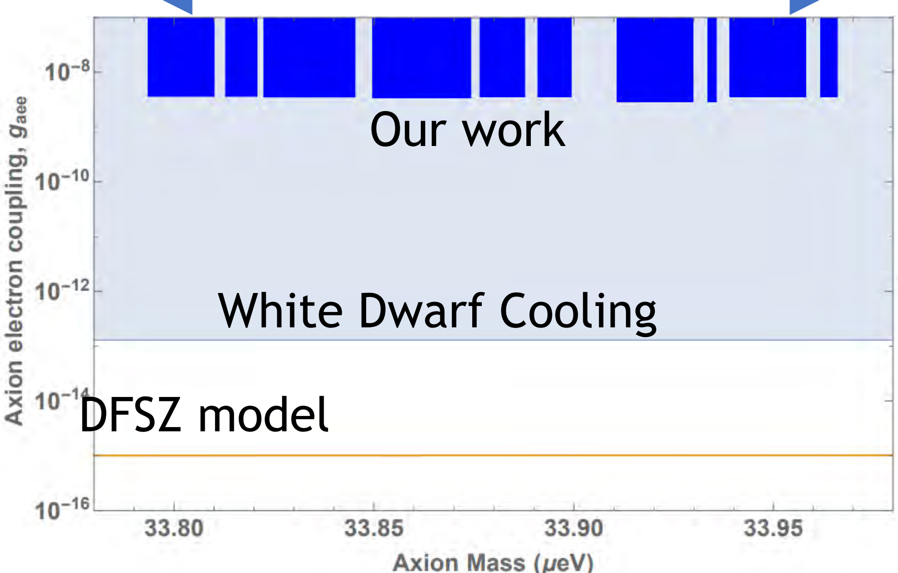

Centred at 8.2GHz

3MHz static range 7x6hrs of averages

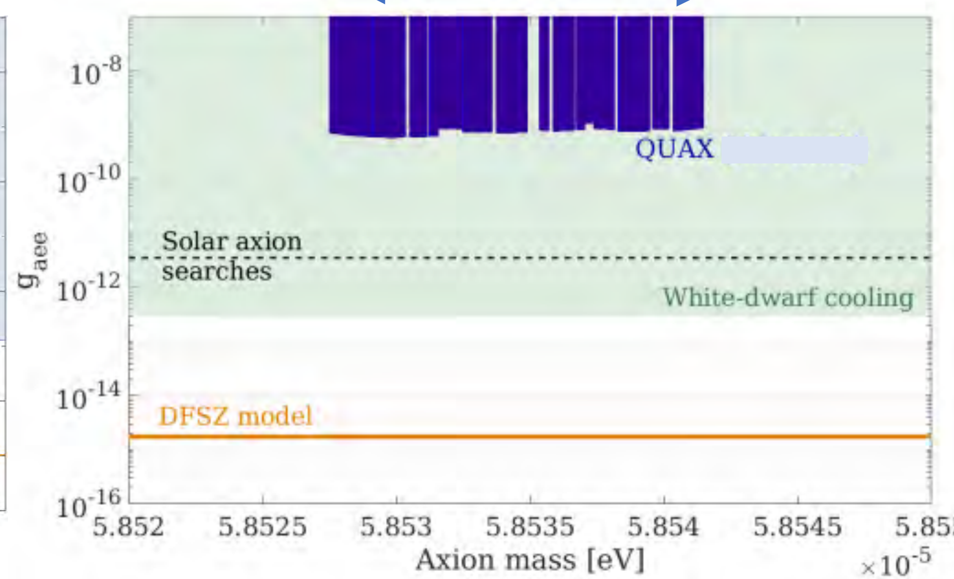

Centred at 14GHz

Axion Detection with Precision Frequency Metrology

THE UNIVERSITY OF WESTERN AUSTRALIA

Maxim Goryachev
Ben McAllister
Mike Tobar

EQU
Australian Research Co
Centre of Excellence f

System for Axion Detection

photonic cavity with two mutually orthogonal modes

optical or microwave

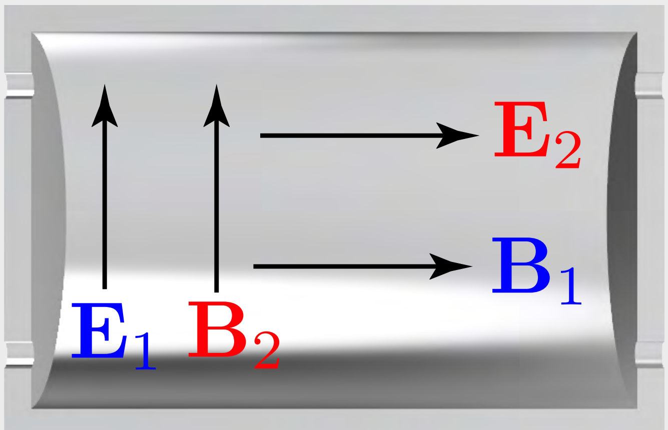

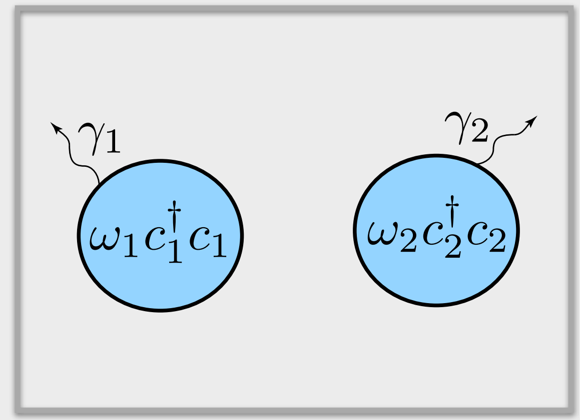

Axion Electrodynamics

$$\mathcal{L} = \frac{1}{2}(\partial_\mu a)^2 - \frac{1}{2}{m_a}^2 a^2 - \frac{1}{4}F_{\mu\nu}F^{\mu\nu} + \frac{1}{4}g_{a\gamma\gamma}aF_{\mu\nu}\tilde{F}^{\mu\nu}$$

Hamiltonian Density

$$\mathcal{H} = \mathcal{H}_{\mathrm{EM}} + \mathcal{H}_a + \mathcal{H}_{\mathrm{int}}$$

$$\mathcal{H}_{\mathrm{EM}} = \frac{\varepsilon_0}{2}\left[\mathbf{E}^2 + c^2\mathbf{B}^2\right]$$

normal ED

$$\mathcal{H}_{\mathrm{a}} = \frac{\phi^2}{2m_a} + V(\theta)$$

axion

$$\mathcal{H}_{\mathrm{int}} = \varepsilon_0 c g_{a\gamma\gamma}\theta\ \mathbf{E}\cdot\mathbf{B}$$

interaction

EQUS Australian Research Council Centre of Excellence for Engineered Quantum Systems

arXiv:1806.07141

System for Axion Detection

photonic cavity with two mutually orthogonal modes

optical or microwave

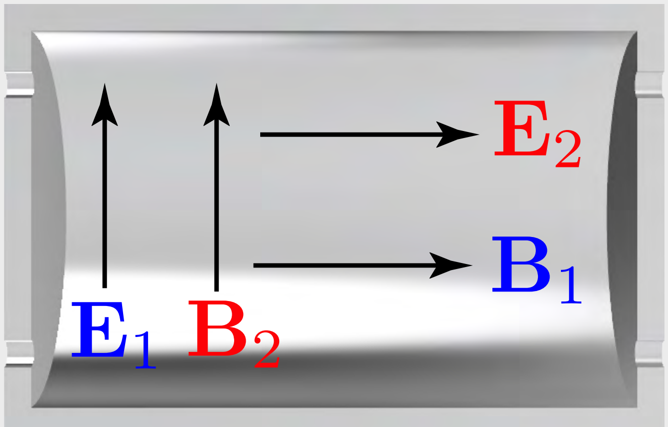

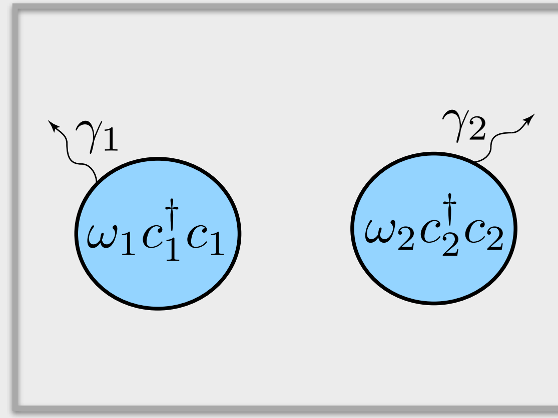

Axion Electrodynamics

$$\mathcal{L} = \frac{1}{2}(\partial_\mu a)^2 - \frac{1}{2}{m_a}^2 a^2 - \frac{1}{4}F_{\mu\nu}F^{\mu\nu} + \frac{1}{4}g_{a\gamma\gamma}aF_{\mu\nu}\tilde{F}^{\mu\nu}$$

Hamiltonian Density

$$\mathcal{H} = \mathcal{H}_{\text{EM}} + \mathcal{H}_a + \mathcal{H}_{\text{int}}$$

$$\mathcal{H}_{\text{EM}} = \frac{\varepsilon_0}{2}\left[\mathbf{E}^2 + c^2\mathbf{B}^2\right]$$

normal ED

$$\mathcal{H}_{\text{a}} = \frac{\phi^2}{2m_a} + V(\theta)$$

axion

$$\mathcal{H}_{\text{int}} = \varepsilon_0 c g_{a\gamma\gamma}\theta\ \mathbf{E}\cdot\mathbf{B}$$

interaction

EQUS
Australian Research Council Centre of Excellence for Engineered Quantum Systems

arXiv:1806.07141

Axion Mediated Mode-Mode Interaction

based on axion Electrodynamics we derive axion induced coupling between two cavity modes

$$H_{\text{int}} = i\hbar g_{\text{eff}}\theta\left[\xi_-(c_1c_2^\dagger - c_1^\dagger c_2) + \xi_+(c_1^\dagger c_2^\dagger - c_1c_2)\right]$$

Dimensionless Orthogonality Form Factors

$$\xi_1 = \frac{1}{\sqrt{V_1V_2}}\int_V d^3r(\mathbf{e}_1\cdot\mathbf{b}_2),$$

$$\xi_2 = \frac{1}{\sqrt{V_1V_2}}\int_V d^3r(\mathbf{e}_2\cdot\mathbf{b}_1).$$

$$\xi_\pm = \xi_1 \pm \xi_2$$

Effective Coupling

$$g_{\text{eff}} = \frac{g_{a\gamma\gamma}}{2}\sqrt{\omega_1\omega_2}$$

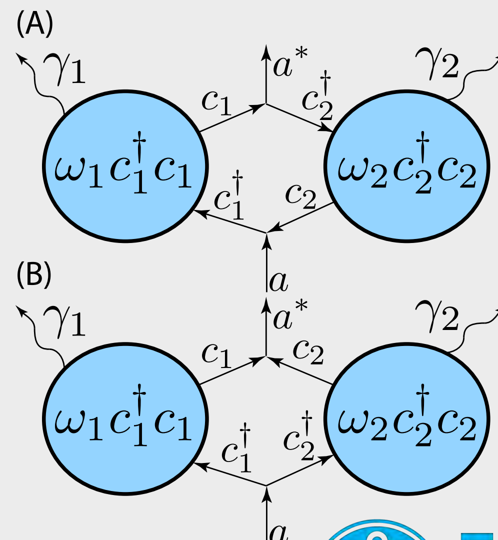

Rotating Wave Approximation

allows optical search at microwaves and mm-wave

Axion UpConversion

$$\omega_a = \omega_2 - \omega_1$$

$$H_{\text{U}} = i\hbar g_{\text{eff}}\xi_-(a^*c_1c_2^\dagger - ac_1^\dagger c_2)$$

beam splitter

allows microwave search at mm-wave

Axion DownConversion

$$\omega_a = \omega_2 + \omega_1$$

$$H_{\text{D}} = i\hbar g_{\text{eff}}\xi_+(ac_1^\dagger c_2^\dagger - a^*c_1c_2)$$

parametric amplification

arXiv:1806.07141

EQUS Australian Research Council Centre of Excellence for Engineered Quantum Systems

Axion Mediated Mode-Mode Interaction

$$H_{\mathrm{U}} = i\hbar g_{\mathrm{eff}}\xi_{-}(a^{*}c_{1}c_{2}^{\dagger} - ac_{1}^{\dagger}c_{2})$$

beam splitter

$$H_{\mathrm{D}} = i\hbar g_{\mathrm{eff}}\xi_{+}(ac_{1}^{\dagger}c_{2}^{\dagger} - a^{*}c_{1}c_{2})$$

parametric amplification

Experimental Approaches

arXiv:1806.07141

Axion Mediated Mode-Mode Interaction

$$H_{\mathrm{U}} = i\hbar g_{\mathrm{eff}}\xi_{-}(a^{*}c_{1}c_{2}^{\dagger} - ac_{1}^{\dagger}c_{2})$$

beam splitter

$$H_{\mathrm{D}} = i\hbar g_{\mathrm{eff}}\xi_{+}(ac_{1}^{\dagger}c_{2}^{\dagger} - a^{*}c_{1}c_{2})$$

parametric amplification

Experimental Approaches

Power Detection

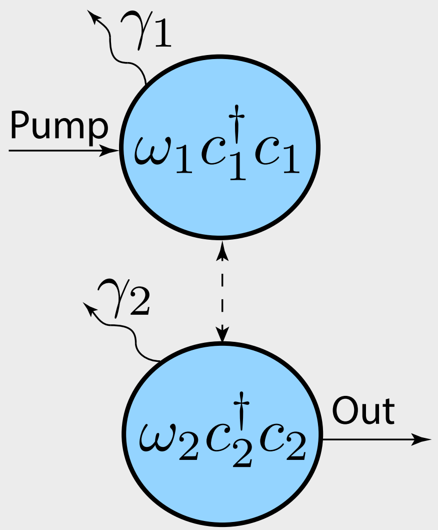

P. Sikivie: arXiv:1009.0762

EQUS Australian Research Council Centre of Excellence for Engineered Quantum Systems

arXiv:1806.07141

Axion Mediated Mode-Mode Interaction

$$H_{\rm U} = i\hbar g_{\rm eff}\xi_{-}(a^{*}c_1c_2^{\dagger} - ac_1^{\dagger}c_2)$$

beam splitter

$$H_{\rm D} = i\hbar g_{\rm eff}\xi_{+}(ac_1^{\dagger}c_2^{\dagger} - a^{*}c_1c_2)$$

parametric amplification

Experimental Approaches

Power Detection

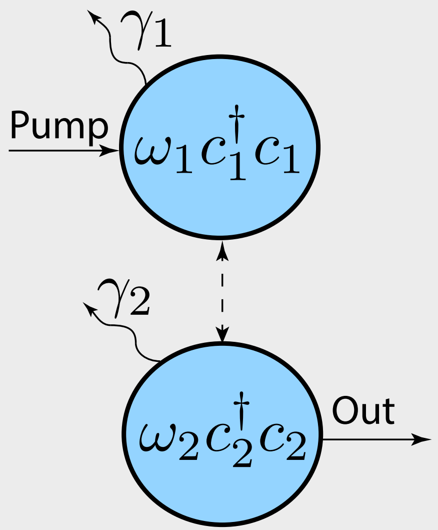

P. Sikivie: arXiv:1009.0762

Cross Correlation

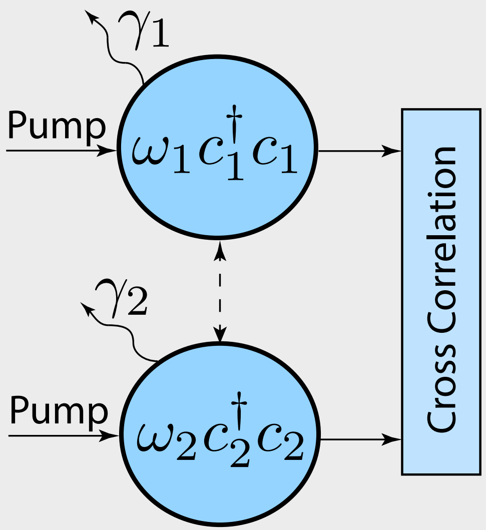

arXiv:1806.07141

EQUS Australian Research Council Centre of Excellence for Engineered Quantum Systems

Axion Mediated Mode-Mode Interaction

$$H_{\rm U} = i\hbar g_{\rm eff}\xi_-(a^* c_1 c_2^\dagger - a c_1^\dagger c_2)$$

beam splitter

$$H_{\rm D} = i\hbar g_{\rm eff}\xi_+(a c_1^\dagger c_2^\dagger - a^* c_1 c_2)$$

parametric amplification

Experimental Approaches

Power Detection

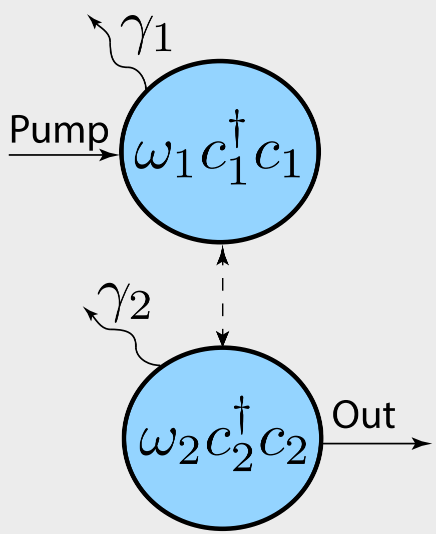

P. Sikivie: arXiv:1009.0762

Cross Correlation

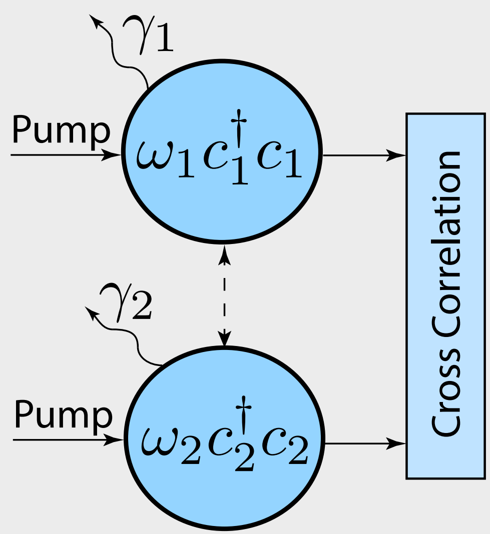

Eigenfrequency Shift

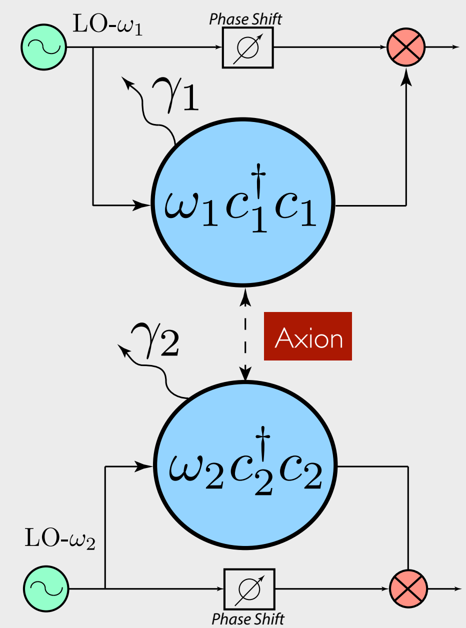

EQUS
Australian Research Council Centre of Excellence for Engineered Quantum Systems

arXiv:1806.07141

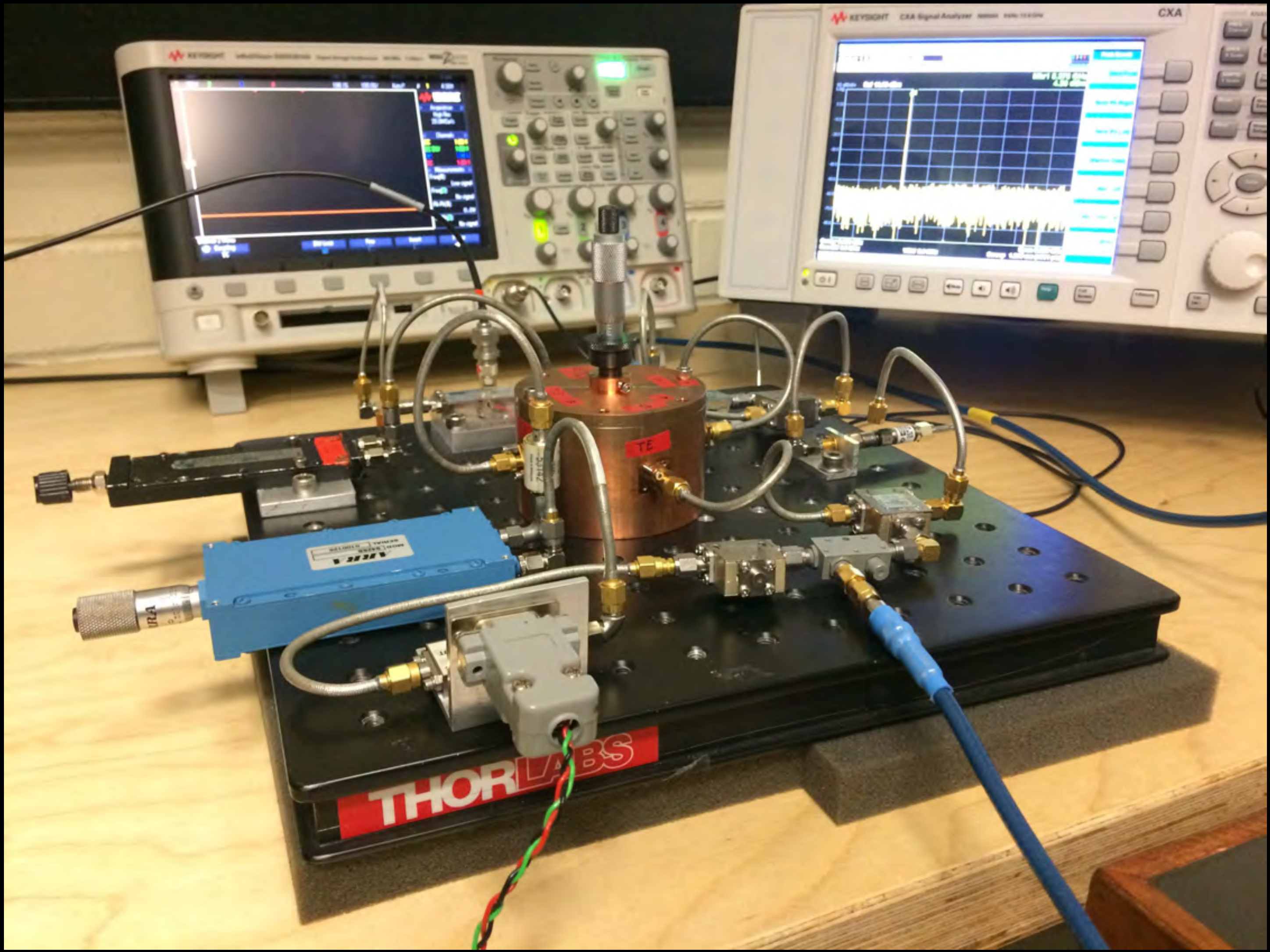
CXA
TE
THORLABS

Design of Cavity

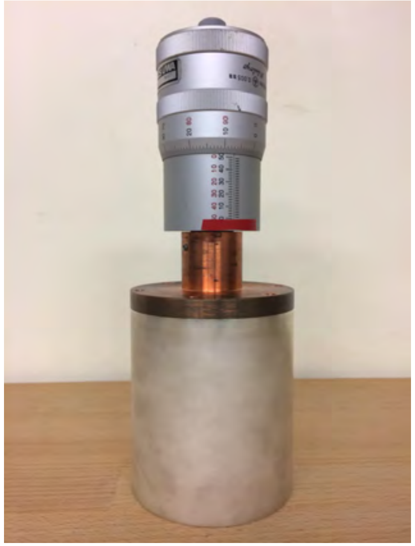

$$\omega_{\mathrm{TM}} = \sqrt{\left(\frac{\varsigma_{m,n}}{R}\right)^2 + \left(\frac{p\pi}{L}\right)^2}\, c \qquad \omega_{\mathrm{TE}} = \sqrt{\left(\frac{\varsigma'_{m,n}}{R}\right)^2 + \left(\frac{p\pi}{L}\right)^2}\, c$$

FREQUENCY DOMAIN AND TUNABILITY

- **Tunable cavity height (lid attached to micrometer)**
- **TM020 mode frequency <u>fixed</u> by cavity radius**

Design of Cavity

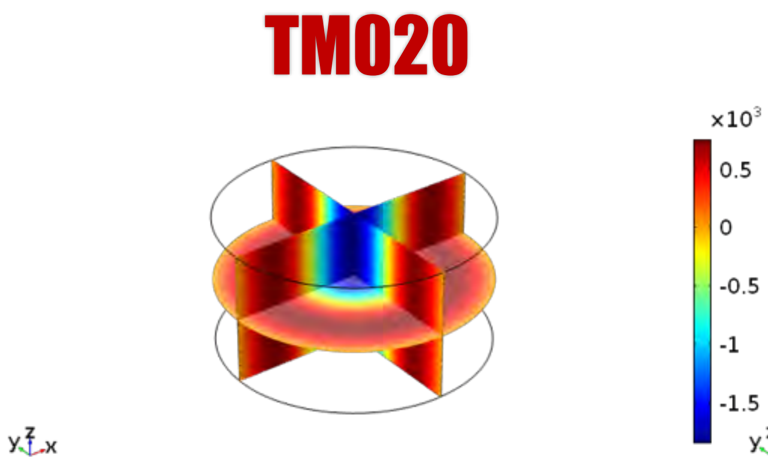

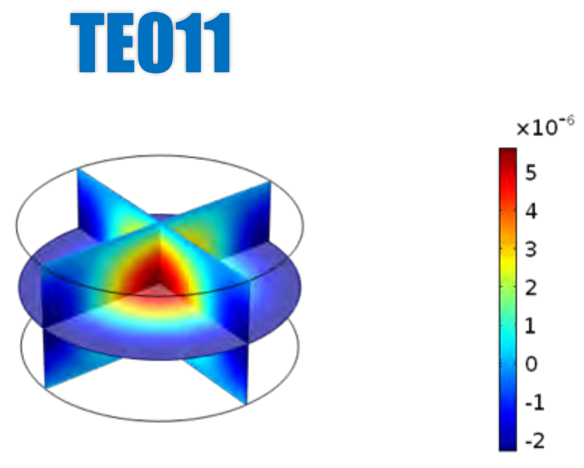

Frequency Space

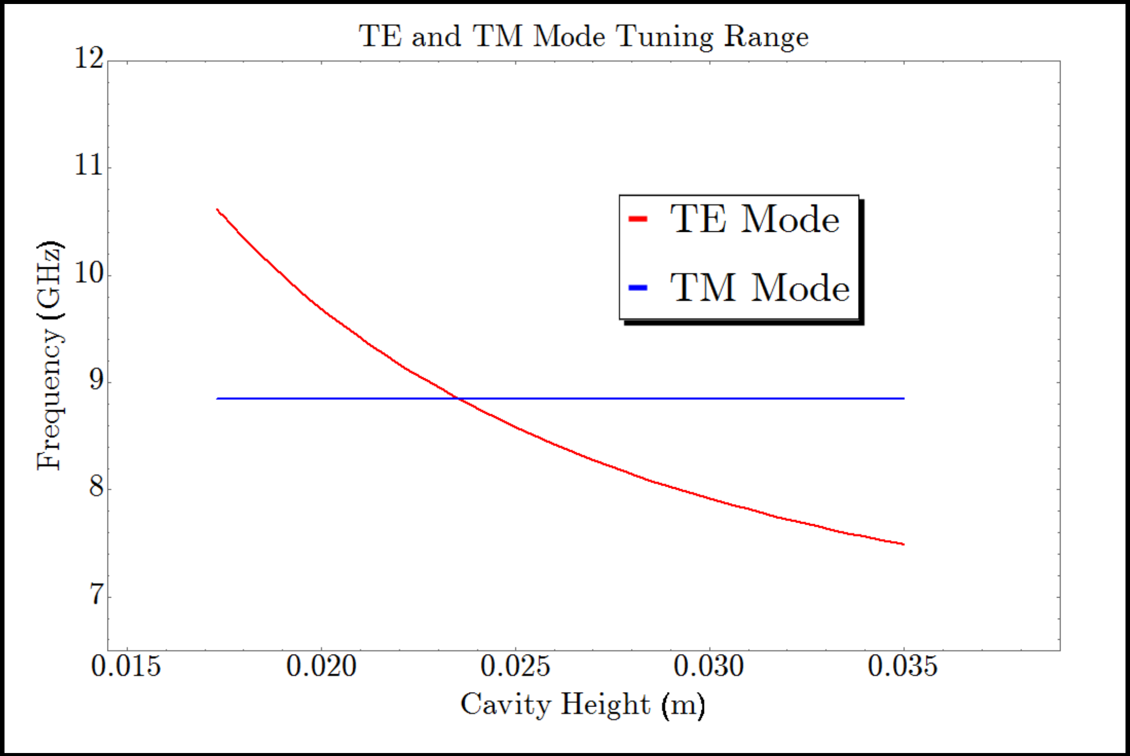

Frequency Space

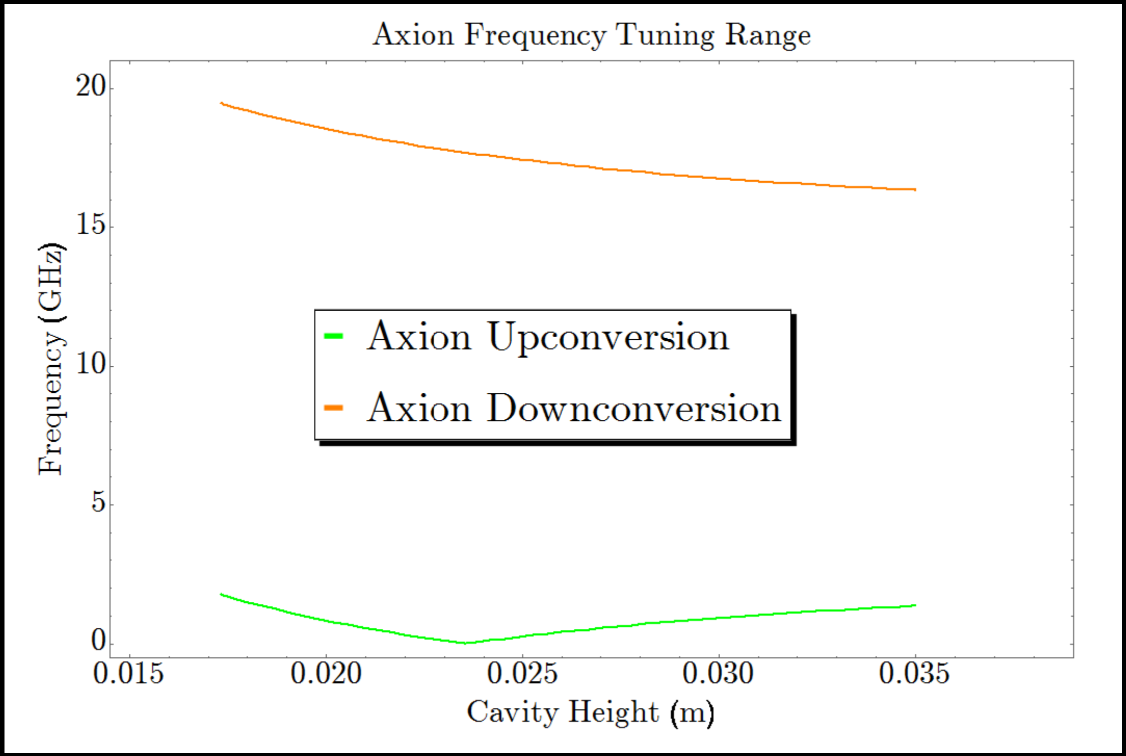

Frequency Space

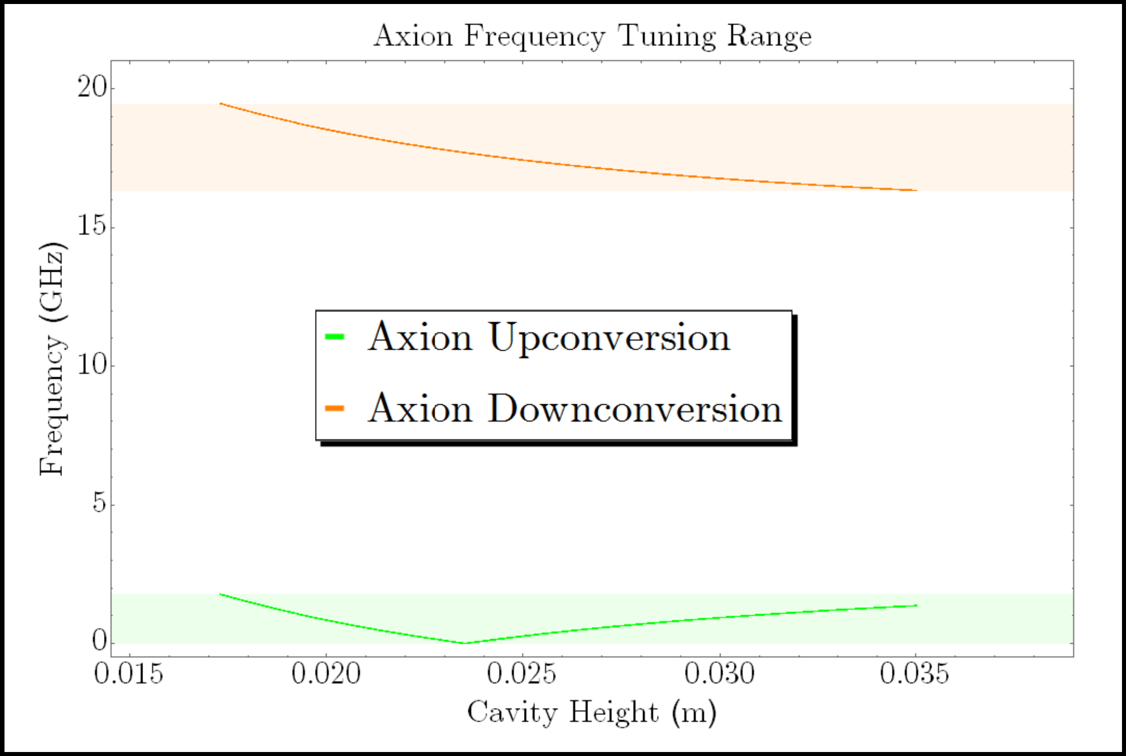

16.3 – 19.5 GHz

DC – 1.77 GHz

Frequency Space

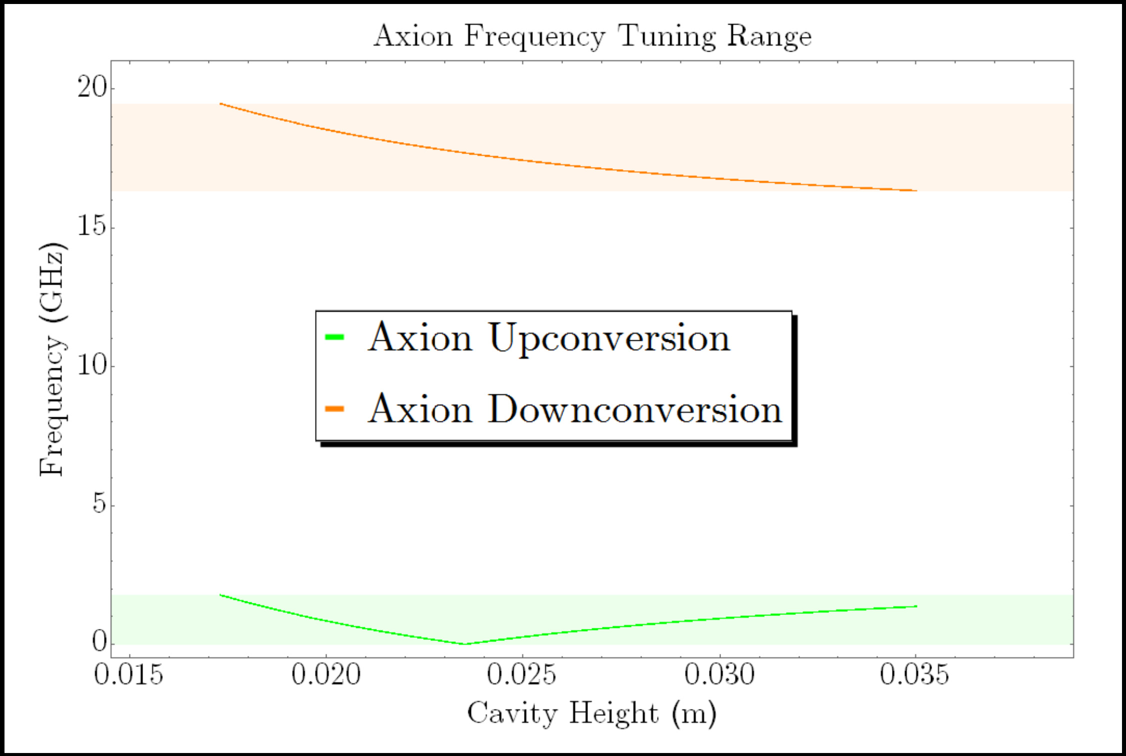

67.5 – 80.47 μeV

DC – 7.32 μeV

Coupling to the Fields

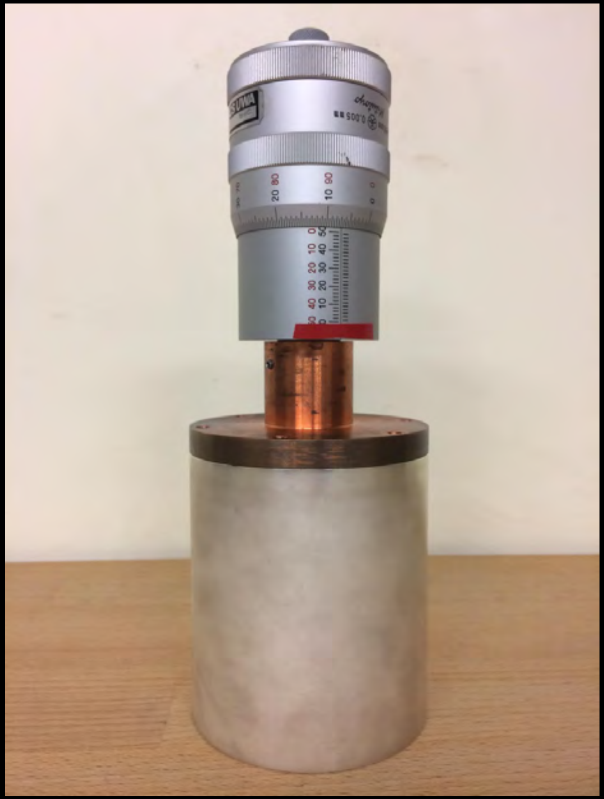

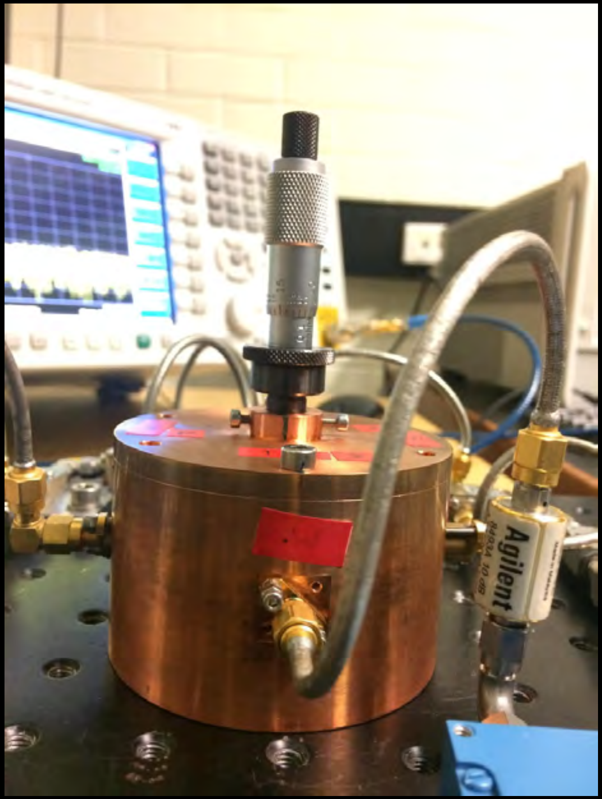

Coupling to the Fields

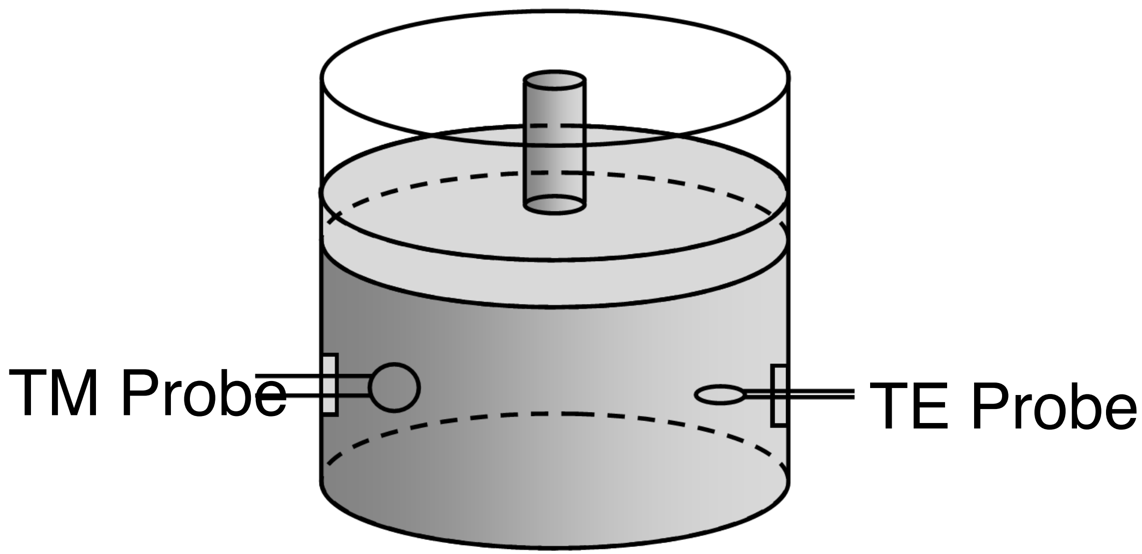

Coupling to the Fields

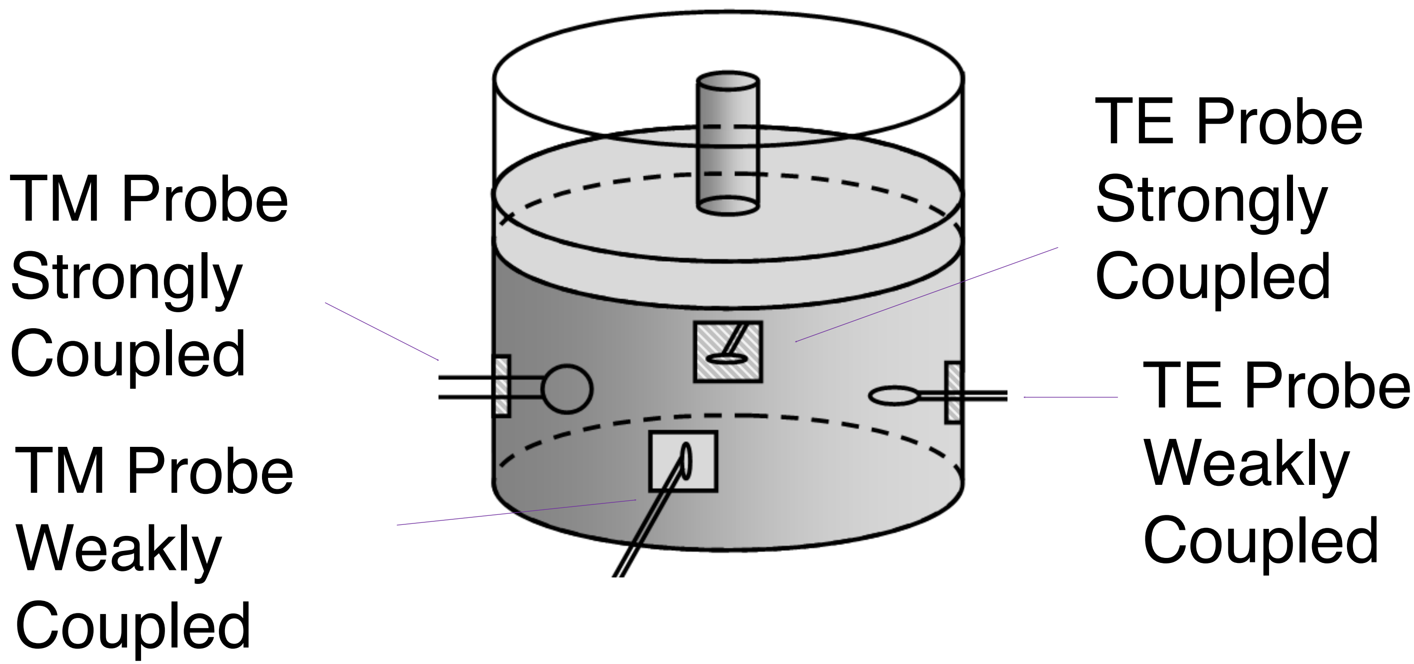

Quality Factor

- Q ~15,000 for two probe copper cavity
- Most significant loss is from cavity wall surface resistance
- Q ~ 10,000 for two probe cavity after silver coating
- **Silver coating** provides a theoretically superior quality factor (smaller surface resistance)
- However, silver coating **deteriorated** the quality factor due to introducing impurities/asymmetry (poor silver coating application)

- Q ~ 10,000 for four probe copper cavity

Theoretical Sensitivity Limits

Sensitivity of the degenerate/broadband mode

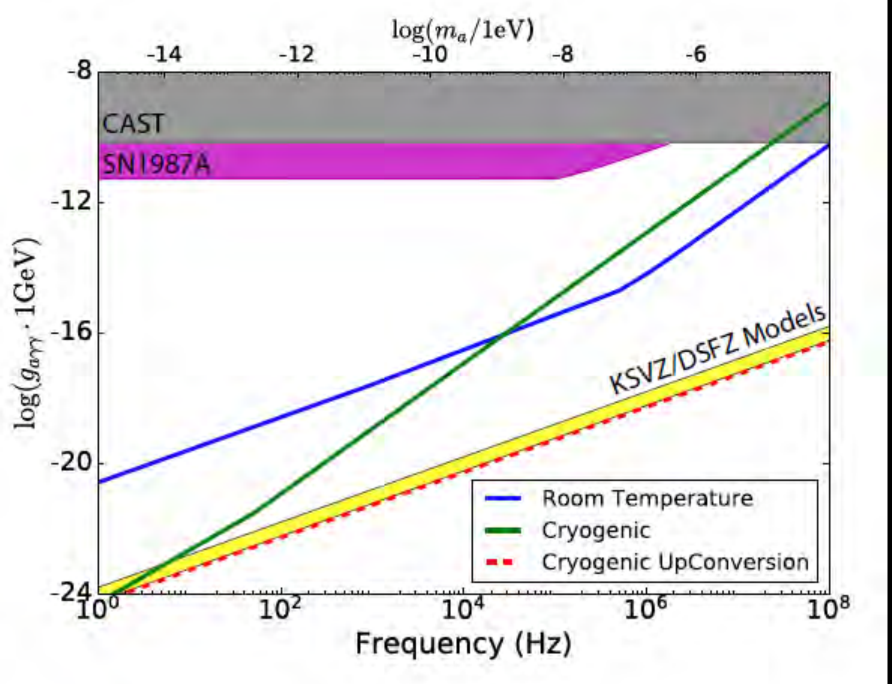

Maxim Goryachev, Ben McAllister, Michael

Theoretical Sensitivity Limits

Sensitivity of the loop oscillator

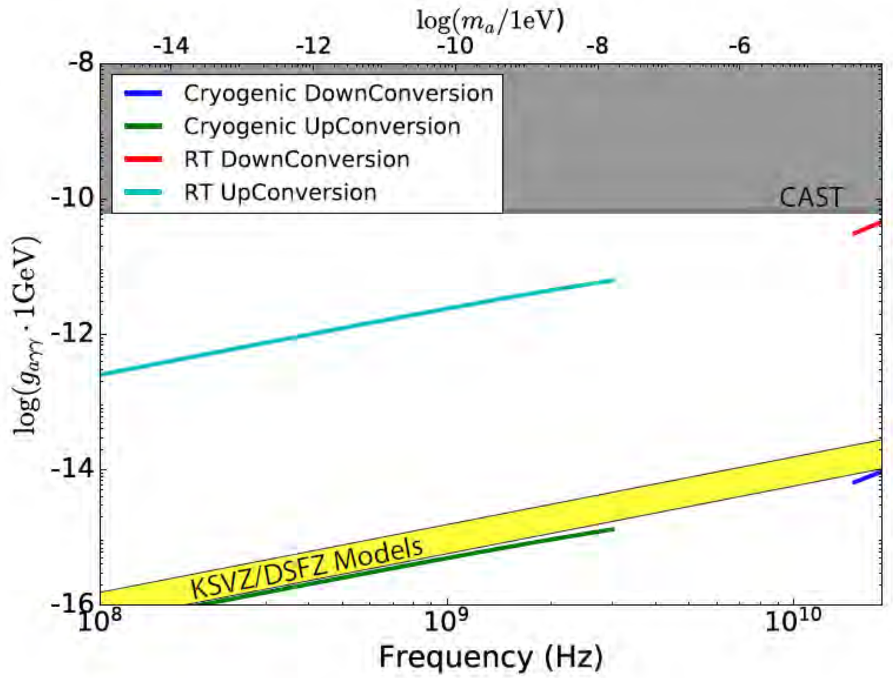

Maxim Goryachev, Ben McAllister, Michael

Free Running Loop Oscillator

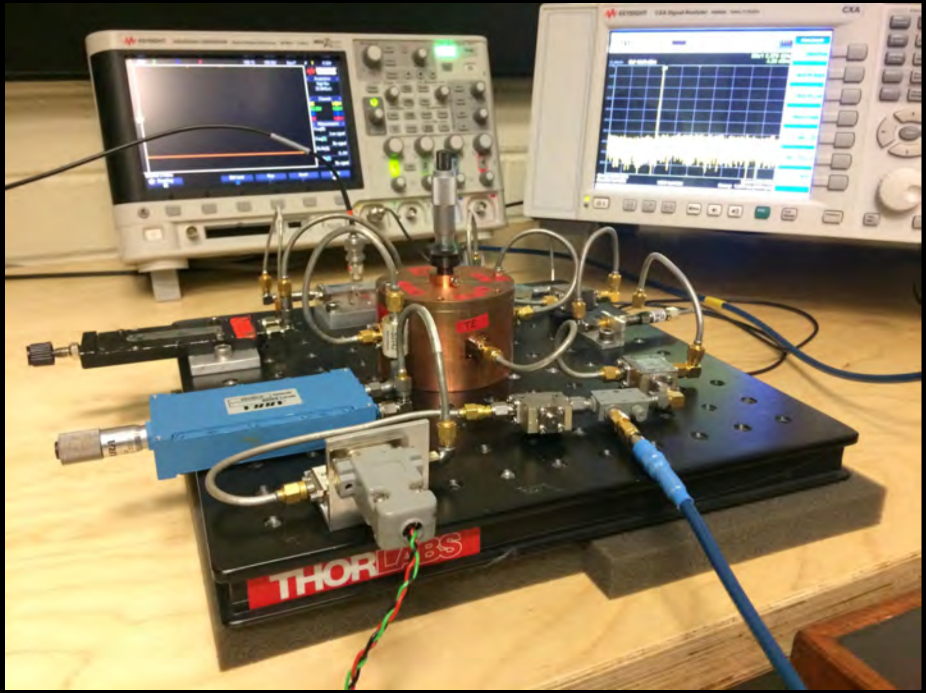

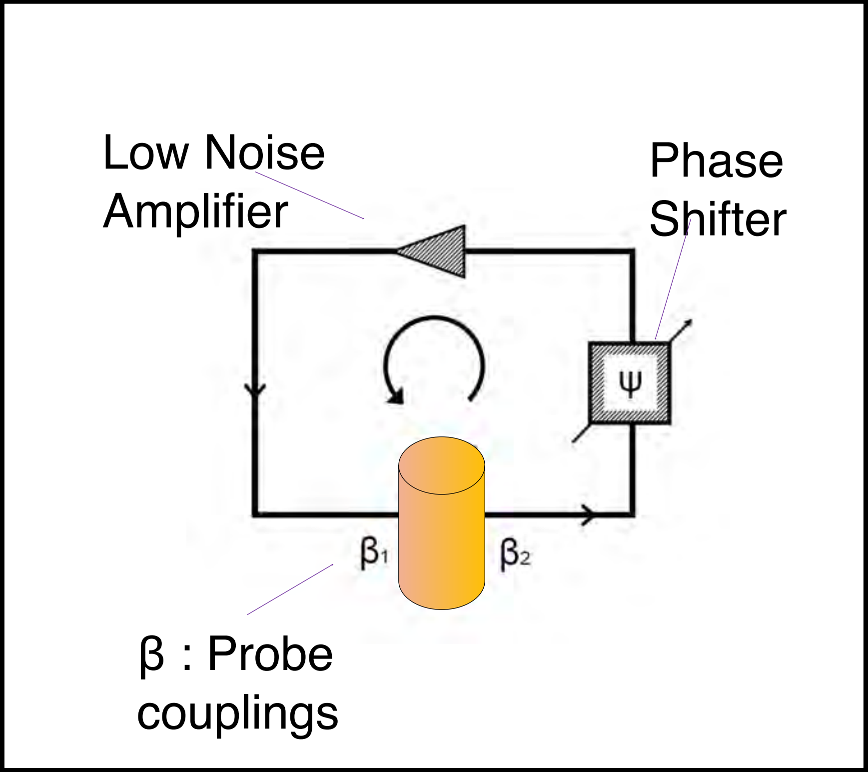

Free Running Loop Oscillator

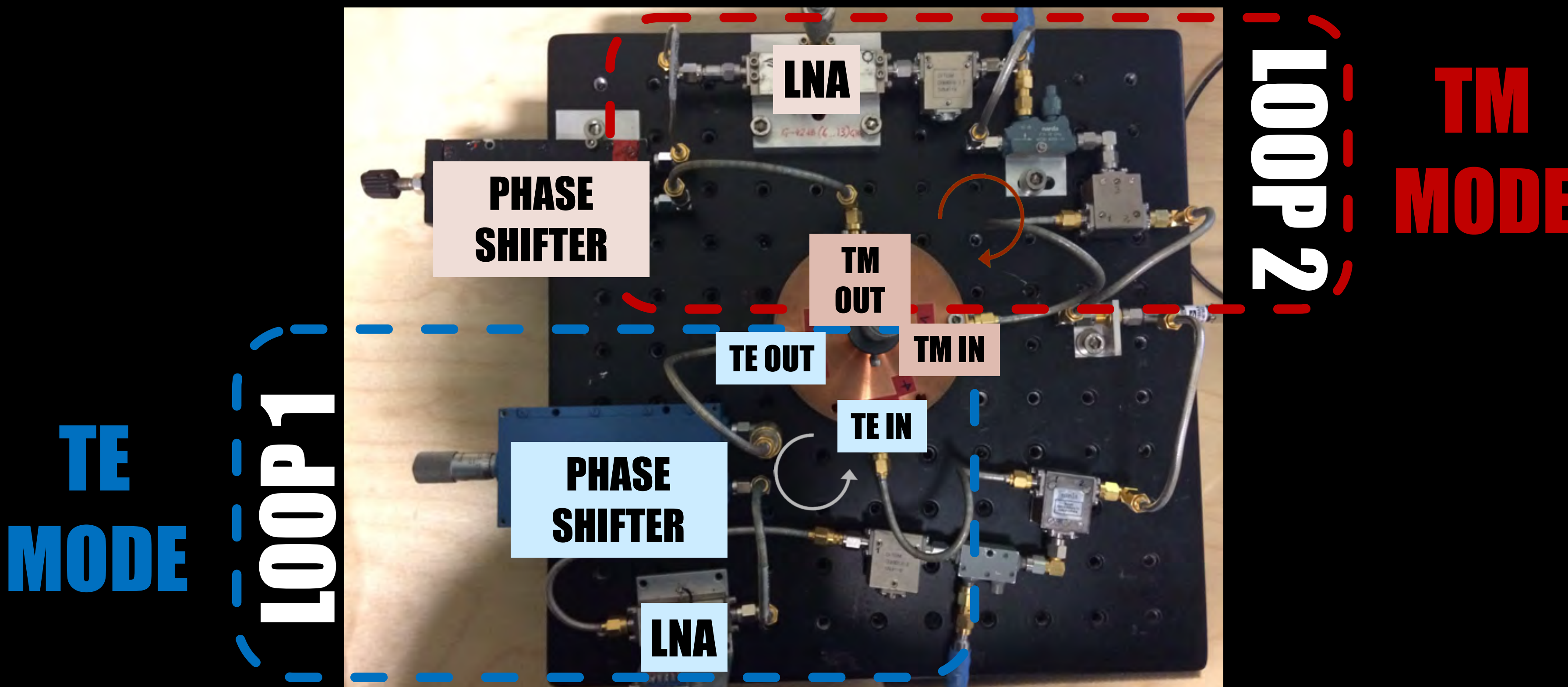

Searching for Axion in Fourier Spectrum of Phase Noise

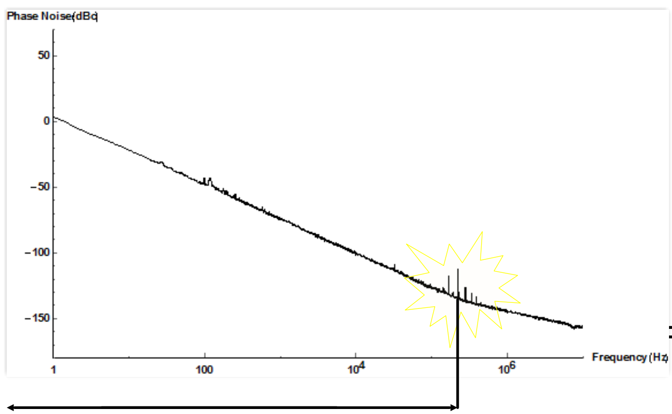

= 9C

$$\omega_a = \omega_1 \pm \omega_2 + 2\pi f$$

$$2\pi f \ll \omega_1$$

$f = 400$ MHz

TE = 9GHz

TE = 8GHz

f_a = 9±8+0.4 GHZ

= 17.4 GHz or 1.4GHz

Phase Noise Detection

FREQUENCY DISCRIMINATOR

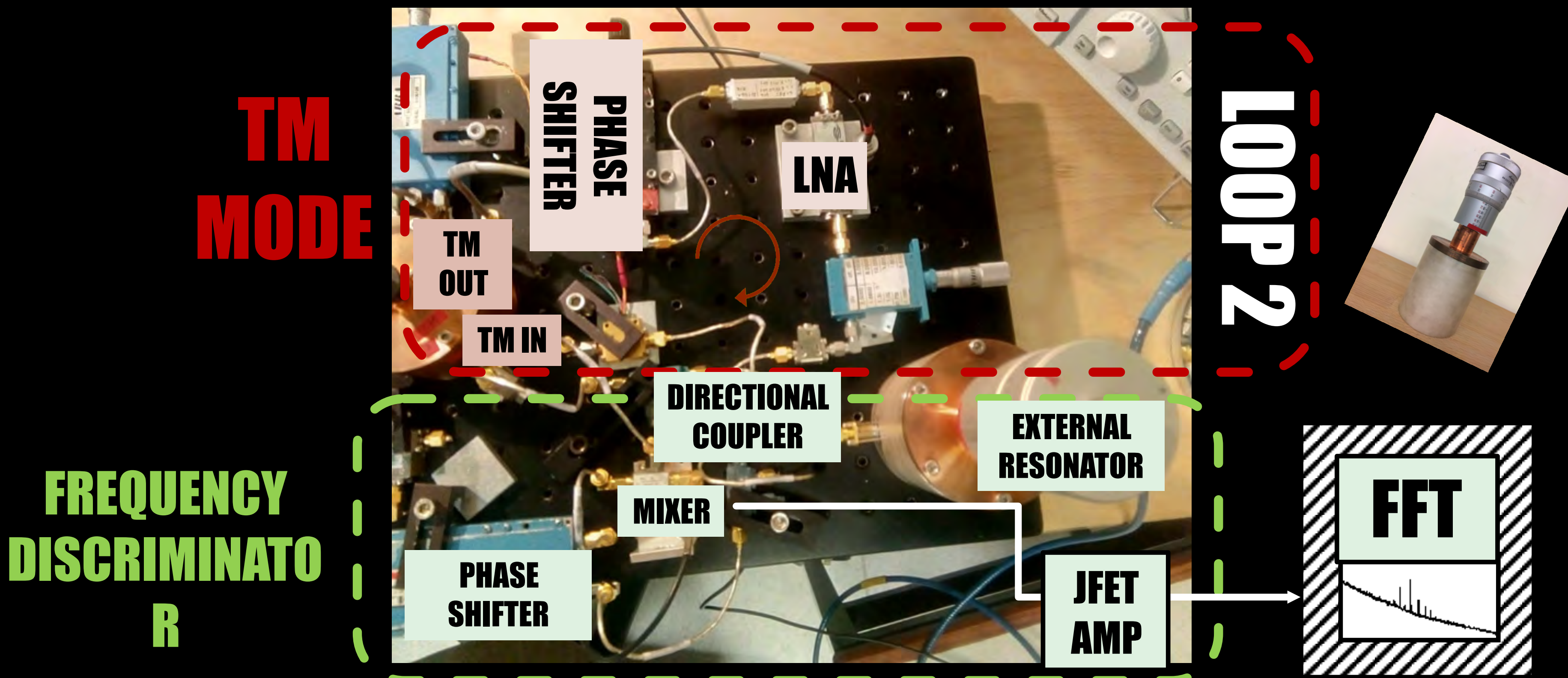

Voltage Noise Detection

FREQUENCY DISCRIMINATOR

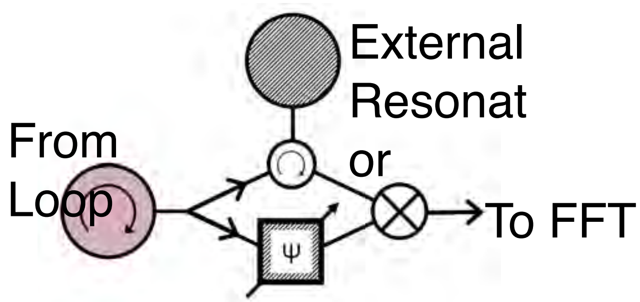

- External resonator **phase** fluctuations into **frequency** fluctuations
- Frequency discriminator turns **frequency** fluctuations into **voltage** fluctuations when phase across the mixer is set to quadrature
- Contains noise of loop, external resonator and tunable cavity
- FFT can produce a voltag
density

FREQUENCY DISCRIMINATOR

Initial Phase Noise Data

TE = 9.5 GHz

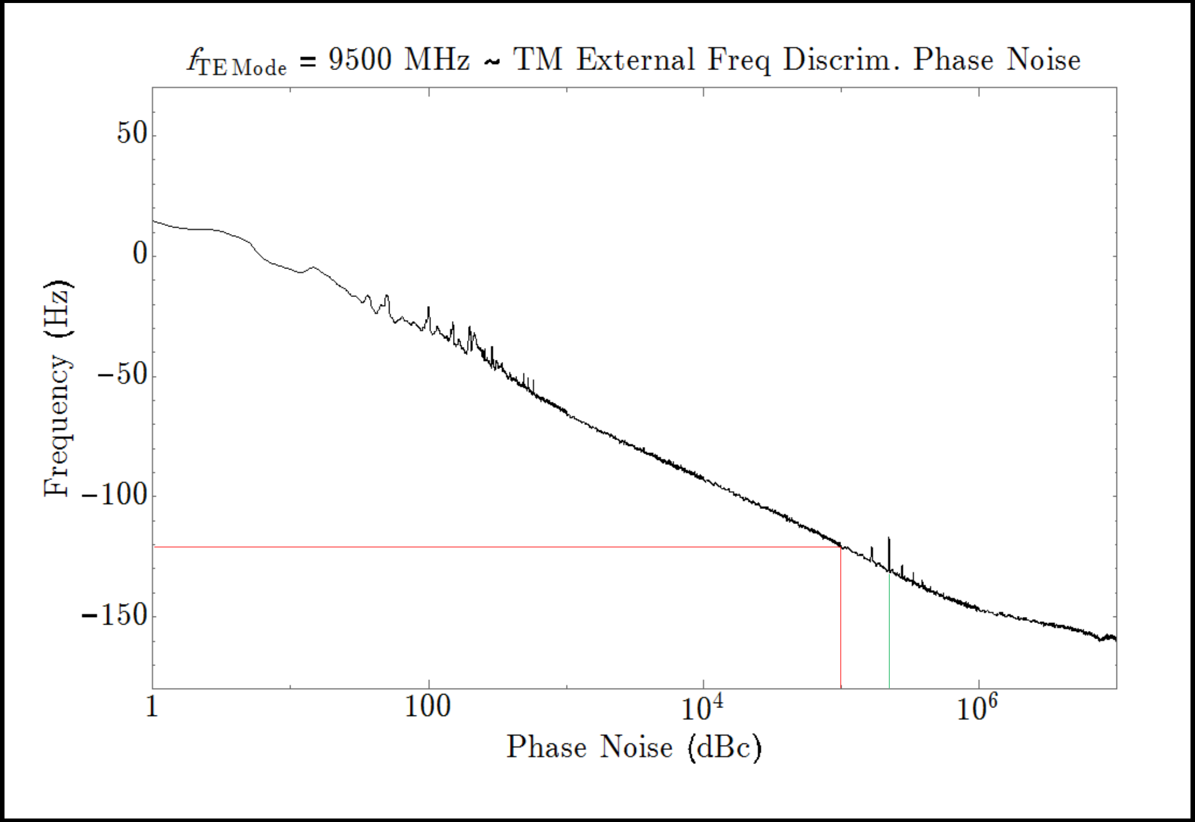

Initial Phase Noise Data

TE = 8.5 GHz

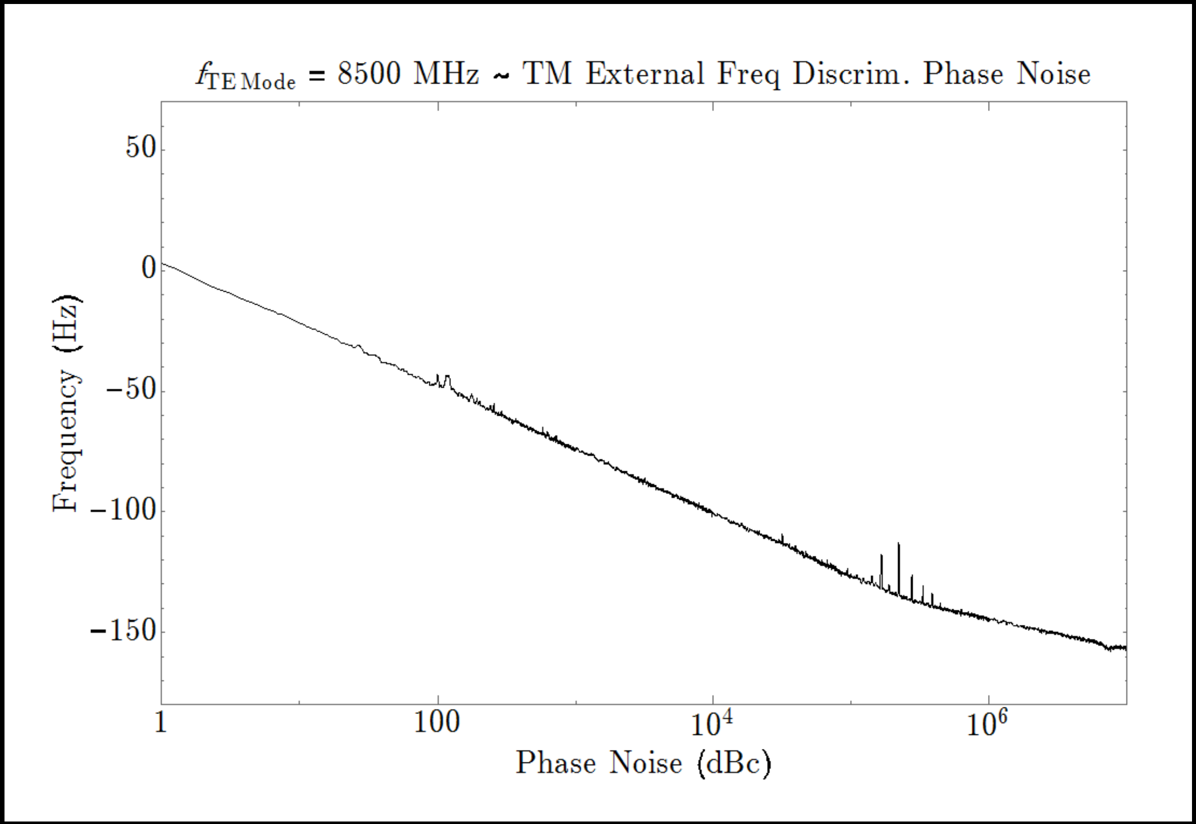

Initial Phase Noise Data

TE = 8 GHz

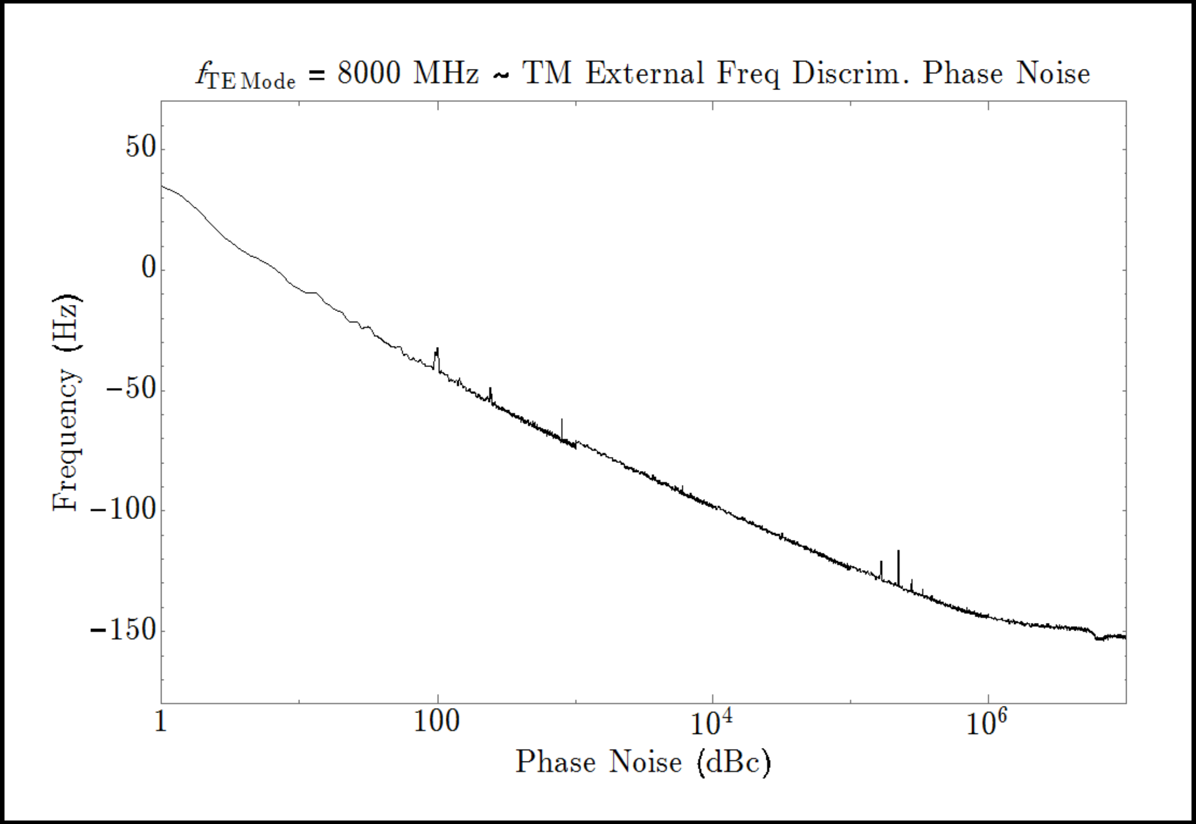

Modified Axion Electrodynamics

$$\vec{\nabla}\cdot\vec{D} = \rho_f + g_{a\gamma\gamma}\sqrt{\frac{\epsilon_0}{\mu_0}}\vec{B}\cdot\vec{\nabla}a$$

$$\vec{\nabla}\times\vec{H} = \vec{J}_f + \frac{\partial\vec{D}}{\partial t} - g_{a\gamma\gamma}\sqrt{\frac{\epsilon_0}{\mu_0}}\left(\vec{B}\frac{\partial a}{\partial t} + \vec{\nabla}a\times\vec{E}\right)$$

$$\vec{\nabla}\cdot\vec{B} = 0$$

$$\vec{\nabla}\times\vec{E} = -\frac{\partial\vec{B}}{\partial t}$$

$$\vec{D} = \epsilon_0\vec{E} + \vec{P}$$

$$\vec{H} = \frac{\vec{B}}{\mu_0} - \vec{M}$$

THE UNIVERSITY OF WESTERN AUSTRALIA

EQU

Australian Research Co

Centre of Excellence fo

Engineered Quantum

Vector Identities

$$\vec{B} \cdot \vec{\nabla} a = \vec{\nabla} \cdot (a\vec{B}) + a(\vec{\nabla} \cdot \vec{B}) \qquad \vec{\nabla} \cdot \vec{B} = 0$$

$$\vec{\nabla} a \times \vec{E} = \left(\vec{\nabla} \times (a\vec{E})\right) - a\left(\vec{\nabla} \times \vec{E}\right) \qquad \vec{\nabla} \times \vec{E} = -\frac{\partial \vec{B}}{\partial t}$$

Modified Gauss' Law and Ampere's Law

$$\vec{\nabla} \cdot \vec{D} = \rho_f + g_{a\gamma\gamma}\sqrt{\frac{\epsilon_0}{\mu_0}}\vec{\nabla} \cdot (a\vec{B})$$

$$\vec{\nabla} \times \vec{H} = \vec{J}_f + \frac{\partial \vec{D}}{\partial t} - g_{a\gamma\gamma}\sqrt{\frac{\epsilon_0}{\mu_0}}\left(\frac{\partial (a\vec{B})}{\partial t} + \vec{\nabla} \times (a\vec{E})\right)$$

Reformulate Modified Electrodynamics

$$\vec{\nabla} \cdot \vec{D_a} = \rho_f$$

$$\vec{\nabla} \times \vec{H_a} = \vec{J_f} + \frac{\partial \vec{D_a}}{\partial t}$$

$$\vec{\nabla} \cdot \vec{B} = 0$$

$$\vec{\nabla} \times \vec{E} = -\frac{\partial \vec{B}}{\partial t}$$

Similar to Standard Model Extension Modifications for Lorentz Invariance Violations

Modification in the Constitutive Relations

$$\vec{D_a} = \epsilon_0 \vec{E} + \vec{P} + \vec{P_a}$$

$$\vec{P}_a = -g_{a\gamma\gamma} a \epsilon_0 (c\vec{B})$$

$$\vec{H_a} = \frac{1}{\mu_0}\vec{B} - \vec{M} - \vec{M_a}$$

$$\vec{M}_a = g_{a\gamma\gamma} a \frac{1}{\mu_0}\frac{\vec{E}}{c}$$

PHYSICAL REVIEW LETTERS

VOLUME 58 4 MAY 1987 NUMBER 18

Two Applications of Axion Electrodynamics

Frank Wilczek

Institute for Theoretical Physics, University of California, Santa Barbara, Santa Barbara, California 93106

(Received 27 January 1987)

$$\Delta \mathcal{L} = \kappa a \mathbf{E} \cdot \mathbf{B}, \tag{1}$$

where κ is a coupling constant. The resulting equations are

$$\nabla \cdot \mathbf{E} = \tilde{\rho} - \kappa \nabla a \cdot \mathbf{B}, \tag{2}$$

$$\nabla \times \mathbf{E} = -\partial \mathbf{B}/\partial t, \tag{3}$$

$$\nabla \cdot \mathbf{B} = 0, \tag{4}$$

$$\nabla \times \mathbf{B} = \partial \mathbf{E}/\partial t + \tilde{\mathbf{j}} + \kappa(\dot{a}\mathbf{B} + \nabla a \times \mathbf{E}), \tag{5}$$

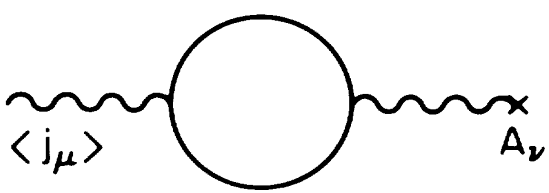

FIG. 3. Expectation of the current in a background field is derived from the vacuum polarization.

UNIFICATION OF COUPLINGS

Recent high-precision experimental results support the predictions of the minimal supersymmetric SU(5) model that unifies electromagnetism and the weak and strong interactions.

Savas Dimopoulos, Stuart A. Raby and Frank Wilczek

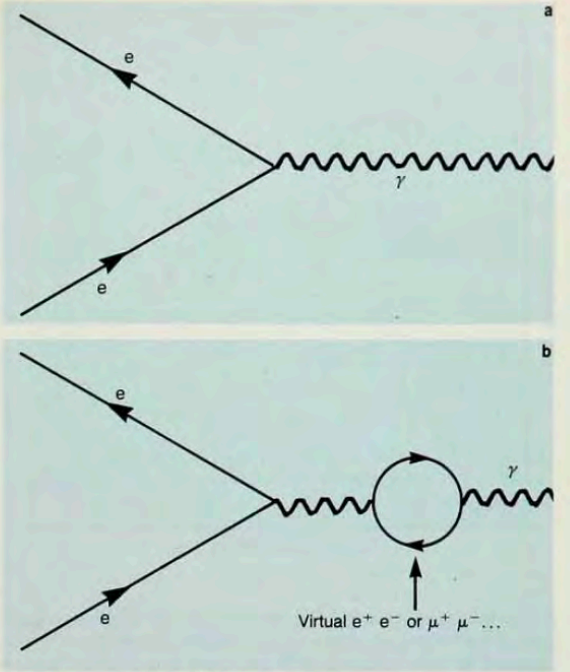

Empty space is a dielectric medium in quantum field theory and can screen charge. These Feynman diagrams represent the interaction between a bare charge and a photon (**a**) and the effect of virtual particles coming between the photon and the charge (**b**). **Figure 5**

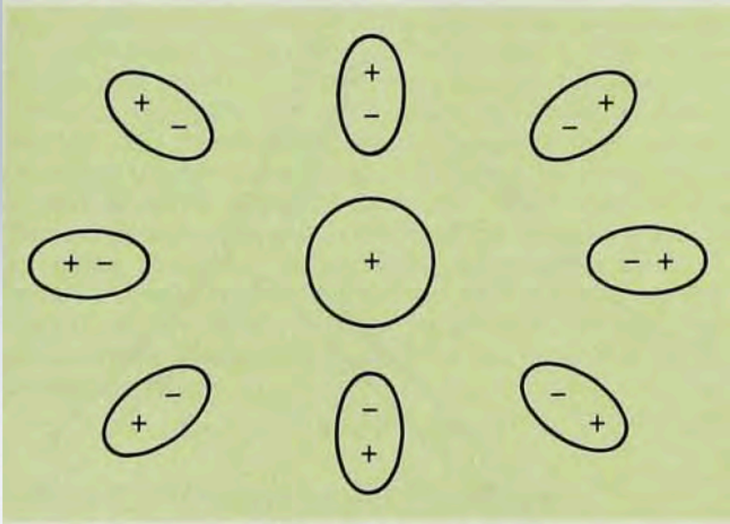

Dielectric screening occurs when a charge in a dielectric medium polarizes the molecules around it. This cloud of polarization partially hides, or screens, the central charge. **Figure 4**

arXiv:hep-th/9609099 v1 11 Sep 1996

Asympt

1.2.

Spin

Fran

School of

Institute fo

Ol

Princet

magnet!

INSTITUTE OF PHYSICS PUBLISHING METROLOGIA

Metrologia **42** (2005) 129–133 doi:10.1088/0026-1394/42/2/007

• hep-ph/0306230

Global representation of the fine structure constant and its variation

Michael E Tobar

Frequency Standards and Metrology Research Group, School of Physics, M013,
University of Western Australia Crawley, 6009, WA, Australia

Received 26 October 2004
Published 9 March 2005
Online at stacks.iop.org/Met/42/129

$$\alpha = \frac{1}{4\sqrt{2}}\sqrt{\frac{\Phi_e}{\Phi_\phi}},$$

Abstract

The fine structure constant, α, is shown to be proportional to the ratio of the quanta of electric and magnetic force associated with the electron. This provides a new representation, which is global across all unit systems. Consequently, a variation in α was shown to occur due to a differential change in the fraction of the quanta of electric and magnetic force, while a variation in $\hbar c$ was shown to manifest due to the common mode change. The representation is discussed with respect to the running of the fine structure constant at high energies (small distances), and a putative temporal drift. It is shown that the running of the fine structure constant is due to equal components of electric screening (polarization of vacuum) and magnetic anti-screening (magnetization of vacuum), which cause the perceived quantum of electric charge to increase at small distances, while the magnetic flux quantum decreases. This introduces the concept of the 'bare magnetic flux quanta' as well as the 'bare electric charge'. With regard to temporal drift, it is confirmed that it is impossible to determine which fundamental constant is varying if α varies.

PHYSICAL REVIEW D **66**, 056005 (2002)

Signals for Lorentz violation in electrodynamics

V. Alan Kostelecký and Matthew Mewes
Physics Department, Indiana University, Bloomington, Indiana 47405
(Received 20 May 2002; published 23 September 2002)

$$\vec{\nabla}\times\vec{H}-\partial_0\vec{D}=0, \quad \vec{\nabla}\cdot\vec{D}=0,$$
$$\vec{\nabla}\times\vec{E}+\partial_0\vec{B}=0, \quad \vec{\nabla}\cdot\vec{B}=0.$$

$$\begin{pmatrix}\vec{D}\\ \vec{H}\end{pmatrix}=\begin{pmatrix}1+\kappa_{DE} & \kappa_{DB}\\ \kappa_{HE} & 1+\kappa_{HB}\end{pmatrix}\begin{pmatrix}\vec{E}\\ \vec{B}\end{pmatrix}$$

PHYSICAL REVIEW D **71,** 025004 (2005)

New methods of testing Lorentz violation in electrodynamics

Michael Edmund Tobar,[1,*] Peter Wolf,[2,3] Alison Fowler,[1] and John Gideon Hartnett[1]
[1]*University of Western Australia, School of Physics, M013, 35 Stirling Highway, Crawley 6009 WA, Australia*
[2]*Bureau International des Poids et Mesures, Pavillon de Breteuil, 92312 Sèvres Cedex, France*
[3]*BNM-SYRTE, Observatoire de Paris, 61 Avenue de l'Observatoire, 75014 Paris, France*
(Received 1 September 2004; published 7 January 2005)

$$\begin{pmatrix}\boldsymbol{D}\\ \boldsymbol{H}\end{pmatrix}=\begin{pmatrix}\epsilon_0(\tilde{\epsilon}_r+\kappa_{DE}) & \sqrt{\frac{\epsilon_0}{\mu_0}}\kappa_{DB}\\ \sqrt{\frac{\epsilon_0}{\mu_0}}\kappa_{HE} & \mu_0^{-1}(\tilde{\mu}_r^{-1}+\kappa_{HB})\end{pmatrix}\begin{pmatrix}\boldsymbol{E}\\ \boldsymbol{B}\end{pmatrix}$$

$$g_{a\gamma\gamma}a \sim \kappa_{DB} \quad \kappa_{HE}$$

Axion Interaction similar to odd parity Lorentz Invariance Violation

www.physics.indiana.edu/~kostelec/

Sidereal Modulations of Constant Background Fields

Oscillating Background Fields Create EM Radiation

Axion is similar to an oscillating odd parity background SME Lorentz invariance violation field.

Cannot shield against these type of violations -> Source Terms.

Axion Induced Vacuum Bound Charges and Currents

Vacuum Bound Charge

$$\rho_a = g_{a\gamma\gamma}\sqrt{\frac{\epsilon_0}{\mu_0}}\vec{\nabla}\cdot(a\vec{B})$$

Vacuum Polarization Current

$$\vec{P}_a = -g_{a\gamma\gamma} a \epsilon_0 (c\vec{B}) \qquad \vec{J}_a = \frac{\partial \vec{P}_a}{\partial t} \qquad \vec{J}_a = -g_{a\gamma\gamma}\sqrt{\frac{\epsilon_0}{\mu_0}}\frac{\partial(a\vec{B})}{\partial t}$$

$$\nabla\cdot\vec{J}_a = -\frac{\partial \rho_a}{\partial t}$$

Satisfies the Continuity Equation

Consider a Capacitor with Linear Dielectric

$$\overrightarrow{D} = \epsilon_0 \overrightarrow{E} + \overrightarrow{P} \qquad \overrightarrow{P} = \epsilon_0 \chi_e \overrightarrow{E} = -\epsilon_0 \overrightarrow{E}_{screen}$$

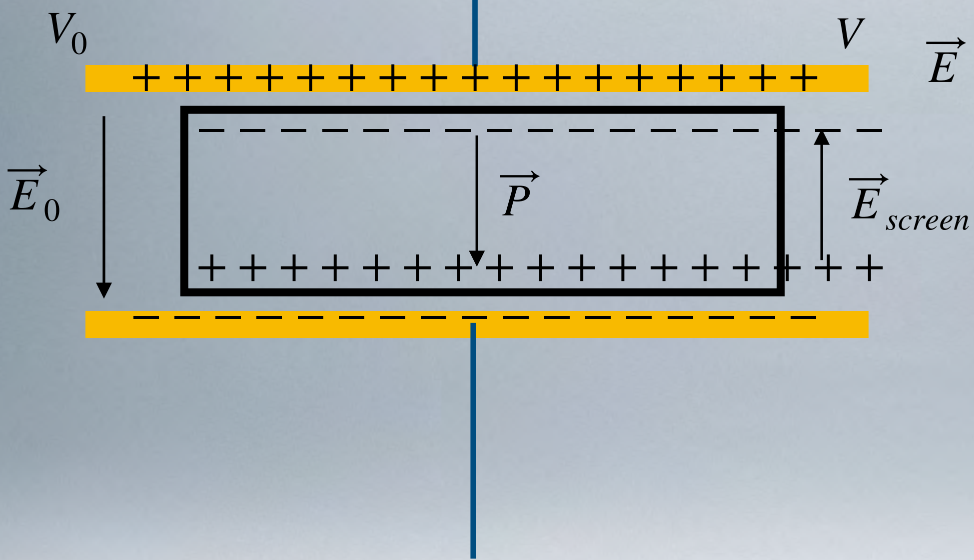

$$\vec{E} = \vec{E}_0 + \vec{E}_{screen}$$

$$\vec{E}_{screen} = -\frac{\chi_e}{\chi_e + 1}\vec{E}_0 = -\chi_e \vec{E}$$

Axion Electrodynamics

$$\overrightarrow{P_a} = -\epsilon_0 (g_{a\gamma\gamma} a c \overrightarrow{B}) \qquad \overrightarrow{E}_{a\ screen} = g_{a\gamma\gamma} a c \overrightarrow{B} \; V/m$$

Note if $\vec{E}_{a\ screen} = 0$ then $\vec{P}_a = 0$ $\qquad \vec{J}_a = \frac{\partial \vec{P}_a}{\partial t} = 0$

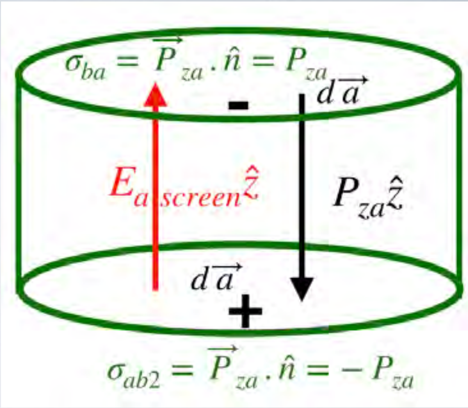

Electromotive Force

$$\overrightarrow{E} = 0 \qquad \overrightarrow{B} = \overrightarrow{B_0} \qquad a(t) = a_0 Cos[\omega_a t]$$

$$\overrightarrow{f_a} = \frac{\overrightarrow{F}_a}{q_a} = -\overrightarrow{E}_{a\ screen} = -g_{a\gamma\gamma} a_0 c \overrightarrow{B_0} Cos[\omega_a t]\ V/m$$

Physics Letters B 265 (1991) 197–200
North-Holland

PHYSICS LETTERS B

A new method for the detectability of oscillating θ

Jooyoo Hong and Jihn E. Kim
Department of Physics and Center for Theoretical Physics, Seoul National University, Seoul 151-742, Korea

Received 27 December 1990; revised manuscript received 29 May 1991

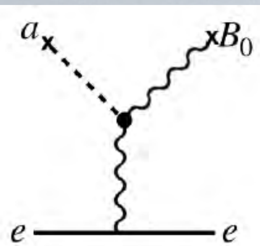

FIG. 2: Feynman diagram showing the Primakoff effect of the axion interacting with the DC $\vec{B}$-field to create an oscillating vacuum polarization, which in turn interacts with an electron [17].

$$\boldsymbol{F}_a = \frac{e\alpha_{em} g_\gamma}{\pi m_a^2} \frac{\partial}{\partial t} (\dot{\theta} \boldsymbol{B})$$

$$\vec{F}_a(t) = e g_{a\gamma\gamma} a_0 (cB_0) \cos(\omega_a) \hat{z}$$

$$\vec{F}_a(t) = -q_a g_{a\gamma\gamma} a_0 (cB_0) \cos(\omega_a) \hat{z}$$

$$\mathcal{E} = \oint_C [\boldsymbol{E} + \boldsymbol{v} \times \boldsymbol{B}] \cdot \mathrm{d}\boldsymbol{\ell}$$

$$+ \frac{1}{q} \oint_C \text{Effective chemical forces} \cdot \mathrm{d}\boldsymbol{\ell}$$

$$+ \frac{1}{q} \oint_C \text{Effective thermal forces} \cdot \mathrm{d}\boldsymbol{\ell} \,,$$

$$+ \frac{1}{q} \oint_C \text{Effective axion forces} \cdot \mathrm{d}\boldsymbol{\ell}$$

$$\vec{E} = 0 \qquad \vec{B} = B_0\,\vec{\theta}$$

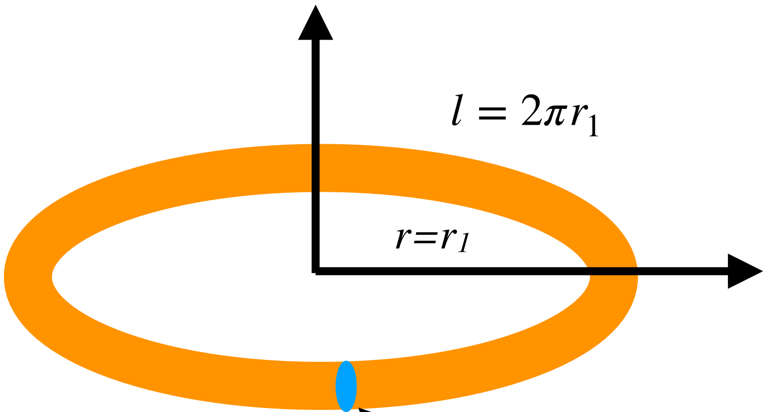

$$\vec{P}_a = -\,\epsilon_0 g_{a\gamma\gamma} a_0 (cB_0) e^{-j\omega_a t}\,\vec{\theta}$$

$$\frac{d\vec{P}_a}{dt} = j\omega_a \epsilon_0 g_{a\gamma\gamma} a_0 (cB_0) e^{-j\omega_a t}\,\vec{\theta}$$

$$\vec{\nabla} \times \vec{P}_a \neq 0$$

$$\vec{f}_a = \frac{\vec{F}_a}{q_a} = -\,\vec{E}_{a\ screen} = \frac{1}{\epsilon_0}\vec{P}_a$$

$$\mathscr{E} = \oint_P \vec{f}_a \cdot d\vec{l} = \frac{1}{\epsilon_0}\oint_P \vec{P}_a \cdot d\vec{l}$$

$$\vec{I} = A\frac{d\vec{P}_a}{dt} = j\omega_a \epsilon_0 g_{a\gamma\gamma} a_0 c B_0 A e^{-j\omega_a t}\,\vec{\theta}$$

$$V = \mathscr{E} = -\,g_{a\gamma\gamma} a_0 c B_0 l e^{-j\omega_a t}$$

$$\frac{V}{I} = -\frac{1}{\epsilon_0}\frac{l}{A}\frac{1}{j\omega_a}$$

COULD NOT DO THIS IN NORMAL ELECTRODYNAMICS

− − − − −

\+ + + + +

PHYSICAL REVIEW D, VOLUME 70, 076006

Lorentz-violating electrostatics and magnetostatics

Quentin G. Bailey and V. Alan Kostelecký
Physics Department, Indiana University, Bloomington, Indiana 47405, USA
(Received 21 July 2004; published 27 October 2004)

The static limit of Lorentz-violating electrodynamics in vacuum and in media is investigated. Features of the general solutions include the need for unconventional boundary conditions and the mixing of electrostatic and magnetostatic effects. Explicit solutions are provided for some simple cases. Electromagnetostatics experiments show promise for improving existing sensitivities to parity-odd coefficients for Lorentz violation in the photon sector.

DOI: 10.1103/PhysRevD.70.076006 PACS numbers: 03.30.+p, 11.30.Cp, 13.40.–f

THE UNIVERSITY OF WESTERN AUSTRALIA

FACULTY OF SCIENCE

Broadband Electric-field Axion Sensing Technique (BEAST)

BT McAllister, M Goryachev, J Bourhill, EN Ivanov, ME Tobar

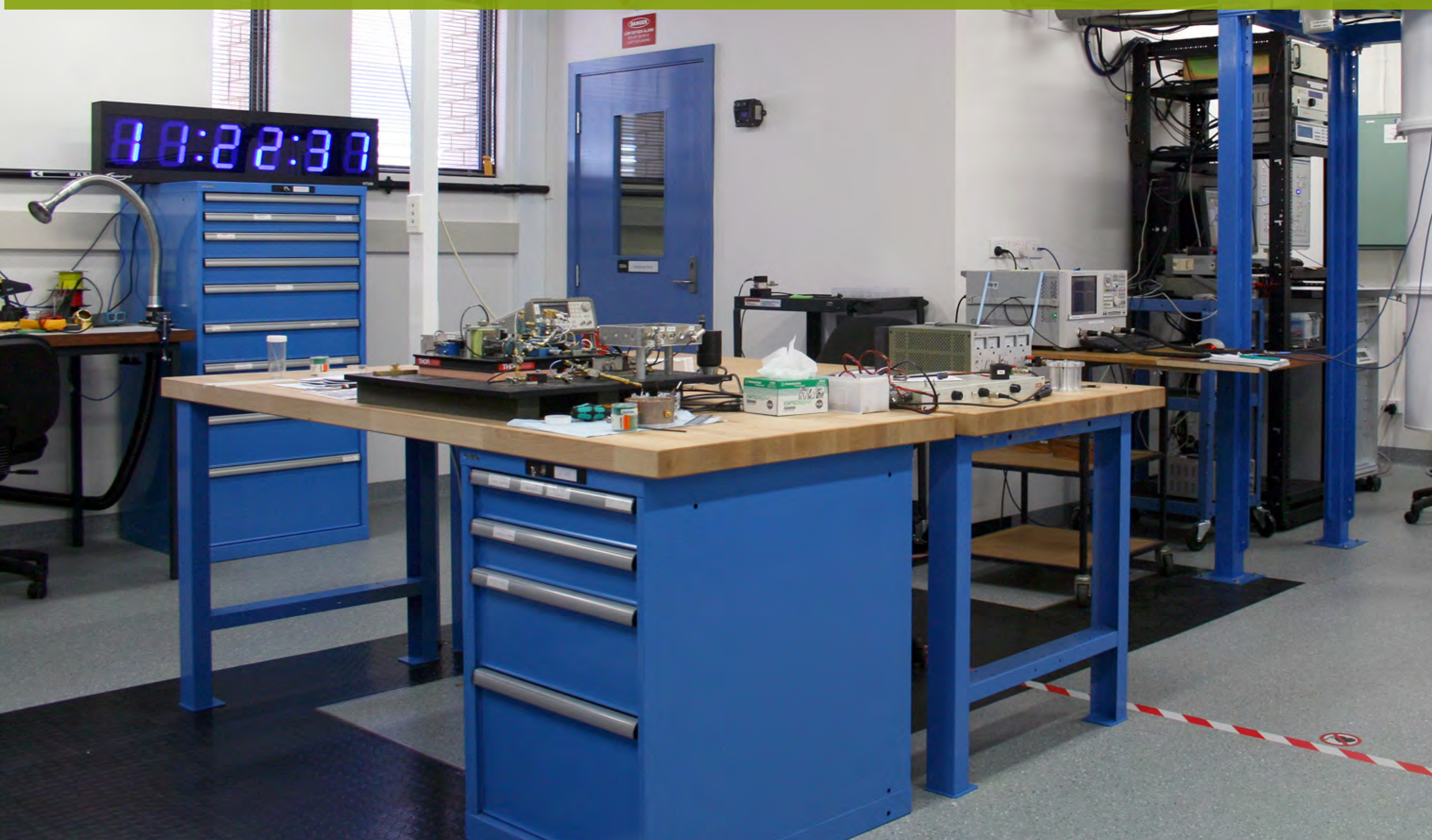

EQUS
Australian Research Council
Centre of Excellence for
Engineered Quantum Systems

BEAST: First Limits

Higher resolution search was conducted around 5 kHz, with the minimal spectral resolution of 4.5 mHz (increasing at higher frequencies)

All sharp peaks greater than 4.4 standard deviations from the mean originating from the SQUID were able to be excluded, due to a similar signal appearing in the flux line

Using this data, we may place the 95 % confidence exclusion limits on axion-photon coupling